MAKALUVAMINES AS CHITINASE INHIBITORS ISOLATED FROM AN ASCIDIAN OF THE GREAT BARRIER REEF

BY

Joshua Luke Haworth

Thesis

Submitted in partial fulfilment of the requirements for the degree of Master of Science by Research at the School of Pharmacy and Biomedical Sciences, University of Central Lancashire, Preston, United Kingdom.

January 2024

Declaration

This thesis describes research conducted within the School of Pharmacy and Biomedical Sciences at the University of Central Lancashire, under the primary supervision of Dr. Jioji Tabudravu from January 2023 to January 2024. I certify that the research described is original and that I have written all text herein, with clear indication to referenced material by suitable citation.  8th January 2024, Joshua Luke Haworth.

Acknowledgements

I would like to thank my primary supervisor Dr. Jioji Tabudravu for the opportunity to embark on this research project, and for the assistance and support that they have provided. I extend my gratitude to the entire analytical suite team of the University of Central Lancashire. In particular I would like to thank Jane Ingram, Kane Fox and Sameera Mahroof for all of the technical support and advice that they have provided throughout this course, in addition to making the analytical lab a pleasant environment to work. Finally I would like to thank my friends and family, who have always been there to offer unconditional support and advice.

Contents

List of Figures

List of Tables

Abstract

This thesis investigates the secondary metabolites isolated from a marine tunicate species of the Great Barrier Reef, Australia. Structural elucidation techniques led to the identification of at least two known compounds belonging to a family of secondary metabolites more commonly isolated from marine sponges. One of the isolated compounds, Makaluvamine H, was used in a preliminary enzyme kinetics assay to assess potential inhibitive properties against chitinase. Additional Makaluvamine compounds from previous studies were obtained and assessed in this assay. This included a purified sample of Makaluvamine P, which was one of the two known compounds isolated and identified from the sample of this investigation. The findings of this research demonstrate that the Makaluvamine compounds assessed do possess inhibitive properties against *Streptomyces* chitinase enzyme. Makaluvamine A demonstrated the highest level of biological activity against the *Streptomyces* chitinase enzyme, with inhibition observed at a molar concentration of 12.4 μM. The lowest molar concentration at which inhibition was observed for the other Makaluvamine compounds were as follows; Makaluvamine P (15.4 μM), Makaluvamine H (23.1 μM) and Makaluvamine C (117 μM). Further investigation into the inhibitive properties of these compounds could potentially lead to their application in commercial sectors such as agriculture and healthcare.

Chapter 1

Introduction

1. Literature review

This literature review aims to establish the relevant background of general natural products research, from the discovery and applications of notable active compounds isolated from living organisms, through to the general techniques used throughout the stages of this discovery process. This will cover topics such as drug discovery and the medicinal history of natural products, medicinal applications of natural products in the modern day, non-medicinal applications of natural products and the challenges and limitations faced in natural products research. A brief discussion on chemical extraction techniques will be featured, in addition to a comprehensive look at natural products from the marine environment, the marine organisms that produce these natural products and the appeal and limitations of this to modern natural product research.

1.1 Drug Discovery and Medicinal History of Natural Products

Throughout history natural products have made a significant contribution to pharmaceutical development and the treatment of illness and disease. From the discovery of penicillin, a compound which changed not only the course of the second world war but also the future outlook of humanities battle against bacterial infections, to paclitaxel, a compound isolated from the bark of the Pacific yew tree that is used in the treatment of several cancers, such as breast and ovarian cancer.[1–3] The majority of natural products are classified as secondary metabolites, which are compounds produced by living organisms that are not deemed essential for the direct growth, development and reproduction of the organism yet may still play a crucial role in the organisms' survival.[4] For example penicillin is a secondary metabolite produced by fungi which, as is commonly known, possesses antibacterial properties. The ability of a fungus to produce an antibacterial compound such as penicillin is likely no accident, as in nature organisms such as fungi often find themselves competing against the likes of bacteria for physical space and nutrients. The secretion of an antibacterial compound therefore can tilt the odds of competition in favour of the fungal organism.[1, 4] This serves as only one small example, however throughout the field of natural products there are a countless array of complex compounds with unique properties produced by organisms ranging from

plants to bacteria, the synthesis of which has been perfected over thousands of years of evolution.

The extensive use of natural products for medicinal purposes far precedes the previous two centuries, in fact it is believed that the medicinal use of these compounds may have preceded recorded human history by thousands of years.[1] This idea has been presented by paleoanthropological studies that found pollen deposits in a neanderthal burial site in Iraq, believed to date back more than 60,000 years ago, alluding to the possibility that neanderthals were aware of medicinal healing properties of plants.[6] As humanity began to form structured civilisations the study and use of natural products grew, and almost every notable ancient civilisation throughout history has demonstrated the use of various naturally derived compounds.[7] Approximately 1,000 plants and plant derived substances were recorded on clay tablets in cuneiform by ancient Mesopotamian civilisations, which are believed to be the oldest form of medical text discovered, written approximately in 2600BC. Included in these ancient medical texts are the oils of *Cupressus sempervirens* (cypress) and *Cedrus* species (cedar), the resin of *Commiphora myrrha* (myrrh) and the juice of the poppy seed *Papaver somniferum*, which are still to present day used in the treatment of coughs, colds and inflammation.[7] Humans continued creating such medicinal records throughout historical civilisations, such as ancient Egypt with the *Ebers papyrus*, 2900BC, a pharmaceutical record comprised of more than 700 plant based drugs through to ancient China, who were responsible for the Materia Medica (1100BC), Shennong Herbal (~100BC) and the Tang Herbal (~659AD).[7] The historical use of natural products remains of significant consideration to modern researchers working within this field, as despite the considerable use of these plant based blends of tonics and ointments throughout history. The active compounds, that is the compounds produced by the plant and responsible for the desired therapeutic effect remained unknown. Advances in technology and chemical knowledge and techniques have allowed researchers to use these historical documents as a foundation upon which the organism can be explored, through the chemical extraction and isolation of individual compounds to the structural characterisation and identification of these compounds with spectroscopic techniques.[8]

1.2 Medicinal Applications of Natural Products in the Modern Day

As discussed the ancient historical use of natural products has primarily involved the direct consumption or application of the natural source, through the form of herbal blends or tonics

and ointments.[7] Today the isolation and discovery of individual secondary metabolites does not restrict the applications to that very compound but can rather inspire the synthesis of structural analogues and derivatives. A notable example of this would be acetylsalicyclic acid, more widely known as Aspirin, a synthetic derivative of the willow tree (*salix alba L*) metabolite salicin, which was initially isolated from the bark.[9] Aspirin serves as a common everyday painkiller that treats headaches and toothaches, in addition to alleviating cold and flu-like symptoms through reducing high body temperatures.

Several alkaloids have been isolated from the poppy *Papaver somniferum*, which includes the ever-significant compound Morphine.[10] A potent pain killer, Morphine is commonly used in clinical situations where a patients pain causes prolonged discomfort, such as active cancer treatment, vaso-occlusive pain during sickle cell crisis and also end of life care to patients. This extends to applications within the emergency department, more commonly when patients have failed to respond to first and second-line pain relief agents.[10] Derivatives of Morphine include diacetylmorphine (Heroin) and codeine.

Quinine is a metabolite used primarily in the treatment of malaria which was isolated from the bark of *Cinchona Succirubra*, a plant native to central and south America.[12] The application of this drug extends to the treatment of fever, indigestion, mouth and throat diseases and also cancer. Since the dawn of chemotherapeutic agents in the mid-20th century natural products have come to dominate the market with their effective chemotherapeutic properties.[13, 14] Since 1940 140 anti-cancer agents have been approved, with over 60% of these being traceable to a natural source and/or product. Of these 140 compounds 126 are classified as small molecules, which are defined as molecules with a molecular weight less than 900Da.[15] 67% of these small molecules originate from a natural source. This is significant as small molecules comprise 90% of all pharmaceutical drugs on the market.[13, 14, 16] From 2016 to 2018, there were 375,400 new cases of cancer in the UK,[17] and the global market for anti-tumour agents was $60 billion in 2007.[3] Examples of notable natural product chemotherapy drugs include paclitaxel (Taxol), Trabectedin (Yondelis),[19] isolated from a marine tunicate and used to treat soft tissue sarcoma and daunorubicin, a compound found in soil dwelling bacteria and used in the treatment of certain blood cancers.

1.3 Natural Products from the Marine Environment

The majority of natural products that were used throughout ancient history found their origin in plants, with natural products from land-based bacteria and fungi predominantly coming

forth in the 19th and 20th centuries.[1, 7, 20–22] However, until recent years ocean dwelling organisms have remained a largely untapped resource with regards to natural products, largely due to the technological limitations for underwater exploration. The emergence of marine based natural products arose from the introduction of SCUBA in the 1970s, along with subsequent advances like manned submersibles (1980s) and remotely operated vehicles (ROVs, 1990).[8, 24] These relatively recent advancements have led to the discovery and isolation of thousands of unique bioactive marine natural products, some of which are currently on the pharmaceutical market and others in some stage of the pharmaceutical pipeline. Examples include the peptide ziconotide (Prialt®, Elan Corporation),[25] an intrathecally administered compound approved for the treatment of pain in 2004 and first isolated and discovered from the venom of the fish-eating marine snail *Conus magus*. Plitidepsin (Aplidin®, PharmaMar)[26] is a cyclic depsipeptide isolated from the marine tunicate *Aplidium albicans*, found off the isle of Es Vedrà in the Balearic Sea. This compound has proved to be effective against a variety of cancers, including melanoma, bladder, small cell and non-small cell lung cancer as well as non-Hodgkin lymphoma and acute lymphoblastic leukaemia. Trabectedin (Yondelis™, PharmaMar)[19] was also isolated from an ascidian, the species *Ecteinascidia turbinata* which inhabits the shallow waters of reefs, pilings and submerged roots. This species of marine tunicate is commonly found in the Caribbean Sea and Gulf of Mexico, but also in some parts of the Mediterranean Sea. The compound trabectedin became the first marine sourced anticancer drug to be approved by the European Union and is currently used in the treatment of advanced soft tissue sarcoma and relapsed ovarian cancer.

Marine sponges are sessile soft-bodied organisms that lack a nervous, digestive and circulatory system that obtain required nutrients from particles within the surrounding seawater.[27–29] The stationary nature of marine sponges limits any physical means of defence, however given their longstanding survival and largely unchanged nature over the last 500 million years this has not proved to be detrimental. The primary mode of defence for these organisms appears to be chemical, and with more than 8,000 known species of marine sponges existing throughout a variety of environments around the world their secondary metabolites too, exhibit diversity and unique properties. This includes an array of medically applicable properties such as cytotoxic, antimicrobial, antiparasitic, antiviral, antioxidant, antiallergic and anti-inflammatory.[30] An important observation to make with marine sponges is the symbiotic relationships that they form with marine-based microorganisms such as bacteria

and fungi which, in many cases have been the organisms responsible for the compounds isolated from marine sponges. Cytarabine (cytosine arabinoside, or Ara-C)[31] is an antimetabolic chemotherapy drug currently available and used in the treatment of acute leukaemia's and some lymphomas. This compound traces its origin back to the 1950s, when pharmaceutical interest in marine sponges emerged. The two nucleosides spongothymidine and spongouridine were discovered and isolated from the Caribbean marine sponge *Cryptotethia crypta*, where they served as a foundation for the synthesis of cytosine arabinoside (Ara-C), as well as Vidarabine (Ara-A), an antiviral drug active against herpes simplex and varicella zoster viruses. Cytarabine was the first marine-derived anticancer agent, and its application as a chemotherapy medication was extended through one of its fluorinated derivatives that has approved use in patients with breast, bladder, pancreatic and lung cancer.[31]

Marine algae are comprised of a diverse and widespread set of organisms that can be mostly classified into two main groups, microalgae and macroalgae. Marine algae have been recognised to produce an array of novel and diverse chemical compounds as they are heavily embedded within marine ecosystems.[32] In a number of cases microalgae has been found to be responsible for the production of natural products that were initially believed to originate from another organism, due to their ability to form symbiotic relationships with other marine life. For example, Dolastatins are a group of cyclic peptides that have been isolated from sea slugs, initially the species *Dolabella Auricularia*.[32] There has been significant doubt cast as to whether these compounds are actually the secondary metabolites of sea slugs, or symbiotic organisms such as microalgae and bacteria. Natural products derived from marine algae have found promising applications in the treatment of inflammatory disease, most notably the pseudopterosin family of chemical compounds.[33] The development of anti-inflammatory medications has grown alongside the biological understanding of inflammatory response, however many of these synthetic and combinatorial compounds cause adverse long-term effects with prolonged use, such as gastrointestinal bleeding, myocardial infarction and stroke.[34] Current medicinal research into the secondary metabolites of marine algae hopes to uncover new anti-inflammatory agents that have reduced side effects yet retain a high potency for effective treatment.

The ocean largely remains an untapped frontier, despite covering over 70% of the Earth's surface. It is said that more than 80% of the ocean has never been mapped or explored, which to put into perspective means humanity is more knowledgeable about the surfaces of the Moon

and Mars than Earth's oceans.[35, 36] As mentioned, the technological advancements of SCUBA and submersibles have been hugely significant in giving way for the emerging study of marine-derived natural products, but on the grand scale of complete ocean exploration these advances are relatively small. Many parts of the ocean remain physically impossible, or at least extremely difficult, to explore and study mostly because of the extreme pressures experienced beyond specific depths.

The Mariana Trench is reported to be the deepest trench on Earth and houses the two lowest recorded points on the planet, both the Challenger Deep with a depth of approximately 36,000 feet (~10,970 meters) and the Sirena Deep, with a depth of around 35,460 feet (~10,800 meters).[37] If the base of Mountain Everest was situated at the deepest point of the Mariana Trench the summit would not even pierce the ocean's surface, with Mount Everest's height standing at roughly 29,000 feet (~8,830 meters). The environment within and surrounding the trench is unique and notably hostile, and despite pressures approximately 1,000 times greater than that at sea level there has been evidence of life within this region.

In general around 226,000 species of ocean life are currently known to scientists, which is believed to make up less than 10% of all ocean life.[35, 36] The extremity and unique conditions of such environments is of great interest to natural product researchers, specifically with regards to the organisms that may live there and how they have adapted to survive in such difficult conditions. These places are likely an untapped resource of novel and diverse compounds that could possess highly valued medicinal properties, among other applications.

1.4 Non-Medicinal Applications of Natural Products

The golden era in natural product research and discovery took place primarily between the 1960s and 1980s, when pharmaceutical companies were motivated to uncover more naturally occurring compounds after the successful introduction of antibiotics from the discovery of penicillin, a secondary metabolite originally obtained from the *Penicillium* moulds *Penicillium Chrysogenum* and *Penicillium Rubens*.[1, 3, 8] In the years since then natural products have been prominent across many pharmaceutical markets, from antibacterials and antivirals, to anti-inflammatories and chemotherapies.[38] The diverse nature and bioactivity of natural products opens them up to an array of possible applications, a notable sector being agriculture.[39] In the last 50 years agricultural productivity has grown significantly as a result of chemical crop treatments, which allow for the control and regulation of pests. The market of such products is primarily comprised of synthetic compounds, known as synthetic chemical

pesticides. Investigations into new pesticides has been a paramount endeavour, as recent studies have shown that the resistance towards synthetic chemical pesticides from insects and mites increased by 13% between 1984 and 1990.[39, 40] Studies on the secondary metabolites of marine algae appear to be uncovering the potential of new natural product pesticides, specifically for those compounds that are related to terpenes. The Chilean red marine alga *Plocamium cartilagineum* has been found to produce compounds that demonstrate insecticidal activity against the Aster leafhopper (*Macrosteles fascifrons*).[41] This insect is one of the primary causes of aster yellow disease in crops, through the transfer of aster yellows phytoplasma when feeding on the host plant. This can have a significant economic impact on agricultural businesses, with common crop losses of 10-25% and occasionally as high as 80-90%.[42] Laurepinnacin, isolated from the red alga *Laurencia pinnata Yamada*, has demonstrated insecticidal activity against the *Culex pipiens* mosquito larva.[43] The soil dwelling bacterium's *Saccharopolyspora spinose* and *Streptomyces avermitilis* are known to produce spinosyn and avermectin, respectively.[44] These two compounds present pesticidal properties through their ability to paralyse insects via the hyperexcitation of their nervous system. The pharmaceutical and biotechnology giant Bayer AG has commercialised the use of the compound phosphinothricin (glufosinate, tradename Finale®), a herbicide produced by *Streptomyces* that causes a fatal build-up of ammonia in plants through the inhibition of the glutamine synthetase enzyme. Fenpicoxamid is a semi-synthetic derivative of a naturally occurring compound also produced by the *Streptomyces* bacteria that has commercial use as a fungicide, through the inhibition of cellular respiration. Combined these two naturally derived compounds account for $1 Billion in sales annually.[45] There are many more natural products with documented properties applicable to the agricultural and agrochemical sector, however the commercial introduction and adoption of such compounds over synthetic competitors can be largely hindered by economic factors, such as high production costs.[46] Increased resistance among insects to pest control agents is not the only concern with current products on the agrochemical market. Recent articles have discussed the adverse implications that come with extensive use of synthetic pesticides, such as the toxic collateral impact on other non-target organisms that reside within the soil.[47] This can unbalance the ecosystem within the soil, essentially depleting it of essential nutrients and organic content. Metabolic products of synthetic pesticides that are formed in the soil may be poorly understood, and thus accumulation of these derivatives, as well as accumulation of the original pesticidal compounds through overuse could be highly toxic and cause harm to other forms of life.[48]

For human health this could be detrimental, as these compounds can easily find their way into the global food supply in undocumented, accumulated quantities.

1.5 Challenges and Limitations of Natural Product Research

Natural products have played a significant role in drug discovery and the development of novel therapeutics, treating a variety of ailments and disease from infections to cancer. The research and discovery of such naturally occurring compounds received significant attention in the last quarter of the 20th century, however by the mid to the end of the 1990's many of the large pharmaceutical companies that were driving this research either reduced or closed their natural product research programmes.[8] This was largely influenced by economic factors, as such natural product-based research programmes proved to be expensive and time consuming to operate, for several reasons. Firstly, the yield of single compounds obtained from an organism can be incredibly low, with fortunate quantities being above 5mg.[49, 50] This can raise many limitations for future analytical experiments, particularly those that are heavily dependent on concentration such as NMR and biological assays. This problem could be subsided by the cultivation of the organism in-house, however cultivation of organisms outside of their natural habitat can prove either difficult or impossible.[51, 52] In cases where cultivation of the organism is possible the problem may still exist, as production of specific secondary metabolites can be heavily dependent on the surrounding environment, meaning a reduction or complete loss of production for the desired compound.[51] Environmental policies may place restrictions on the amount of an organism that can be collected, particularly in protected areas of environmental conservation such as ocean reef systems and in organism's native to a particular region, such as certain plants. The characterisation and structural elucidation process for natural products can be notoriously time consuming and difficult, generally requiring specialised knowledge and a sufficient quantity of the single desired compound to be achieved effectively.[53] This process runs the risk of spending time identifying compounds that are already known, which for the sake of efficiency need to be identified and discarded from the investigation at the earliest possible stage. This places significant pressure on establishing effective dereplication techniques, that is analytical processes that allow for the prompt identification of known compounds, which may or may not be so effective.[51] Finally, advances in computer technology such as robotics, automated processes and software have opened up the possibility of high-throughput screening (HTS) to pharmaceutical companies. This involves the rapid and reproducible testing of thousands of compounds for biological activity at various levels, including cellular and molecular.[54] Each

of these tests are carried out by automated robots in single wells on a well plate, with multiple well plates held, and with each plate possibly consisting of more than 3000 wells. One report documented the testing of more than 150,000 compounds within 8 hours.[55, 56] High-throughput screening relies on a source of chemical compounds to be tested, which is known as a screening library. These screening libraries are commercially available, with chemical manufacturing companies such as ThermoFisher offering libraries with over 51,000 synthetic organic compounds.[57] Unfortunately the industrial adoption of high-throughput screening also played a role in drawing attention away from natural products within the pharmaceutical sector, as screening libraries for natural products do not typically exist. This is likely due to how difficult and laborious the process would be to create an extensive screening library comprised of thousands of compounds with diverse bioactive properties, a requirement for HTS to be effective. The synthesis of many natural products has proved to be difficult, with commercial scale production of such compounds regarded completely unfeasible.

1.6 Chemical Extraction Techniques for Natural Products

Extraction is usually the first point of call in a natural products investigation, a process where compounds are initially isolated from their source. The extraction approach can vary depending on a number of factors, such as the overall goals of the investigation, the state of the original sample and environmental and cost considerations. Solid-liquid extraction techniques are commonly used for the extraction of natural products from their raw source, such as plant or fungal matter. An array of solid-liquid extraction techniques exist, such as maceration, percolation, reflux extraction and Soxhlet extraction, to name a few.[58] Maceration is one of the simplest solid-liquid extraction techniques, where the solid sample matter is ground and soaked in a particularly selected solvent. The solvent diffuses into the solid matrix of the raw material, where compounds of similar miscibility to the chosen solvent dissolve. The change in concentration gradient causes this solvent to diffuse out of the matrix along with the relevant compounds, where they can then be collected.[50, 59] Whilst simple to perform relative to other techniques there are drawbacks to this method, particularly low efficiency and poor extraction yield. Percolation is a technique that builds upon maceration, where instead fresh solvent is continuously supplied to the ground sample matter and simultaneously filtered through a filtration medium and collected. This has improved efficiency over the standard maceration method, but typically requires more solvent which can be costly, both financially and environmentally.[50, 59] Reflux extraction significantly improves efficiency in comparison to both standard maceration and percolation methods, with

reduced extraction time because of the use of hot solvent that is continuously added back into the extraction vessel upon condensation.[50, 59] Soxhlet extraction works in a similar fashion to a typical reflux extraction, but with a slightly different configuration of apparatus that automates the siphoning for process for the collection of solvent extract. Again this improves efficiency through reduced extraction time compared to maceration and percolation.[50, 59] A significant disadvantage of reflux and Soxhlet extraction is the use of heat, which prohibits the extraction of thermolabile compounds. This can be a significant issue that rules out the use of these extraction techniques in an investigation despite their efficiency advantages, as compounds of interest, particularly those with potential bioactive properties, cannot be obtained due to their thermolability. Crude extracts such as those obtained from solid-liquid extractions can be subject to further partitioning through liquid-liquid extraction, the Kupchan scheme being a prevalent example within the natural products field.[60] This process involves adding two immiscible solvents to the crude extract in a separating funnel, for example those of opposite polarity such as hexane and water. These two solvents are collected separately (fractionated) from the separating funnel, with the higher density solvent first followed by the less dense solvent.[60] Following this solvents of varying polarity are subsequently added to one of the collections, such as chloroform to the water fraction. This process is repeated with varying solvents until several fractions are obtained, each falling within a different region of the polarity scale. This allows for the natural products of the crude extract to be further separated into fractions based on their polarity, which can be then used in preliminary assays to quickly identify which fraction possesses active compounds. Typically this region of active compounds lies somewhere directly between polar and non-polar.

1.7 Aims of Research

The aims of this research project were to successfully isolate and identify compounds from an extract of a marine tunicate of the Great Barrier Reef. Following this any compounds successfully isolated and identified were to be evaluated in an enzyme kinetics assay for active inhibition against chitinase of the bacteria *Streptomyces griseus*.

Chapter 2

2.1 Introduction

2.1.1 Chitin, Chitinase and the Significance of Chitinase Inhibitors

Chitin is a linear polymer consisting of repeating β (1,4)-*N*-acetylglucosamine units.[61] It is the second most abundant natural polysaccharide on the planet after cellulose, and predominantly functions as both an internal and external structural component in various organisms, including arthropods (such as crab and shrimp) and insects, and is additionally utilised in fungi and some bacteria.[61, 62] Chitinases refer to enzymes that possess the ability to degrade chitin.[63] These enzymes play a crucial role in the very organisms that utilise chitin as a structural component, as strict enzymatic control of the synthesis and degradation of chitin is required to maintain homeostasis.[61, 63, 64] Bacteria typically use chitinase for the degradation of chitin which can in turn be utilised as a source of energy.[65] This is a notable observation of marine dwelling bacteria like those of the genus *Vibrio*, who solely live on chitin due to its abundance in marine ecosystems. Chitin is present in the cell wall of fungi and thus acts as a structural component, where fungal chitinases then play a regulatory role for the growth and development of the fungal organism. In mycoparasitic fungi such as *Trichoderma* the chitinase enzymes have demonstrated two-fold degradation of chitin in both self and non-self-cell walls.[64, 66] This is achieved by selectively restricting the access of chitinase to the chitin within the self-cell wall by cell surface receptor proteins. Chitinases themselves are of increasing importance with respect to their biotechnological applications, as for example they can be used in agriculture as a biocontrol agent to manage fungal pathogens and insects that have an adverse impact on crops.[61, 63] They can be used in the processing of biological waste such as the chitinous biomass of marine organisms, where degraded chitooligomer products can then go on to be applied in various food and chemical industries. Chitin has not been found to be synthesised by mammals, yet of all mammals studied (including humans) they do appear to encode chitinases. One prominent chitinase enzyme expressed in humans is the acidic mammalian chitinase, known as AMCase.[67] Whilst the physiological function and endogenous substrates for AMCase remain unknown expression of this enzyme appears to be increased in human asthma patients and has also been induced in mice in an aeroallergen asthma model.[67, 68] Chitin is a structural component in the exoskeleton of house dust mites (HDM), which as an inhaled allergen directly correlates with cases of asthma and thus could explain the increased expression for the chitolytic AMCase

enzyme. In the mouse asthma model inhibition of AMCase appeared to reduce inflammation and hyperresponsiveness of the airway. There is significant potential that chitinase inhibiting compounds could be utilised in the treatment of asthma as an anti-inflammatory, as well as therapeutic applications in other related diseases.[67, 68]

2.1.2 Makaluvamines

Makaluvamines (**Figure 2.5.54**) are a family of compounds belonging to the class of pyrroloiminoquinone alkaloids, alongside other families such as discorhabdins, epinardins, batzellines and veiutamine. These compounds have been notably isolated from marine sources, particularly marine sponges of the genera *Latrunculia, Batzella, Prianos* and *Zyzzya*.[28, 49] A characteristic feature of all Makaluvamines is the tricyclic pyrroloiminoquinone core, which holds potentially potent bioactive properties that make this family of compounds attractive targets for organic synthesis and drug discovery. One study investigated 14 analogues of Makaluvamines (**Figure 2.5.55**) for antibacterial activity against *Streptococcus mutans* and inhibition of *Streptococcus mutans* biofilm formation.[69] A biofilm is a collection of surface-attached microbial cells, such as bacteria, that are enclosed in an extracellular polymeric substance matrix, for example that of polysaccharides.[70] The ability that some bacteria have in forming biofilms is largely beneficial, as the biofilm can offer increased resistance to the immune response of the host, antibiotics and biocides.[69] *Streptococcus mutans* is largely associated with tooth decay, and the ability of this bacteria to form biofilms is attributed as a major factor in causing this disease. The study found that all 14 Makaluvamine analogues displayed biofilm inhibition, with IC_{50} values ranging from 0.4 μM to 88 μM. The observed bactericidal activity for most of the analogues coincided with the anti-biofilm activity, leading to the conclusion that the biofilm inhibition was achieved by the makaluvamine analogues' ability to kill *Streptococcus mutans*. Makaluvamines have also demonstrated considerable cytotoxic activity,[71, 72] opening them up to potential therapeutic applications in the future for the treatment of diseases such as cancer. Makaluvamines, alongside fellow marine derived alkaloids, have faced many limitations that have withheld their potential medicinal applications, despite their notably potent bioactivity. The yield obtained from the natural source for these compounds is typically low, which limits the experimental research that can be carried out on them. In addition synthetic methods for the production of these compounds and their analogues have proved difficult to establish at a scale feasible for commercial production.[49, 71]

2.2 Experimental

2.2.1 Ascidian Tunicate Sample Collection

The marine tunicate sample from which the extracts in this investigation were derived was collected from Davies Reef, a mid-region of the Great Barrier Reef in Australia. This task was carried in out August 2006 by a free diving expedition over the course of a four-day diving period, where a total of 13 marine organism samples were collected across two reef regions. Each sample was allocated an identification code, and some biological experiments were carried out to taxonomically identify each species that was obtained. Extracts of 9 of the 13 collected marine samples were sent to the University of Central Lancashire for natural product related research. Extracts of DAV-09 were the focal sample in this investigation, which was specifically obtained from a coral habitat in site GBR DAV-3A (coordinates: S: 18.49.943; E: 147.37.163) of Davies Reef, at a depth of 7.2 m. Though not yet completely confirmed it is believed that the ascidian tunicate sample DAV-09 is that of *Polysyncraton pedunculatum*, a tunicate of the *Didemnidae* family.

2.2.2 Preliminary Chitinase Inhibition Assay of Original Extracts

The preceding investigation to that of this thesis looked for inhibitive activity against chitinase amongst the nine extracts received from Australia. This began with a preliminary chitinase inhibition bioassay that was performed on each of the nine crude extracts using a chitinase enzyme produced by the bacteria *Streptomyces griseus*, and a synthetic compound structurally analogous to that of chitin labelled as 4-nitrophenyl *N*, *N*'-diacetyl-β-d-chitobioside (>99%) (**Figure 2.5.53**). The preliminary bioassay found that 5 of the 9 original extracts demonstrated inhibitive activity against the chitinase enzyme of *Streptomyces griseus*. A solid phase extraction consisting of three subsequent solvent washes (25, 50 and 100% methanol) was performed on each of the 5 active extracts, resulting in a total of 15 solid phase extracted fractions. Included within this were the three solid phase extracted fractions of DAV-09.

2.2.3 HPLC Compound Isolation from DAV-09-SPE Fraction

The investigation outlined in this thesis began with the method development for compound isolation from the DAV-09 solid phase extracted fractions, using an Agilent Technologies 1220 Infinity HPLC instrument. This was largely a trial and process of varying solvent systems, gradient methods and HPLC columns. The first method tested involved a Phenomenex® Luna 5 µm C8(2) 100 Å 250 mm × 10 mm HPLC column, and an isocratic methanol (80%) water

(20%) solvent system. The flow rate was set to 2 mL/min and the column oven was kept inactive. The diode array detector was configured for a spectrum range of 190 nm to 400 nm, with specific signals set at various wavelengths; 230, 254, 270, 290, 300, 350 and 400 nm, with a bandwidth of 20 nm. Chromatogram observation was set to the wavelength of 254 nm. Over several 3.50 µL sample injection runs varying adjustments were made, such as the flow rate reduction to 1.0 mL/min and the change of solvent ratios from methanol-water (80:20) to 90:10 and then 75:25. A gradient method was also tested over a 20 minute period, starting with no methanol that ramped up to 10% over the course of the first 5 minutes, then up to 100% over the next 5 minutes where it remained for the foreseeable run. Both trifluoroacetic acid (TFA) and ammonia (NH_3) were added to the water (to give 0.05% TFA/NH_3) in separate runs to test how acidity and basicity of the solvent system would affect the quality of the chromatogram. Ultimately no changes made with this column provided a well resolved chromatogram for compound isolation. This was the same outcome for the following HPLC columns; Phenomenex® Luna 5 µm C18(2) 100 Å 250 mm × 10 mm, and the X Select CSH 130 C18 5 µm 250 mm × 10 mm. For each of these column trial sets varying adjustments were again made to solvent ratios and gradient/isocratic methods. At one stage methanol was swapped out for acetonitrile, however this change was quickly reverted as it negatively impacted the chromatogram. The configuration for the diode array detector remained the same as at the start of the method development, as was the column oven (inactive) and injection volume (3.50 µL).

The fourth column trialled was an ACE 5 C18 V17-1586. The first test began with a reduced sample injection volume of 2.50 µL and a gradient solvent system of methanol-water starting at 50:50 for the first 3 minutes, ramped to 60:40 over the following 3 minutes and finally increased to 70:30 over the next 3 minutes where it remained for the foreseeable run. This provided a much more clearly resolved chromatogram than had been seen previously with the other columns. Trifluoroacetic acid was reintroduced into the solvent system (at 0.05% TFA in the water solvent) to check whether slight acidity would further improve the resolution of the chromatogram with this column. This solvent system was isocratic (methanol-water (0.05% TFA), 75:25), and the TFA did appear to improve the resolution of the peaks in the chromatogram. After a few further adjustments the initial HPLC method deemed ideal for compound isolation was an isocratic 50:50 methanol-water (with 0.05% TFA) solvent system, at a flow rate of 1 mL/min. The water solvent containing TFA had a pH of approximately 3.0, which was tested using litmus paper. All other configurations for the diode array detector and

column oven remained unchanged from the beginning of the method development. From this point the sample injection volume was gradually increased from 2.50 µL to improve the time efficiency for isolating compounds from the DAV-09 solid phase extracted fractions. Close attention was paid to the quality of the chromatogram as the injection volume was increased, as to be cautious not to push the volume too high and overload the instrument. The maximum sample injection volume used for peak collection was 30.0 µL, as values greater than this would start to distort the chromatogram. The final HPLC method used for peak collection at 30.0 µL sample injections was a gradient solvent system (with instant ratio changes) of methanol-water (0.05% TFA), starting at 40:60 for the first 10 minutes, then switched to 50:50 for the following 15 minutes and finally back to 40:60 for the remainder of the run. Total runtime was approximately 35 minutes. In total 6 compounds were isolated from the solid phase extracted DAV-09-25% and DAV-09-50% methanol fractions, with each sample appearing to contain the same 6 compounds based on identical chromatograms and ultraviolet profiles. Prior to the transfer of each sample into a crimp vial for HPLC they were centrifuged in an Eppendorf vial for approximately 5 minutes. The chromatogram was observed at a wavelength of 254 nm during peak collection, with each peak being collected in individual 50 mL plastic centrifuge tubes that were labelled accordingly.

2.2.4 Drying of HPLC Isolated Samples by Rotary Evaporation

Once the two DAV-09 solid phase extracted fractions had been processed through HPLC they were dried using an IKA rotary evaporator (model RV 10D S93) that was configured to an RPM of 210, and a water bath temperature of 40˚C. It was imperative that the water bath temperature did not exceed this as not to adversely affect the structural characteristics of the isolated compounds, should they have been thermolabile for example. Matching peaks from both the DAV-09-25% and DAV-09-50% methanol solid phase extracted fractions were combined and dried as one. After each peak had been sufficiently dried by the rotary evaporator a small amount of methanol solvent was added to allow for the transfer of each isolated sample into individual, pre-weighed glass specimen vials. These specimen vials were subsequently dried under nitrogen gas in a fume hood, before being weighed.

2.2.5 Sample Preparation for NMR on an 800 MHz Instrument

A challenge faced with natural product analysis is the typically small quantity of compound that is obtained, which can place limitations on concentration dependant analytical techniques such as NMR. For this NMR sample preparation 3 mm NMR tubes were used as opposed to

the standard 5 mm NMR tubes, which allowed for a smaller volume of deuterated methanol solvent (175 μL) to be added to each of the HPLC isolated samples. These samples were in turn (H2 through H6) transferred to individual 3 mm NMR tubes. The 3 mm NMR tubes were then inserted into 5 mm NMR tubes, ensuring that the inner 3 mm NMR tubes' movement was restricted by adding a small amount of cotton wool into the top of the tube and tube-cap. This method achieved a higher sample concentration whilst maintaining probe compatibility and sample visibility and to the NMR instrument. These samples were temporarily stored in the refrigerator prior to four of them (H2-H5) being sent to the University of Edinburgh, where 1-dimensional proton (^{1}H) and 2-dimensional COSY (^{1}H-^{1}H), HSQC (^{1}H-^{13}C) and HMBC (^{1}H-^{13}C) NMR were performed using a Bruker 800 MHz UltraStabilised spectrometer.

2.2.6 Preliminary Mass Spectrometry Analysis

A preliminary mass spectrometry experiment was performed on the HPLC isolated samples using a high-resolution Agilent 6546 Quadrupole Time-of-Flight (Q-TOF) mass spectrometer.

2.2.7 Further Purification of HPLC Isolated Samples

Further purification work was carried out on both HPLC isolated samples H3 and H5 by size exclusion chromatography using Sephadex® LH-20 gel. This was prepared by adding methanol to the powdered Sephadex® LH-20 material to form a slurry, where a small amount was then transferred (~5-10 cm^3) to a suitable glass separating column with an equal amount of methanol and left to swell. This was left to swell as other lab work was carried out for probably at least 30 minutes. A solvent system comprised of methanol (13 mL), chloroform (7.0 mL) and distilled water (8.0 mL) was prepared and added to each of the HPLC samples, where they were in turn purified through the size exclusion column. The flow rate was maintained at approximately 1 droplet per second, which was adjusted accordingly using the valve of the separating column. Multiple washes of the solvent system were applied when necessary, and the experiment ended once the HPLC isolated samples had cleared the column. This was monitored visually as the samples were red in colour. Throughout the size exclusion experiment collections of approximately 0.5 to 1.0 mL were continuously made into plastic sample tubes until the sample had completely passed through the column. For H3 this yielded eight Sephadex® fractions, and for H5 a total of six Sephadex® fractions were obtained.

At a later stage further purification was carried out using the same Sephadex® LH-20 exclusion medium and solvent system (7.0 mL methanol, 13 mL chloroform and 8.0 mL of

distilled water), though with the addition of 15 µL of trifluoroacetic acid (TFA). The first three Sephadex® fractions of the H3 sample from the previous size exclusion experiment were combined and repurified in this second purification. The flow rate was again adjusted to approximately 1 droplet per second and collections of around 0.5 mL were made in individual plastic sample tubes throughout the experiment until the sample had completely cleared the column. This yielded a total of ten Sephadex® fractions.

2.2.8 Sample Preparation of Sephadex® Fractions for NMR

The initial NMR experiment for the Sephadex® fractions was performed on the eight fractions of H3 and the six fractions obtained from H5, using a Bruker UltraShield 400 MHz. The sample preparation method followed that for the first NMR experiment that was conducted at the University of Edinburgh, with the sample dissolved in around 175 µL of deuterated methanol and transferred into a 3 mm NMR tube. This tube was then inserted and secured in a 5 mm NMR tube using a small amount of cotton wool. The NMR instrument was configured to run a single 1-dimensional proton (^{1}H) experiment for each of the fractions, where wavescans were set to 64 and rotation to 20 Hz. The same NMR experiment was also performed on three samples from an external study, labelled as Makaluvamines A, C and P.

The first three Sephadex® fractions of the H3 sample were recovered from their respective NMR tubes and combined as one sample. This sample would then go on to be repurified to yield ten new Sephadex® fractions. Proton NMR (^{1}H) was performed on all ten of these fractions following the same preparation method and instrument configuration.

2.2.9 HRMS Preparation of Makaluvamine and Sephadex® Samples

A total of six samples were prepared for HRMS, these were Makaluvamine A, Makaluvamine C, Makaluvamine P, H3 Sephadex® fraction 4 and H3 Sephadex® fraction 5.

Fractions 5, 6 and 7 of the ten fractions obtained from the repurification of H3 fractions 1, 2 and 3 were combined as one sample (**Figure 2.5.56**) (referred to as the repurified H3 Sephadex® fraction), which was the sixth sample used in the HRMS experiment. 100 µL of each sample was transferred (using methanol solvent) from their original sample vial into clean, pre-weighed glass vials. These were subsequently dried to give initial masses of; 0.2 mg (for Makaluvamine A, C and P), 0.5 mg (H3 Sephadex® fraction 4), 0.6 mg (H3 Sephadex® fraction 5) and 1.0 mg (for the repurified H3 Sephadex® fraction). 1.0 mL of LCMS grade methanol was added to each sample and used as a solvent to transfer the samples

into crimp vials. 100 µL of Makaluvamine A, C and P was transferred into individual crimp vials, where they were made up to 1.0 mL to give a new concentration of 0.02 mg/mL. 50 µL of H3 Sephadex® fraction 4 was transferred and up to 1 mL in the crimp vial to give a concentration of 0.025 mg/mL. 25 µL of H3 Sephadex® fraction 5 was transferred and made up to 1 mL for a concentration of 0.015 mg/mL. And finally 10 µL of the repurified H3 Sephadex® fraction was transferred and made up to 1.0 mL for a resulting concentration of 0.01 mg/mL.

2.2.10 Enzyme Kinetics Assay of Chitinase Inhibition

2.2.10.1 Phosphate Buffer Preparation

The chitinase inhibition assay began with the preparation of a phosphate buffer. For this the compounds sodium phosphate monobasic dihydrate ($NaH_2PO_4.2H_2O$, molecular mass of 156.01 $gmol^{-1}$) and sodium phosphate dibasic dodecahydrate ($Na_2HPO_4.12H_2O$, molecular mass of 358.14 $gmol^{-1}$) were used. The target molarity for the total phosphate buffer solution was 0.05 M, and so 0.025 mol of each phosphate compound was required. Based on the volume preparation for each compound this equated to 3.90025 g of the monobasic dihydrate and 8.95350 g of the dibasic dodecahydrate. Actual masses obtained in the lab were 3.90030 g and 8.95325 g, respectively. Each of the weighed-out compounds were transferred to separate 500 mL volumetric flasks, where they were each made up to the 500 mL mark with distilled water. After sufficient mixing both these solutions were transferred to a 1.0 L volumetric flask, mixed further and transferred to a large screwcap glass bottle which was then stored in the refrigerator. Before being used in the kinetics assay the pH of the phosphate buffer solution was adjusted to 6 (6.08) using phosphoric acid and a digital pH meter.

2.2.10.2 Sample Solvent Preparation

Absolute ethanol (99%) was diluted with distilled water to give an ethanol solution of 75%. This was used as a solvent for the potentially active compounds investigated in the assay.

2.2.10.3 Sample Preparation

The approximate quantities of compound available for each sample to be used in the assay were as follows; Makaluvamine A (0.5 mg), Makaluvamine C (23.5 mg), Makaluvamine P (6.2 mg), H3 Sephadex® fraction 4 (0.5 mg), H3 Sephadex® fraction 5 (0.6 mg) and repurified H3 Sephadex® fraction (1.0 mg). Varying volumes of the 75% ethanol-water were added to the following samples to give concentrations of; 200 µL to Makaluvamine A (2.5

mg/mL), 1.0 mL to Makaluvamine C (23.5 mg/mL), 300 µL to Makaluvamine P (20.7 mg/mL) and 200 µL to repurified H3 Sephadex® fraction (5.0 mg/mL).

2.2.10.4 Substrate Preparation

The substrate used in this enzyme kinetics assay was 4-nitrophenyl *N*, *N*'-diacetyl-β-D-chitobioside (≥99%) (**Figure 2.5.53**), as it is structurally analogous to chitin. The entirety of the vial which contained 5.0 mg of the compound was transferred to a plastic 50 mL centrifuge tube. To this 22.5 mL of the prepared phosphate buffer solution was added, resulting in a substrate concentration of ~0.2 mg/mL. This total substrate solution was kept heated in a water bath at 25˚C throughout the duration of the assay.

2.2.10.5 Enzyme Preparation

For this assay chitinase enzymes originating from the bacteria *Streptomyces griseus* and the fungal species *Trichoderma* were used. The masses for each enzyme that were weighed-out were 2.0 mg and 0.4 mg, respectively. A proportionate volume of distilled water was added to each enzyme to provide a resulting concentration of 1.0 mg/mL (2.0 mL added to the former, 0.4 mL added to the latter). The enzyme was stored in an ice bath throughout the experiment.

2.2.10.6 Enzyme Kinetics Procedure

The instrument used to perform this enzyme kinetics assay was a Shimadzu UV-3600 UV-VIS-NIR Spectrophotometer, set to the default method configuration for enzyme kinetics. 1.0 mL of phosphate buffer solution was added to a clean cuvette and used as a reference throughout the duration of the assays. The duration of each kinetics assay was set to 90 seconds. The assay began with the preparation of a control that consisted of 900 µL of substrate solution, 50 µL of enzyme solution (*Streptomyces griseus*) and 50 µL of ethanol-water (75%). Satisfied with the results of the control the assay for each Makaluvamine sample was performed, following the same format as the control (50 µL of sample solution as opposed to sole ethanol) at the initial concentrations at which each sample was prepared. From here the concentration of each sample was subsequently diluted by 50% to monitor the affects of dilution on activity. This began with the repurified H3 Sephadex® fraction (diluted to 2.5 mg/mL) and subsequently followed by Makaluvamine A (diluted to 1.25 mg/mL), Makaluvamine P (diluted to 10.35 mg/mL, followed by a second dilution to 5.18 mg/mL) and Makaluvamine C (diluted to 11.75 mg/mL). Following this set of assays the same procedure was carried out using the chitinase enzyme from *Trichoderma*, though this was only

comprised of a control, Makaluvamine C (11.75 mg/mL) and both the original and diluted (2.5 mg/mL) repurified H3 Sephadex® fractions.

2.3 Results and Discussion

2.3.1 Structural Elucidation of Makaluvamine H from DAV-09-H3

The structural characterisation of Makaluvamine H was achieved through the combined interpretation of 1-dimensional proton (^{1}H) (**Figure 2.5.2**) and 2-dimensional COSY (^{1}H-^{1}H) (**Figure 2.5.3**), HSQC (^{1}H-^{13}C) (**Figure 2.5.4**) and HMBC (^{1}H-^{13}C) (**Figure 2.5.5**) NMR, alongside HR-ESIMS and MS/MS data. Computer aided structural elucidation techniques also provided valuable supplementary insight into the structure elucidation process, in addition to the use of chemical databases.

The analysis began with the interpretation of the preliminary high-resolution mass spectrometry data of the HPLC isolated DAV-09-H3 sample using ACD Labs software package (**Figure 2.5.21**). Six peak regions of notable interest were identified from the chromatogram of the LC-HRMS data based on their respective UV-Vis profiles, which were of a similar pattern to the UV-Vis profiles seen during the compound isolation stage with the HPLC. The retention times for each peak region were as follows; peak region one (4.06 min), peak region two (4.09 min), peak region three (4.12 min), peak region four (4.25 min), peak region five (4.29 min) and finally peak region six (4.69 min). Notable *m/z* values measured in ESI+ positive mode amongst the six peak regions were (approximately); 217.099 *m/z* and 216.118 *m/z* (the most prominent m/z peaks seen), 563.060 *m/z*, 493.141 *m/z*, 341.222 *m/z* and 250.075 *m/z*. These *m/z* values were used to generate a possible list of corresponding molecular formula within the ACD Labs software (**Figure 2.5.22**), which were then used as a search aid in chemical databases such as Chemspider, COCONUT, Antibase etc.

NMR data obtained from the experiments performed with the Bruker 800 MHz UltraStabilised spectrometer were used for the structural elucidation of Makaluvamine H. Interpretation of the NMR data began downfield with the assignments of quaternary carbons, identified as such by the cross reference of the 2-dimensional HMBC and HSQC-edited spectrograms. This process continued working meticulously upfield with the assignments of protonated carbons from the HSQC-edited data and their corresponding protons from the 1-dimensional proton NMR data. After relevant carbon (^{13}C) and proton (^{1}H) assignments were made the focus switched to interpretation of 2-dimensional correlation data, COSY (^{1}H-^{1}H)

and HMBC (^{1}H-^{13}C), that were used to pinpoint any relationships between assigned atoms and thus which of them likely formed a single chemical structure. As a result of this the following notable ^{13}C carbon peaks were identified (**Table 2.3.1.1**); quaternary carbon 8 (167.66 δ/ppm), quaternary carbon 5a (156.73 δ/ppm), quaternary carbon 7 (156.62 δ/ppm), protonated carbon 2 (130.43 δ/ppm, CH), quaternary carbon 8b (123.42 δ/ppm), quaternary carbon 8a (123.26 δ/ppm), quaternary carbon 2a (117.74 δ/ppm), protonated carbon 6 (85.43 δ/ppm, CH), protonated carbon 4 (52.75 δ/ppm, CH_2), protonated carbon 10 (38.30 δ/ppm, CH_3), protonated carbon 9 (35.09 δ/ppm, CH_3) and protonated carbon 3 (18.81 δ/ppm, CH_2). ^{1}H proton assignments were made to their corresponding carbon, as identified from the HSQC-edited data; proton 2 (7.11 δ/ppm, singlet), proton 6 (5.77 δ/ppm, singlet), proton 4 (3.94 δ/ppm, triplet), proton 10 (3.40 δ/ppm, singlet), proton 9 (3.96 δ/ppm, singlet) and proton 3 (2.99 δ/ppm, triplet). The following 2-dimensional HMBC correlations were subsequently identified; carbon 3 (proton 4), carbon 4 (protons 3 and 10), carbon 10 (proton 4), carbon 5a (proton 6), carbon 7 (protons 9 and 10), carbon 2a (protons 9, 3 and 6), carbon 8b (protons 6 and 2), carbon 8a (protons 9 and 2), carbon 2 (proton 9) and carbon 8 (protons 2 and 6). Clear 2-dimensional COSY correlations were only seen between protons 4 and 3.

From this analysis a total of twelve carbons and twelve protons were identified, yielding a possible molecular mass of ~156 $gmol^{-1}$, which excluded the likely presence of other atomic species such as oxygen and nitrogen. Nevertheless this was used as a foundation for database searches and molecular formula generation, where additional atomic species were added to the molecular formula to increase the molecular mass to closely match the *m/z* values observed in the HRMS data. Ultimately this yielded a database hit for the compound Makaluvamine H using a combination of Antibase, COCONUT and Chemspider databases for added validity. From Chemspider the molecular formula for Makaluvamine H was listed as $C_{12}H_{14}N_3O^{+}$, with a monoisotopic mass of 216.1131 $gmol^{-1}$. This mass correlated with the intense m/z values seen in the HRMS data. ACD Labs Structure Elucidator Suite was then used to generate carbon-13 NMR chemical shift values for the Makaluvamine H structure, which was then cross referenced with the assigned carbon-13 NMR values for the HPLC isolated DAV-09-H3 sample obtained from the Bruker 800 MHz instrument. The lettered assignments of the NMR data made previously were reassigned to a numbered format corresponding to the molecular structure of Makaluvamine H (**Figure 2.3.1.1**) and the atomic positions within it.

Figure 2.3.1.1: Structure of Makaluvamine H

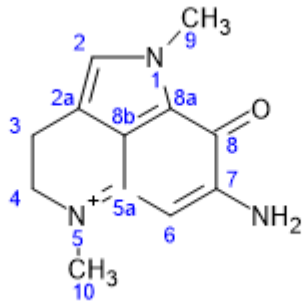

Table 2.3.1.1: NMR Data for Makaluvamine H in CD_3OD-d_4 (800 MHz)

	^{1}H, d, *J* (Hz)	^{13}C, ppm	HMBC	COSY
2	7.11, s	130.43	C-9	
2a		117.74	C-9; C-3; C-6	
3	2.99, t, *7.58*	18.81	C-4	4
4	3.94, t, *7.30*	52.75	C-3; C-10	3
5a		156.73	C-6	
6	5.77, s	85.43		
7		156.62	C-9; C-10	
8		167.66	C-2; C-6	
8a		123.26	C-9; C-2	
8b		123.42	C-6; C-2	
9	3.96, s	35.09		
10	3.40, s	38.30	C-4	

The NMR assignments made for DAV-09-H3 from the Bruker 800 MHz UltraStabilised experiments were used as a reference guide for the further purification of the DAV-09-H3 sample. After each purification of the DAV-09-H3 sample using Sephadex® LH-20 a proton NMR was performed on each of the obtained Sephadex® fractions, using the Bruker 400 MHz UltraShield. The proton NMR data for each fraction was briefly observed to identify the presence of peaks corresponding to Makaluvamine H, as previously assigned, as well as to see if other unrelated peaks had been expelled from successful purification. Of the eight fractions obtained from the first Sephadex® purification fractions 4 (**Figure 2.5.13**) and 5 (**Figure 2.5.14**) appeared to be the most successfully purified, based on the proton NMR data. This influenced the decision to recombine fractions 1, 2 and 3 for a second attempt at purification using the same Sephadex® LH-20 method and approach. Fractions 6 to 8 were not of much significance, as these did not appear to contain the desired Makaluvamine H compound. The second Sephadex® purification yielded a total of ten fractions, all of which were again prepared for proton NMR. From this it was concluded that repurified Sephadex®

fractions 5 (**Figure 2.5.15**), 6 (**Figure 2.5.16**) and 7 (**Figure 2.5.17**) were the most successfully purified. Fractions 5, 6 and 7 were combined to give one sample and this, along with fractions 4 and 5 from the first Sephadex® purification would go on to be used in the enzyme kinetics assay, as they each equated to Makaluvamine H. This was further verified by LC-HRMS using the Agilent 6546 Q-TOF mass spectrometer, where the most prominent *m/z* value for each of these three samples was 216 *m/z* (**Figures 2.5.34, 2.5.36** and **2.5.38**).

2.3.2 Structural Elucidation of Makaluvamine P from DAV-09-H5

The structural elucidation of Makaluvamine P was achieved through the combined interpretation of 1-dimensional proton (^{1}H) (**Figure 2.5.6**) and 2-dimensional COSY (^{1}H-^{1}H) (**Figure 2.5.7**), HSQC (^{1}H-^{13}C) (**Figure 2.5.8**) and HMBC (^{1}H-^{13}C) (**Figure 2.5.9**) NMR, alongside HR-ESIMS and MS/MS data. Computer aided structure elucidation techniques were also applied, alongside the use of chemical databases such as Chemspider and COCONUT which provided valuable guidance in the structure elucidation process.

The analysis began with the interpretation of the preliminary high-resolution mass spectrometry data of the HPLC isolated DAV-09-H5 sample, using ACD Labs software package (**Figure 2.5.23**). One peak of notable interest was identified from the chromatogram of the LC-HRMS data that had a UV-Vis profile which closely matched the pattern seen for the UV-Vis profile during the compound isolation stage with the HPLC. The retention time and most prominent *m/z* value (measured in ESI+ positive mode) for this peak was 5.14 min and 336.171 *m/z*, respectively. This *m/z* value was used to generate a possible list of corresponding molecular formula within the ACD Labs software, which were then used as a search aid in chemical databases such as Chemspider and COCONUT.

NMR data obtained from the experiments performed with the Bruker 800 MHz UltraStabilised spectrometer were used for the structural elucidation of Makaluvamine P. Interpretation of the NMR data began downfield with the assignments of quaternary carbons, identified as such by the cross reference of the 2-dimensional HMBC and HSQC-edited spectrums. This process continued working meticulously upfield with the assignments of protonated carbons from the HSQC-edited data and their corresponding protons from the 1-dimensional proton NMR data. After relevant carbon (^{13}C) and proton (^{1}H) assignments were made the focus switched to interpretation of 2-dimensional correlation data, COSY (^{1}H-^{1}H) and HMBC (^{1}H-^{13}C), that were used to pinpoint any relationships between assigned atoms and thus which of them likely formed a single chemical structure. As a result of this the

following notable ^{13}C carbon peaks were identified (**Table 2.3.2.1**); quaternary carbon 8 (167.15 δ/ppm), quaternary carbon 15 (156.04 δ/ppm), quaternary carbon 7 (155.90 δ/ppm), protonated carbon 2 (130.64 δ/ppm, CH), protonated carbon 17 (129.75 δ/ppm, CH), quaternary carbon 12 (128.90 δ/ppm), quaternary carbon 8b (123.30 δ/ppm), quaternary carbon 8a (122.90 δ/ppm), quaternary carbon 2a (117.69 δ/ppm), protonated carbon 16 (115.16 δ/ppm, CH), protonated carbon 4 (52.70 δ/ppm, CH_2), protonated carbon 10 (45.19 δ/ppm, CH_2), protonated carbon 19 (38.34 δ/ppm, CH_3), protonated carbon 18 (35.09 δ/ppm, CH_3), protonated carbon 11 (33.41 δ/ppm, CH_2) and protonated carbon 3 (18.82 δ/ppm, CH_2). ^{1}H proton assignments were made to their corresponding carbon, as identified from the HSQC-edited data; proton 2 (7.10 δ/ppm, singlet), proton 17 (7.08 δ/ppm, doublet), proton 16 (6.73 δ/ppm, doublet), proton 4 (3.90 δ/ppm, triplet), proton 10 (3.66 δ/ppm, overlapped), proton 19 (3.34 δ/ppm, singlet), proton 18 (3.95 δ/ppm, singlet), proton 11 (2.92 δ/ppm, triplet) and proton 3 (2.97 δ/ppm, triplet). The following 2-dimensional HMBC correlations were subsequently identified; carbon 12 (protons 16 and 10), carbon 15 (proton 16), carbon 4 (protons 15 and 19), carbon 2 (proton 18), carbon 7 (protons 4 and 19) and carbon 2a (protons 4 and 3).

From this analysis a total of sixteen carbons and seventeen hydrogens were identified, yielding a possible molecular mass of ~209 $gmol^{-1}$, which excluded the likely presence of other atomic species such as oxygen and nitrogen. At this stage Makaluvamine H had already been characterised from the NMR and HRMS data of the HPLC isolated DAV-09-H3 sample, and so the first assumption made for this compound was that it could be another member of the Makaluvamine family. Database searches for Makaluvamines with a molecular mass close to the *m/z* value seen in the HRMS data (336.171 *m/z*) quickly returned a match for Makaluvamine P, which as listed on Chemspider has a monoisotopic mass of 336.170654 $gmol^{-1}$. The assigned carbon-13 NMR values for the HPLC isolated DAV-09-H5 sample (obtained from the Bruker 800 MHz instrument) were cross referenced with the assigned NMR data for Makaluvamine P found in literature. The lettered assignments of the NMR data made previously were reassigned to a numbered format corresponding to the molecular structure of Makaluvamine P (**Figure 2.3.2.1**) and the atomic positions within it.

Figure 2.3.2.1: Makaluvamine P

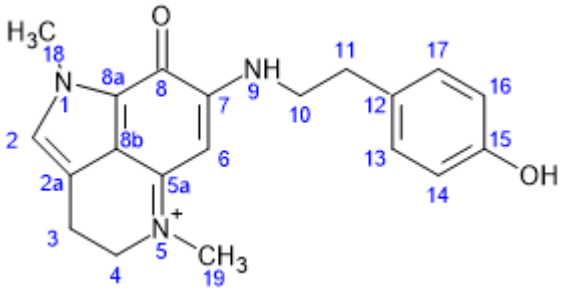

Table 2.3.2.1: NMR Data for Makaluvamine P in CD_3OD-d_4 (800 MHz)

	1H, d, *J* (Hz)	13C, ppm	HMBC	COSY
2	7.10, s	130.64	C-18	
2a		117.69	C-4; C-3	
3	2.97, t	18.82		4
4	3.90, t	52.70	C-15; C-19	3
5a	~	~	~	~
6	~	~	~	~
7		155.90	C-4; C-19	
8		167.15		
8a		122.90		
8b		123.30		
10	3.66, overlap	45.19		11
11	2.92, t	33.41		10
12		128.90	C-16; C-10	
13	~	~	~	~
14	~	~	~	~
15		156.04	C-16	
16	6.73, d, *8.48*	115.16		17
17	7.08, d, *8.41*	129.75		16
18	3.95, s	35.09		
19	3.34, s	38.34		

The initial plan for the next stage was to further purify the HPLC isolated DAV-09-H5 sample, as was carried out for the DAV-09-H3 sample. A single further purification step of DAV-09-H5 was carried out using the established Sephadex® LH-20 method, which yielded six fractions, and a proton NMR was performed on each of these six fractions using the Bruker 400 MHz UltraShield instrument. However a purified sample of Makaluvamine P was obtained from work carried out in another study, and so this was the sample that would go on to be used in the enzyme kinetics assay.

2.3.3 Enzyme Kinetics Assay of Chitinase Inhibition

Prior to the enzyme kinetics assay an LC-HRMS was performed on each of the samples that were to be used, which was done to verify that the molecular masses for each sample corresponded to their compound identity. The *m/z* values for the most intense *m/z* peak observed from the HRMS, alongside the literature monoisotopic molecular masses of each corresponding compound for each sample were as follows; Makaluvamine A (202.0976 *m/z*, 201.090210 $gmol^{-1}$) (**Figure 2.5.25**), Makaluvamine C (202.0977 *m/z*, 202.090210 $gmol^{-1}$) (**Figure 2.5.28**), Makaluvamine P (336.1713 *m/z*, 336.170654 $gmol^{-1}$) (**Figure 2.5.31**) and Makaluvamine H (216.1131 *m/z*, 216.113144 $gmol^{-1}$) (**Figures 2.5.34**, **2.5.36** and **2.5.38**). There were three samples that corresponded to Makaluvamine H, these were H3 Sephadex® Fraction 4, H3 Sephadex® Fraction 5 and the repurified H3 Sephadex® Fraction, the latter of which was used in the enzyme kinetics assay.

Enzyme inhibitive activity of each compound was observed by monitoring the change in absorbance over a set 90 second period. For the two controls a linear increase in absorbance over this period was observed, as the chitinase enzymes cleaved the ether bond of the substrate. In comparison to one another the chitinase enzyme from *Trichoderma* appeared to be much more active than that of *Streptomyces*, as the former presented a far more prominent linear increase over the set time-period than the latter (**Figure 2.5.40**).

The first set of kinetics assays were performed against the *Streptomyces* chitinase enzyme, where all four Makaluvamine compounds demonstrated significant inhibition at their initial concentrations, as observed by the constant unchanged absorbance relative to the linear increase of the control (**Figures 2.5.41, 2.5.43, 2.5.45** and **2.5.47**). Makaluvamine H did not appear to show any inhibitive activity against chitinase following the dilution from 5.0 to 2.5 mg/mL (**Figure 2.5.46**). This was also the case for Makaluvamine A, diluted from 2.5 mg/mL to 1.25 mg/mL (**Figure 2.5.42**) and Makaluvamine C, diluted from 23.5 mg/mL to 11.75 mg/mL (**Figure 2.5.44**). Makaluvamine P did demonstrate strong inhibition against the *Streptomyces* chitinase upon the first dilution from 20.7 to 10.35 mg/mL (**Figure 2.5.48**). Inhibitive activity was again observed following the second dilution of Makaluvamine P, from 10.35 to 5.175 mg/mL (**Figure 2.5.49**), though the inhibition appeared milder than that at previous concentrations for this compound. The lowest molar concentration at which each compound demonstrated inhibitive activity against *Streptomyces* chitinase were calculated as follows; Makaluvamine A (12.4 μM), Makaluvamine C (117 μM), Makaluvamine P (15.4

μM) and Makaluvamine H (23.1 μM). From the compounds tested Makaluvamine A appeared to demonstrate the most potent inhibitive activity, closely followed by Makaluvamine P.

A second set of kinetic assays were prepared to test for active inhibition against the chitinase of *Trichoderma*. Makaluvamine H was tested at an initial concentration of 5.0 mg/mL (**Figure 2.5.51**) followed by the diluted concentration of 2.5 mg/mL (**Figure 2.5.52**), neither displayed any inhibitive activity against the enzyme. Makaluvamine C was also tested, again showing no activity against the chitinase of *Trichoderma* (**Figure 2.5.50**).

The varying level of activity between each of the Makaluvamine compounds and between the two subsequent enzymes could arise from several factors. A notable observation made from the control experiments was that the *Trichoderma* chitinase appeared to cleave the substrate more aggressively than that of the *Streptomyces* chitinase. This could be due to differing modes of action between each enzyme, possibly through different conformations of their respective active sites, with that of *Trichoderma* being predominantly more active against the substrate. This possible differing conformation could explain why Makaluvamine H and C displayed active inhibition against *Streptomyces* chitinase, but no activity at all against *Trichoderma*. The structural conformations of Makaluvamine H and C may grant them the ability to inhibit the active site of the former enzyme, but not the latter as the shape of these active sites may differ. This remains as only one possibility, as no primary experimental work has been carried out to determine how inhibition of chitinase is achieved by the Makaluvamine compounds. The inhibition could take place at an allosteric site of the enzyme, perhaps a site that is present in the *Streptomyces* chitinase but not the *Trichoderma*. This form of inhibition would alter the conformation of the active site of the enzyme, negating its ability to bind to the substrate. With respect to the differing levels of inhibitive activity against *Streptomyces* chitinase between each of the Makaluvamine compounds the respective chemical structure likely plays a significant role. Makaluvamine A and P appeared to be the most potent of the four Makaluvamines tested, as they showed inhibitive activity at the lowest molar concentrations. Makaluvamines A and C possess almost identical structures, consisting of the core pyrrole-quinoline type structure that features a ketone and an amine group. The one difference is the location of a methyl group, which finds itself attached to the nitrogen of the pyrrole structure in the former and to the nitrogen of the quinoline structure in the latter. The potency based on the molar concentrations at which these two compounds were active were completely opposite, which could indicate that the relatively minor difference in structure could have a more than significant impact on their inhibitive ability against *Streptomyces*

chitinase. Makaluvamine H also consists of the core pyrrole-quinoline type structure as seen for A and C, though features two methyl groups, one attached to the nitrogen of the pyrrole structure and the other to the nitrogen of the quinoline structure. The single ketone and amine groups remain in the same positions across the three of these compounds. Makaluvamine P is comprised of the same core structure as Makaluvamine H, though is bridged via an amide linkage in place of where the amine is situated in the other three other Makaluvamines to a 4-ethylphenol structure. Considering all of this the molar concentration at which Makaluvamine C was active stands as a significant outlier, possibly as a result of the absence of a methyl group on the nitrogen of the pyrrole. The presence of a methyl on the nitrogen of the quinoline structure could have been highlighted as a possible cause for this, however both Makaluvamine P and H feature this same methyl and the respective molar concentrations at which these two compounds were active were much more in line with that of Makaluvamine A.

2.4 Conclusion and Future Work

In conclusion to this investigation two compounds have been isolated and identified from the extract of an Ascidian sample of the Great Barrier Reef through structural dereplication, using a combination of high-resolution mass spectrometry and 1D and 2D NMR spectroscopic techniques. Chemical database searches and computer-assisted structural elucidation programs were also a valuable aid in identifying the two compounds, in combination with the experimental data gathered. The two compounds were identified as Makaluvamine H and Makaluvamine P. In a previous study a preliminary enzyme kinetics assay was carried out with the crude Ascidian extract to test for inhibitive activity against chitinase of the bacteria *Streptomyces griseus*. This crude Ascidian extract from which Makaluvamine H and P were isolated demonstrated strong chitinase inhibition. With this information the enzyme kinetics experiment was replicated and performed on the purified Makaluvamine H compound, alongside pure samples of Makaluvamine P, A and C obtained from a separate study. All Makaluvamine compounds demonstrated active inhibition against chitinase of *Streptomyces griseus*. The most potent compound, based on the lowest molar concentration at which inhibitive activity was observed, was Makaluvamine A.

Further work needs to be carried out to definitively identify the Ascidian from which the extract was derived. At present the Ascidian is believed to be *Polysyncraton pedunculatum*, of the *Didemnidae* family. Future work relating to this study could involve the structural

elucidation of other compounds that were present in the extract samples, that may or may not belong to the family of Makaluvamines. The enzyme kinetics procedure outlined in this study could be carried out on any further identified compounds to assess them for inhibitive activity against the chitinase of *Streptomyces griseus*. The potency of each of the Makaluvamine compounds that were tested could be more accurately described by further experimental work, such as a measure of the half maximal inhibitory concentration (IC_{50}). In producing this data the inhibitive activity of each of the Makaluvamine compounds could be accurately plotted against increasing molar concentrations at regular intervals. An investigation into the mode by which Makaluvamines inhibit chitinase would also be of interest, this could determine whether inhibition is competitive or non-competitive. Finally, the focal point of this study was to investigate whether the Makaluvamine compounds identified from the Ascidian extract expressed inhibitive activity against the chitinase of *Streptomyces griseus*. As discussed in the literature review natural products can possess a range of applicable properties, most notably as therapeutics. Future work could include different biological assays that screen these Makaluvamine compounds for potential therapeutic activity against a range of diseases and ailments.

2.5 Supplementary Information

Figure 2.5.1: Photographs of DAV-09 marine tunicate taken during diving expedition.

Figure 2.5.2: DAV-09-H3 proton NMR data – 800 MHz - MeOD

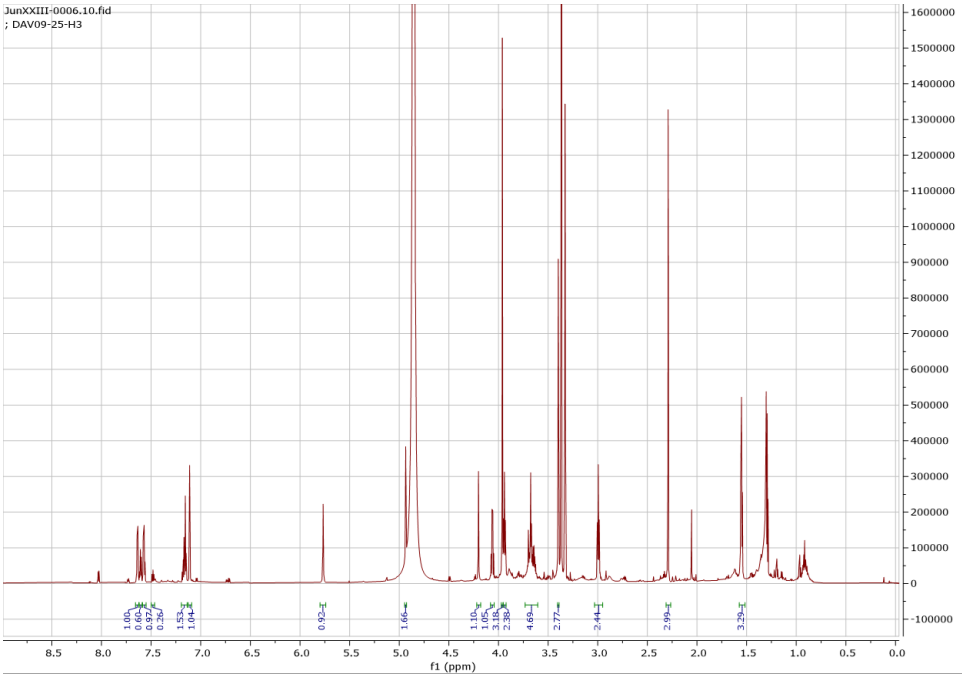

Figure 2.5.3: DAV-09-H3 COSY NMR data – 800 MHz – MeOD

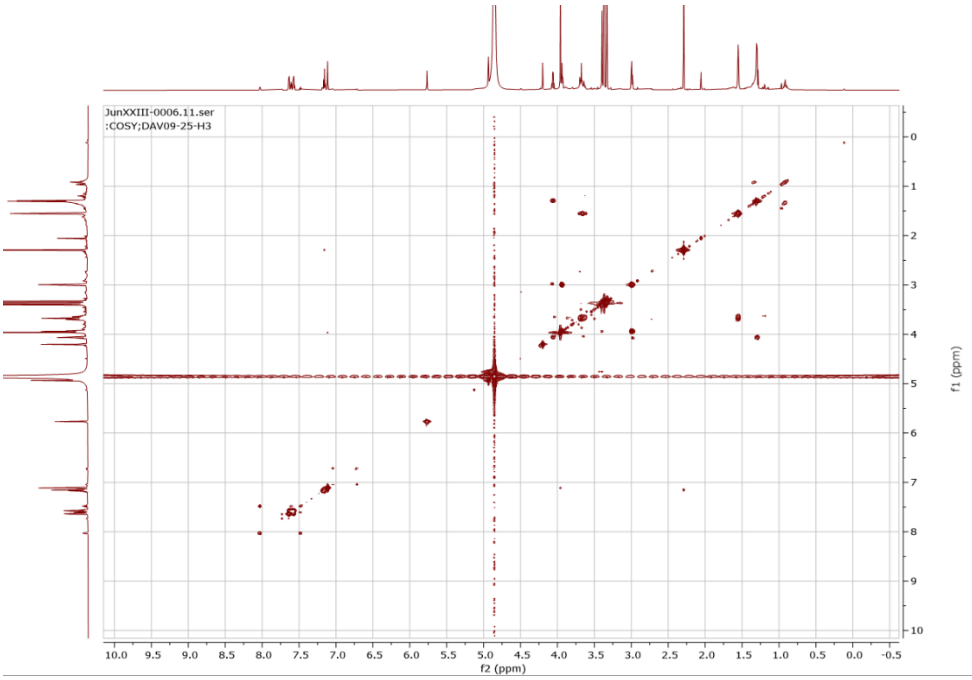

Figure 2.5.4: DAV-09-H3 HSQC-edited NMR data – 800 MHz – MeOD

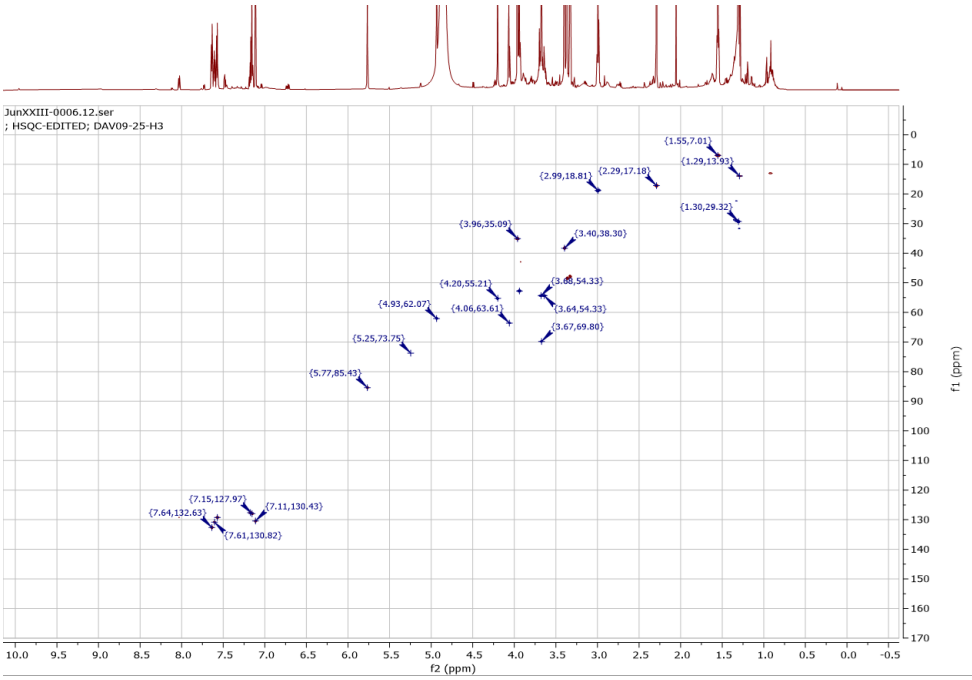

Figure 2.5.5: DAV-09-H3 HMBC NMR data – 800 MHz – MeOD

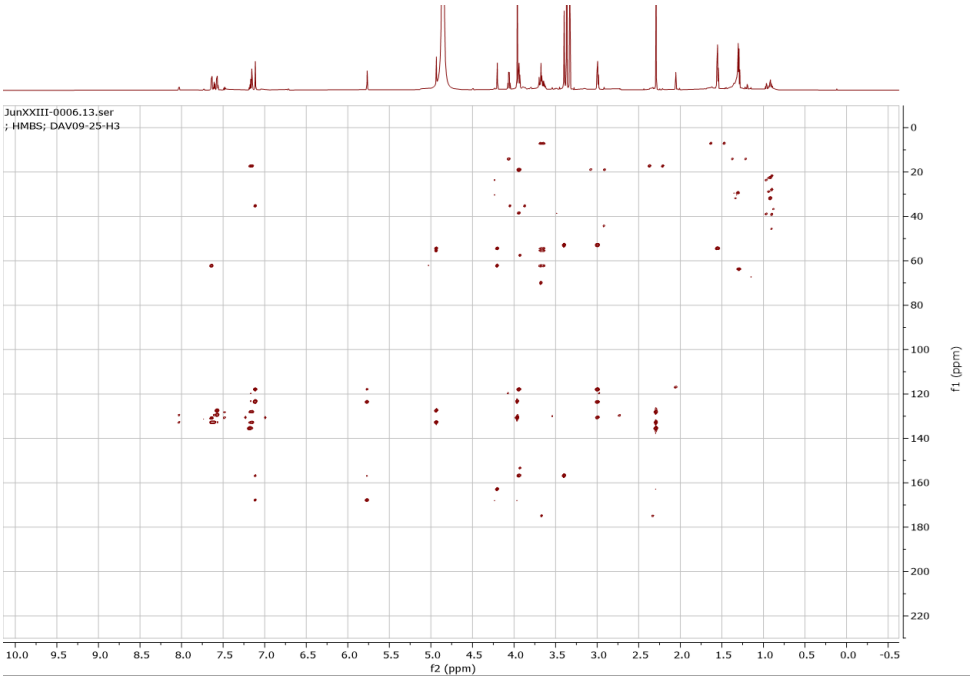

Figure 2.5.6: DAV-09-H5 proton NMR data – 800 MHz – MeOD

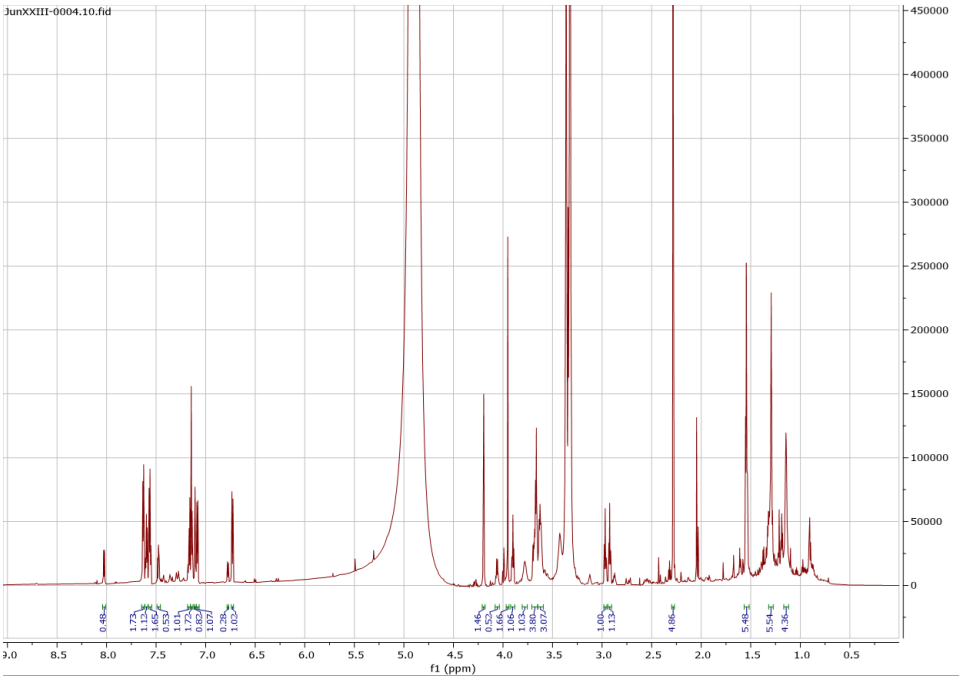

Figure 2.5.7: DAV-09-H5 COSY NMR data – 800 MHz – MeOD

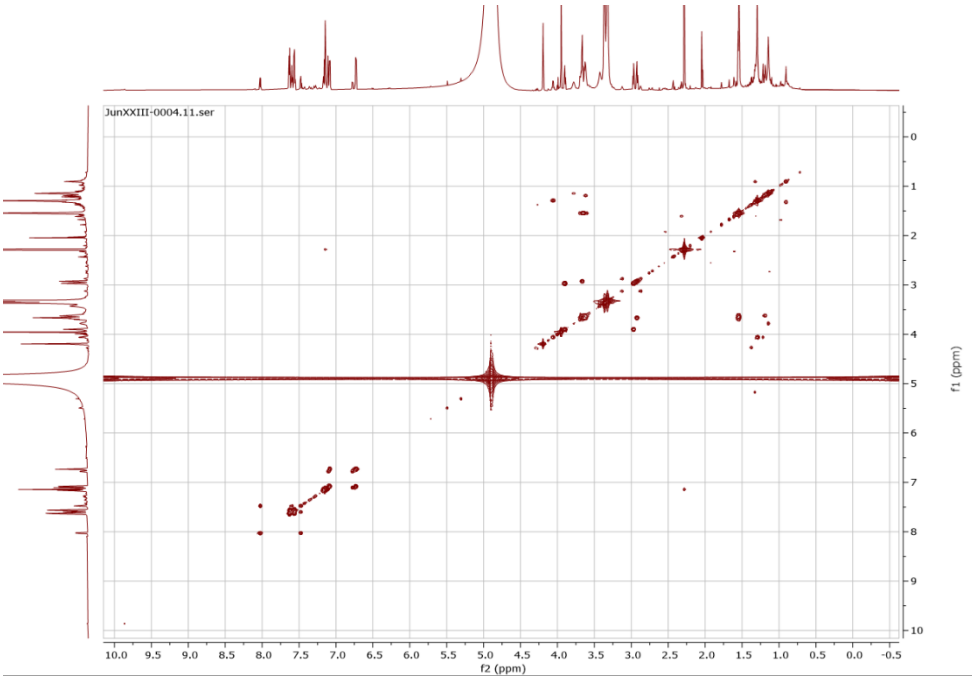

Figure 2.5.8: DAV-09-H5 HSQC-edited NMR data – 800 MHz – MeOD

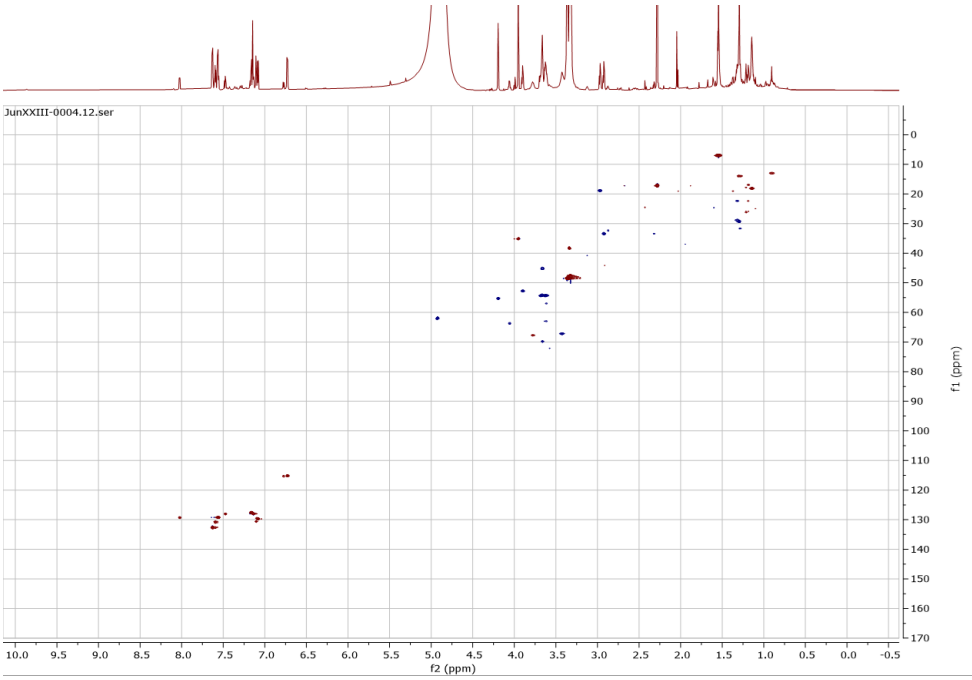

Figure 2.5.9: DAV-09-H5 HMBC NMR data – 800 MHz – MeOD

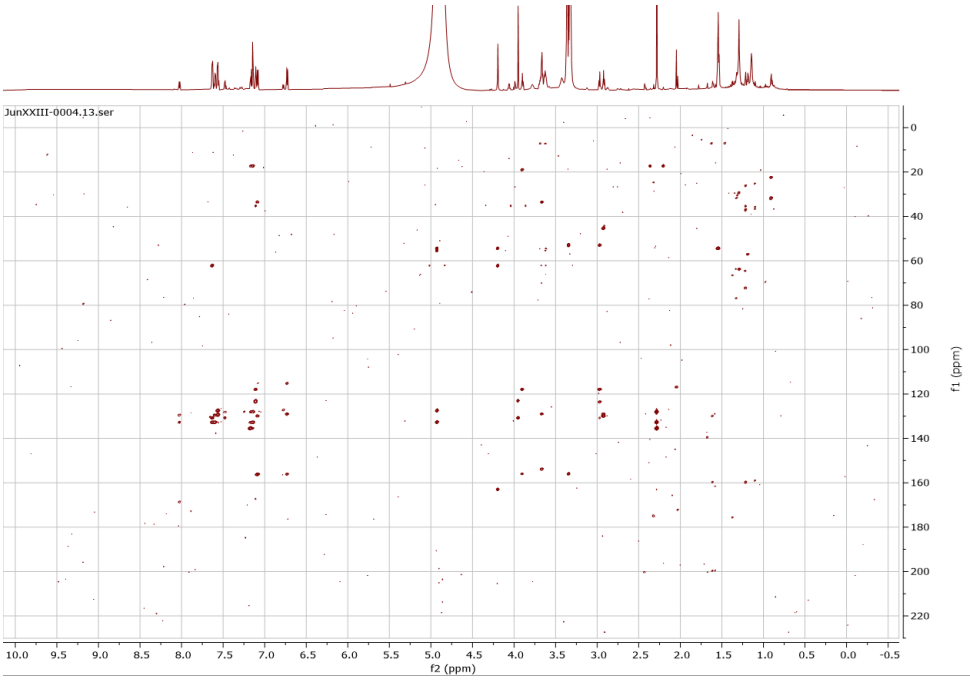

Figure 2.5.10: Makaluvamine A proton NMR data – 400 MHz – MeOD

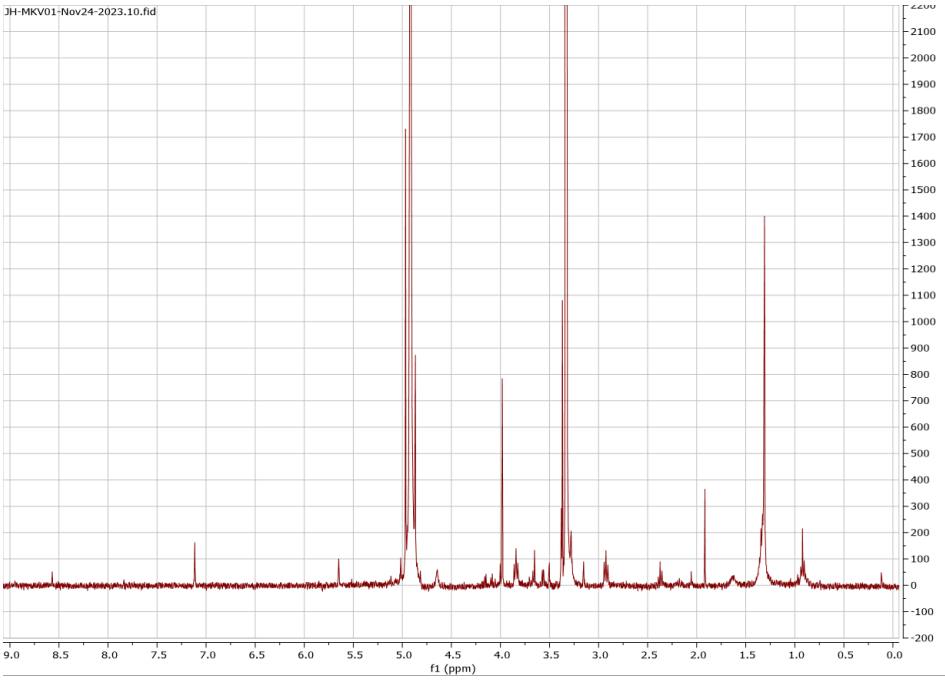

Figure 2.5.11: Makaluvamine C proton NMR data – 400 MHz – MeOD

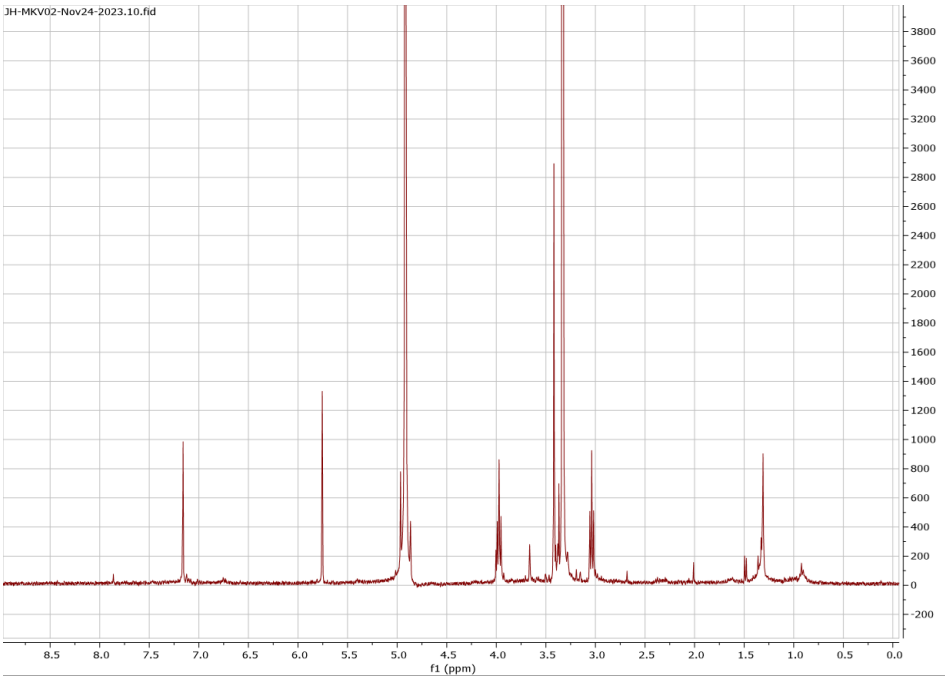

Figure 2.5.12: Makaluvamine P proton NMR data – 400 MHz – MeOD

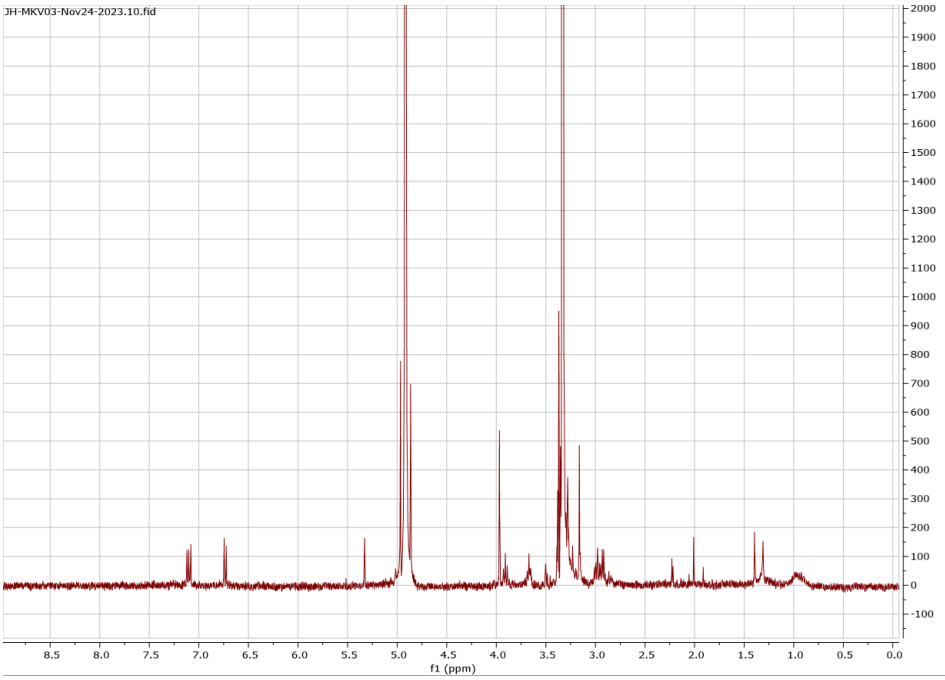

Figure 2.5.13: DAV-09-H3 Sephadex® 4 proton NMR data – 400 MHz – MeOD

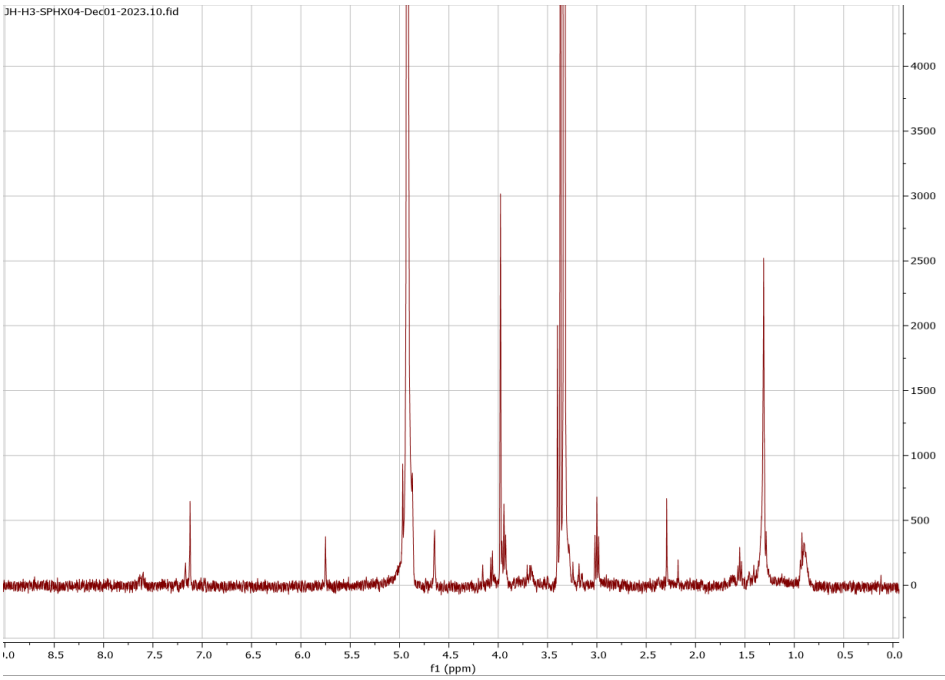

Figure 2.5.14: DAV-09-H3 Sephadex® 5 proton NMR data – 400 MHz – MeOD

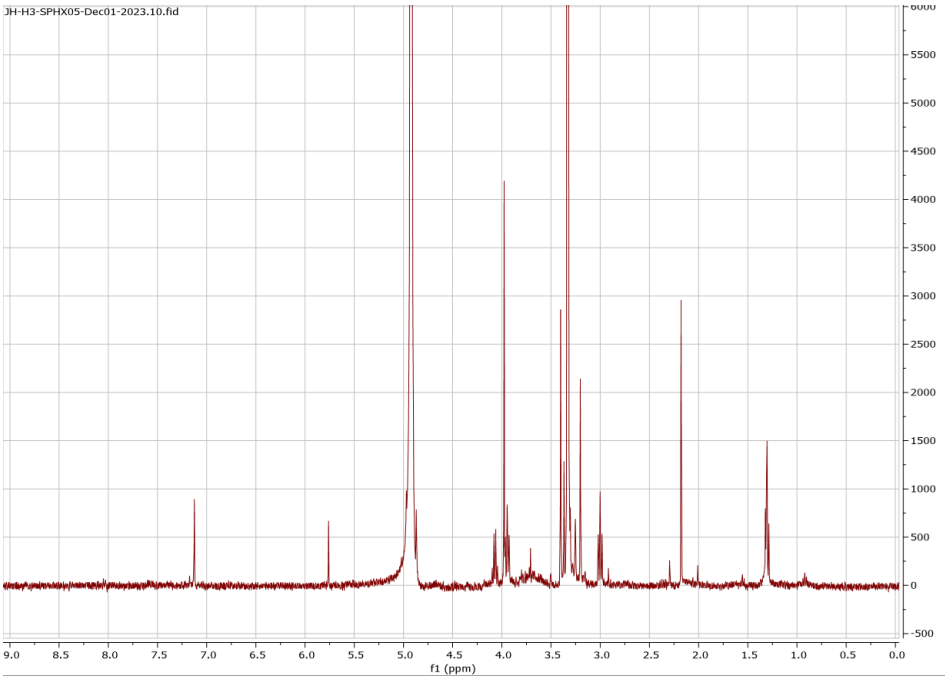

Figure 2.5.15: DAV-09-H3 re-Sephadex® 5 proton NMR data – 400 MHz – MeOD

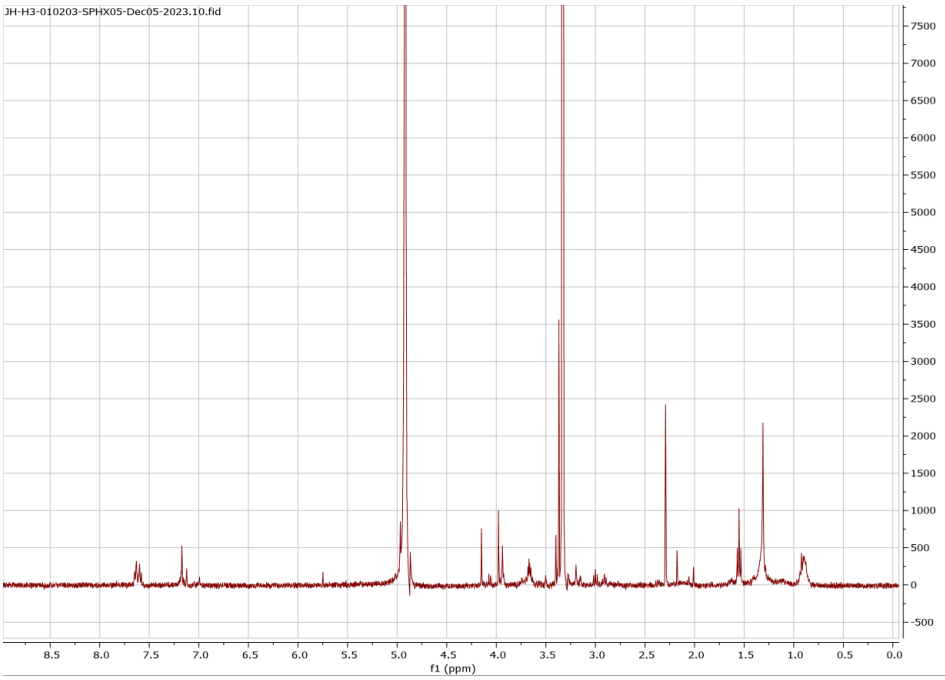

Figure 2.5.16: DAV-09-H3 re-Sephadex® 6 proton NMR data – 400 MHz – MeOD

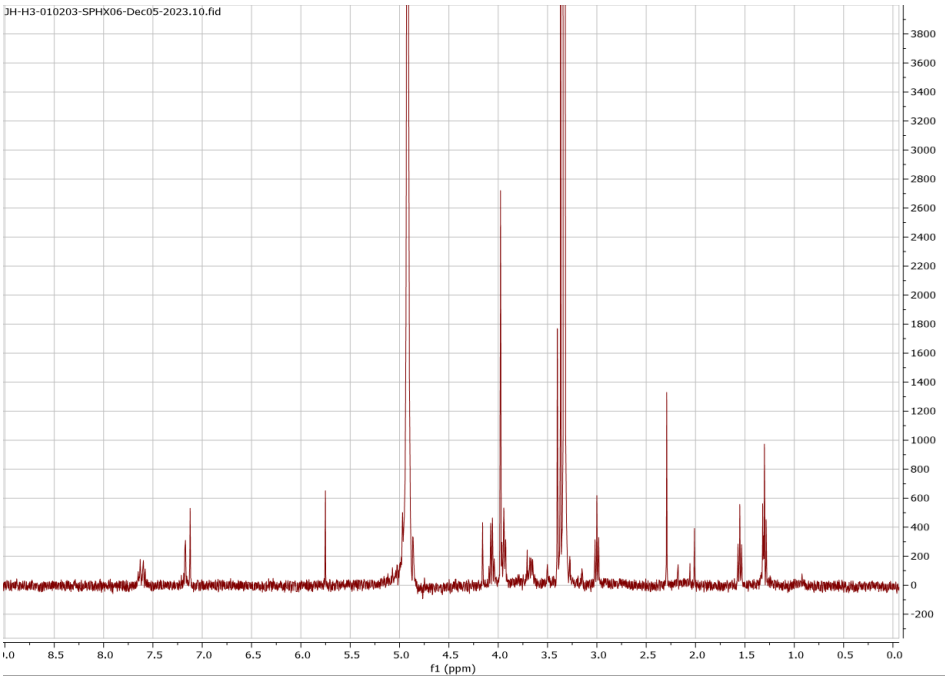

Figure 2.5.17: DAV-09-H3 re-Sephadex® 7 proton NMR data – 400 MHz – MeOD

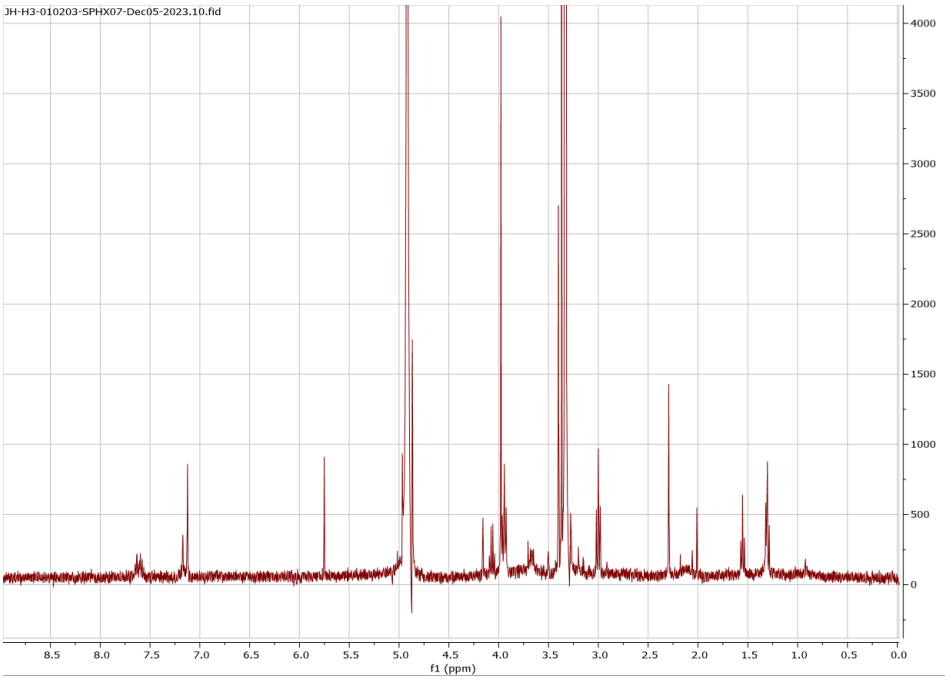

Figure 2.5.18: DAV-09-25% SPE HPLC Chromatogram

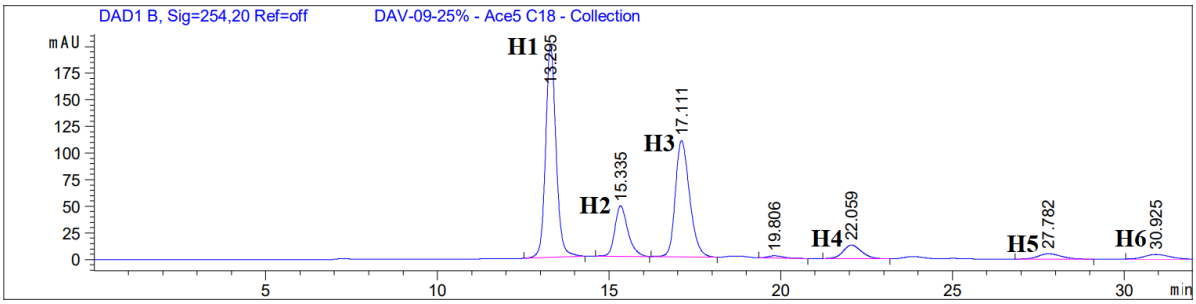

Figure 2.5.19: DAV-09-25% HPLC UV-Vis profiles of H1(*Top*) – H6(*Bottom*)

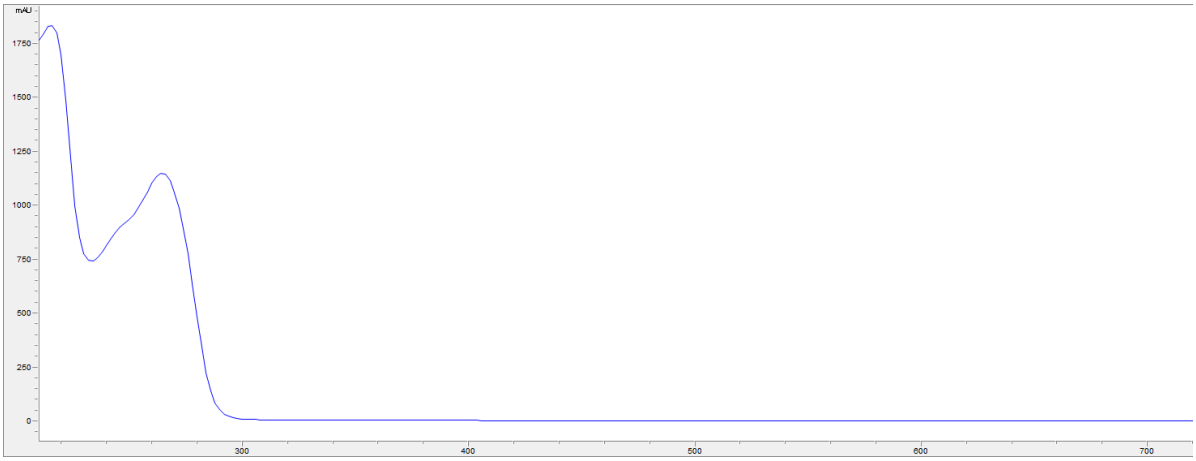

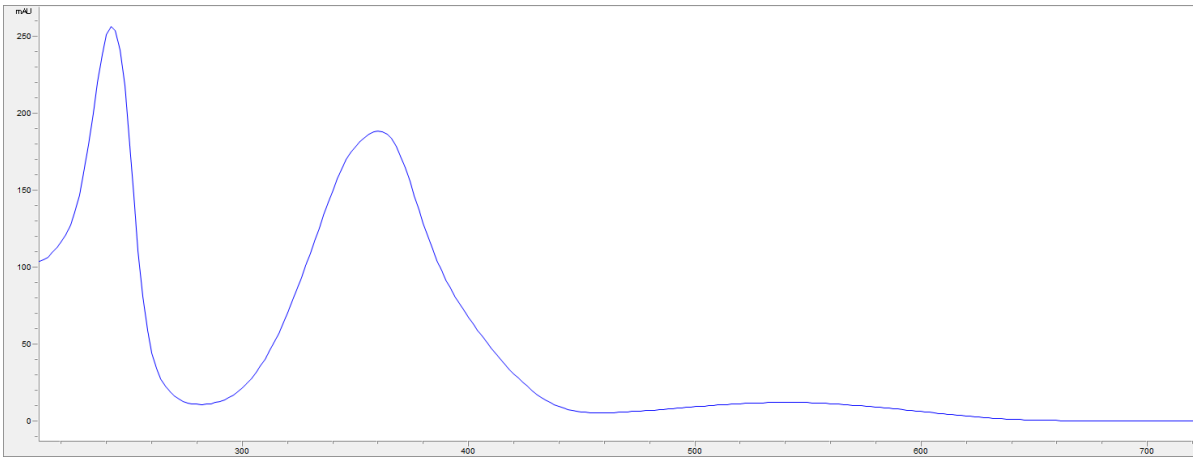
mAU
250
200
150
100
50
0
300
400
500
600
700

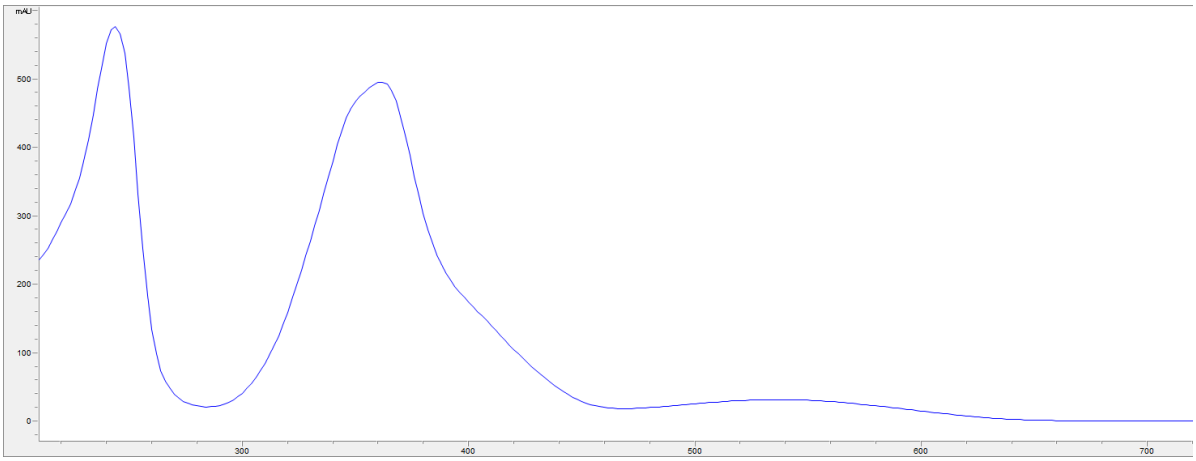
mAU
500
400
300
200
100
0
300
400
500
600
700

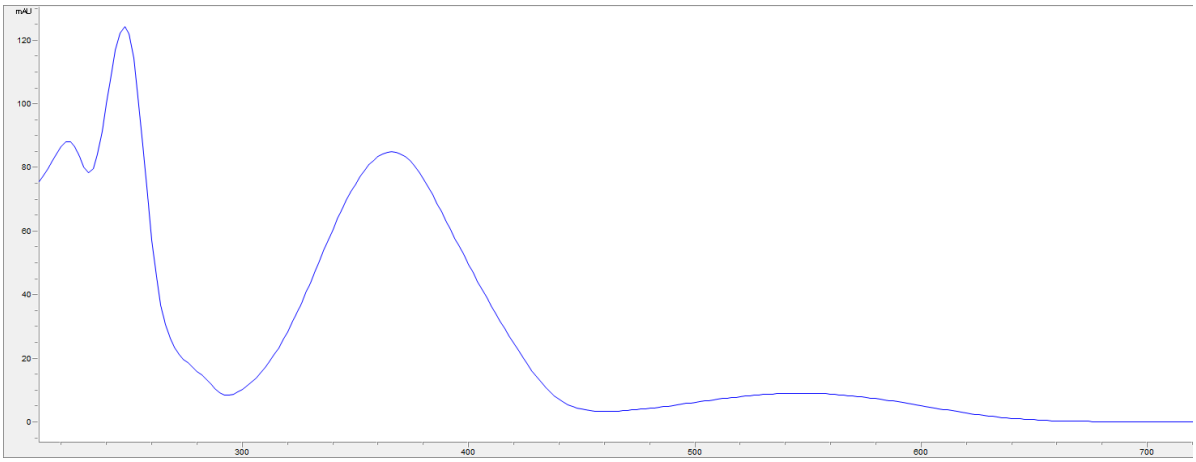
mAU
120
100
80
60
40
20
0
300
400
500
600
700

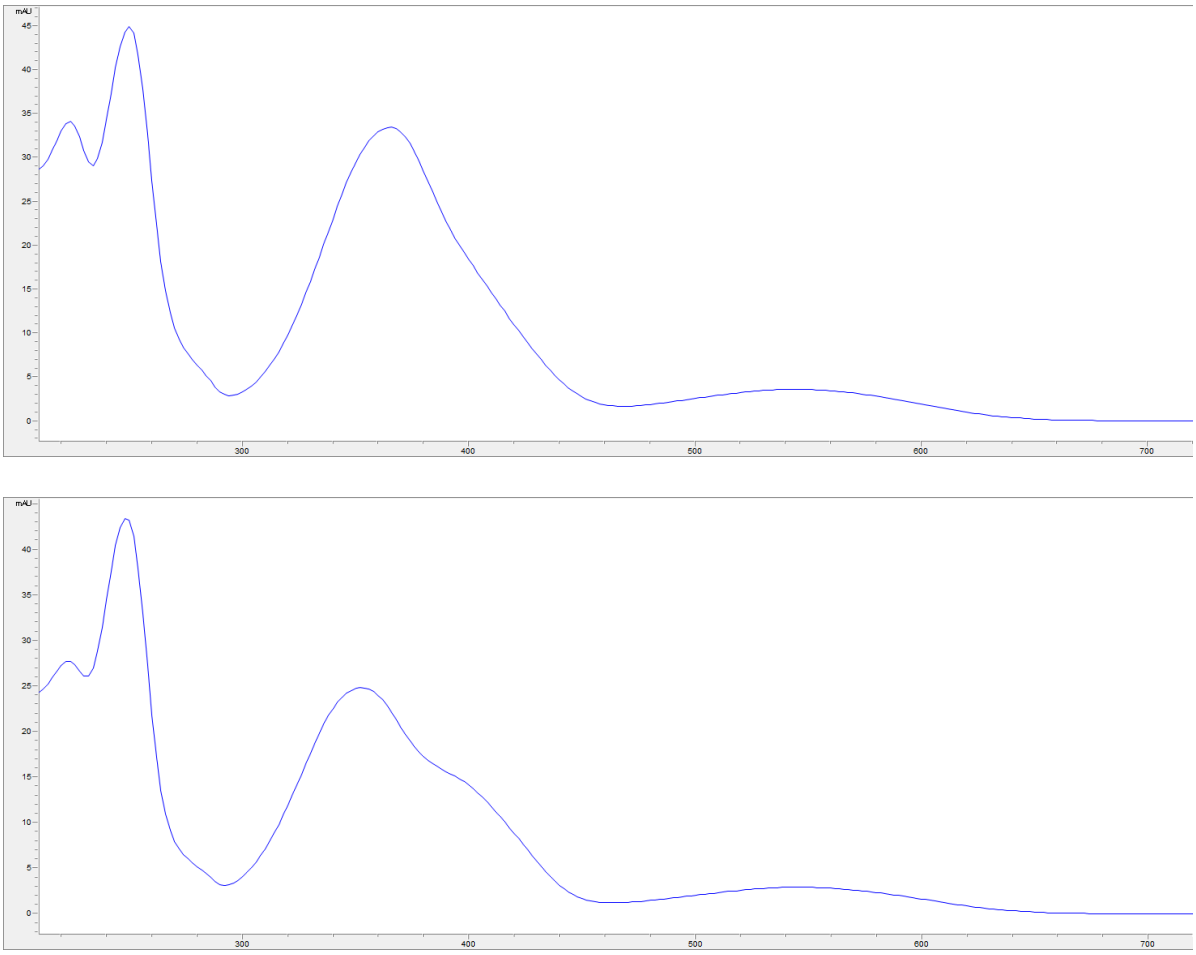

Figure 2.5.20: DAV-09-50% SPE HPLC Chromatogram

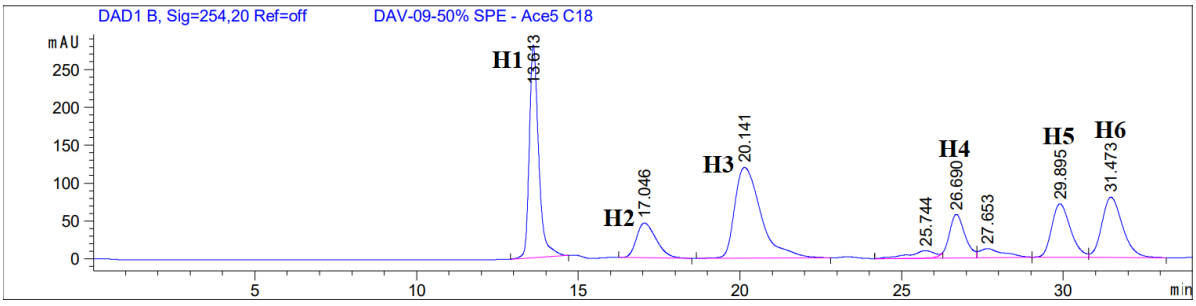

Figure 2.5.21: DAV-09-H3 LC-HRMS analysis in ACD/Labs software

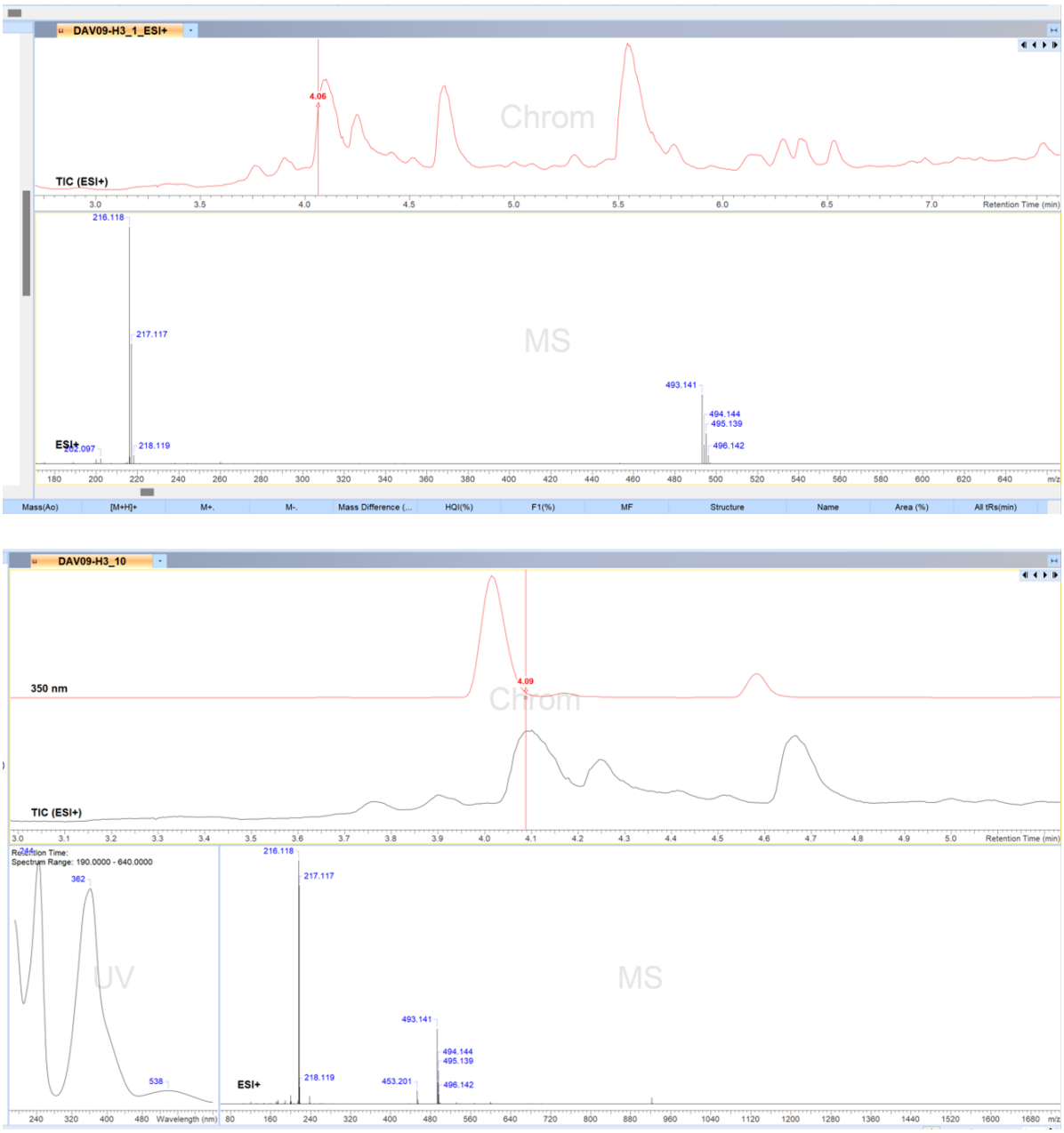

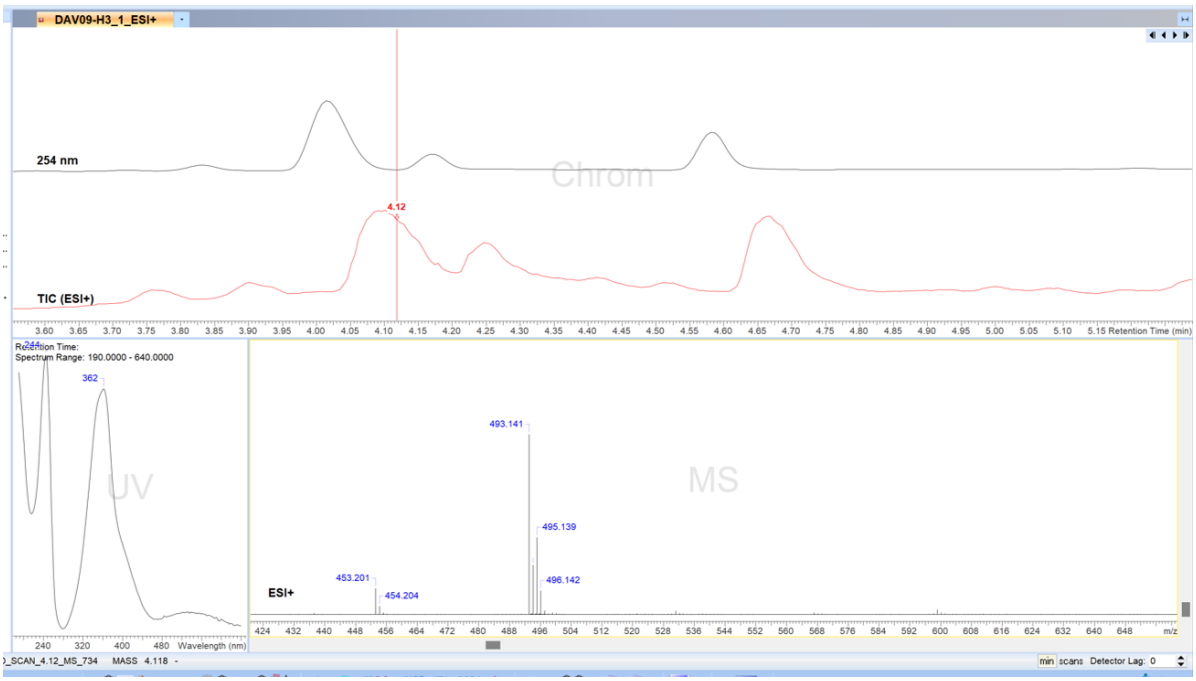
DAV09-H3_1_ESI+
254 nm
Chrom
4.12
TIC (ESI+)
Retention Time (min)
Retention Time:
Spectrum Range: 190.0000 - 640.0000
362
UV
Wavelength (nm)
493.141
MS
495.139
453.201
454.204
496.142
ESI+
m/z
_SCAN_4.12_MS_734
MASS 4.118
min scans Detector Lag: 0

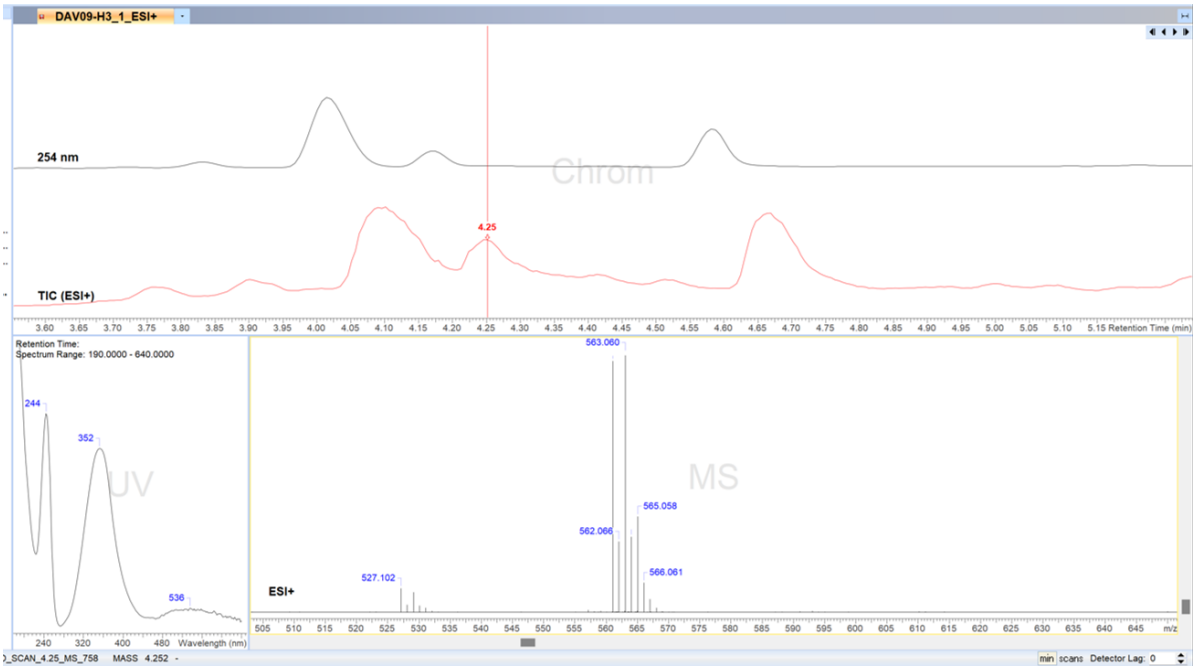
DAV09-H3_1_ESI+
254 nm
Chrom
4.25
TIC (ESI+)
Retention Time (min)
Retention Time:
Spectrum Range: 190.0000 - 640.0000
244
352
UV
536
Wavelength (nm)
563.060
MS
565.058
562.066
566.061
527.102
ESI+
m/z
_SCAN_4.25_MS_758
MASS 4.252
min scans Detector Lag: 0

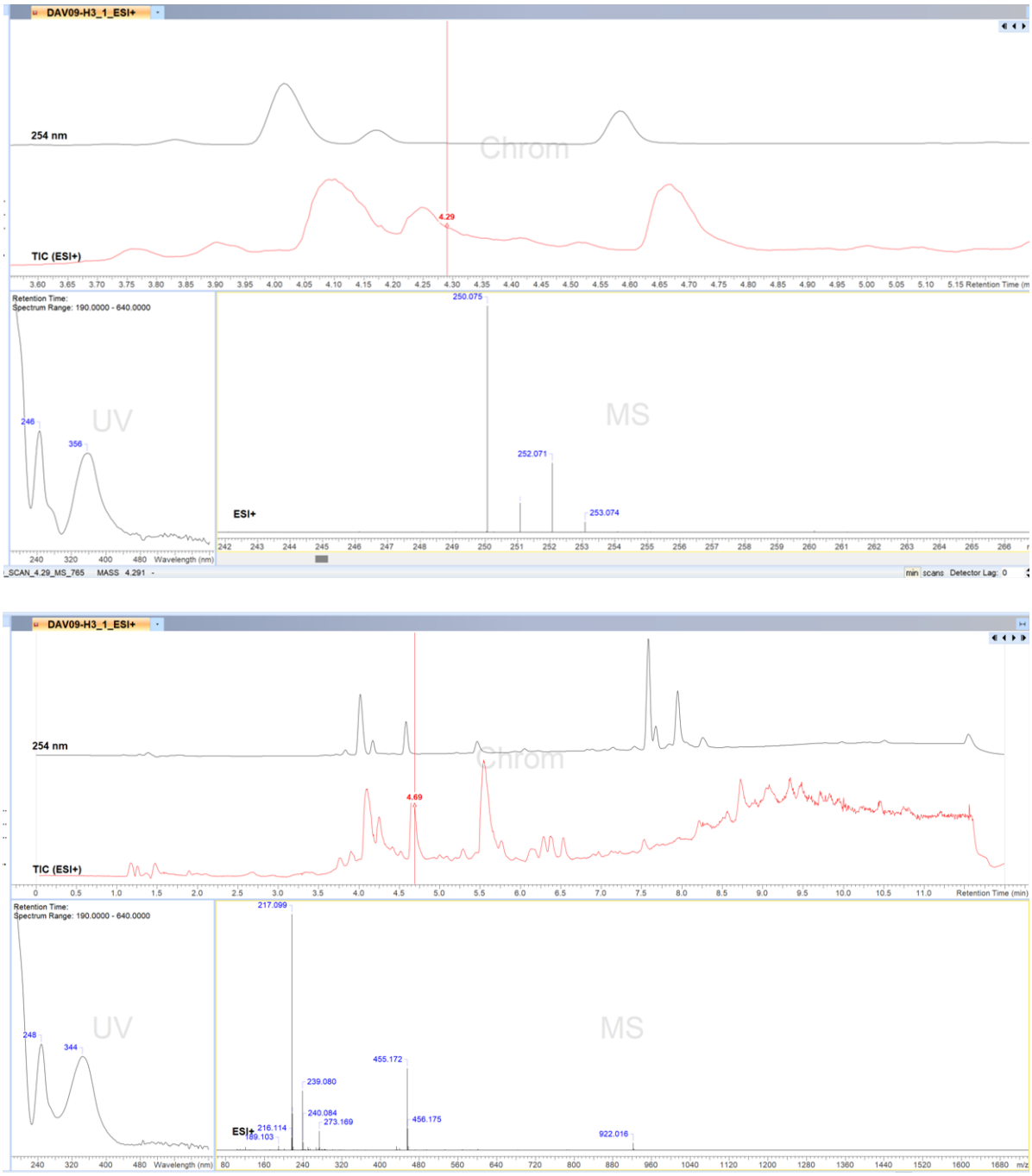

Figure 2.5.22: DAV-09-H3 molecular formula generation for 217 m/z ACD/Labs software

No.	Formula	Monoisotopic Mass	Error (Da)	FFQ	RDBE
1	C17H13	217.102	-0.001	11.5	
2	C9H17N2O2S	217.101	0.000		10.5;11.5;12.5;13.5;14.5
3	C3H23NO5S2	217.102	-0.001		13.0 - 18.0
4	C2H17N8S2	217.102	-0.001		1.5 - 10.5
5	CH21N4O4S2	217.100	0.001		9.5 - 17.5
6	CH13N8O5	217.101	0.000		19.5 - 27.5

Figure 2.5.23: DAV-09-H5 LC-HRMS analysis and molecular formula generation in ACD/Labs software

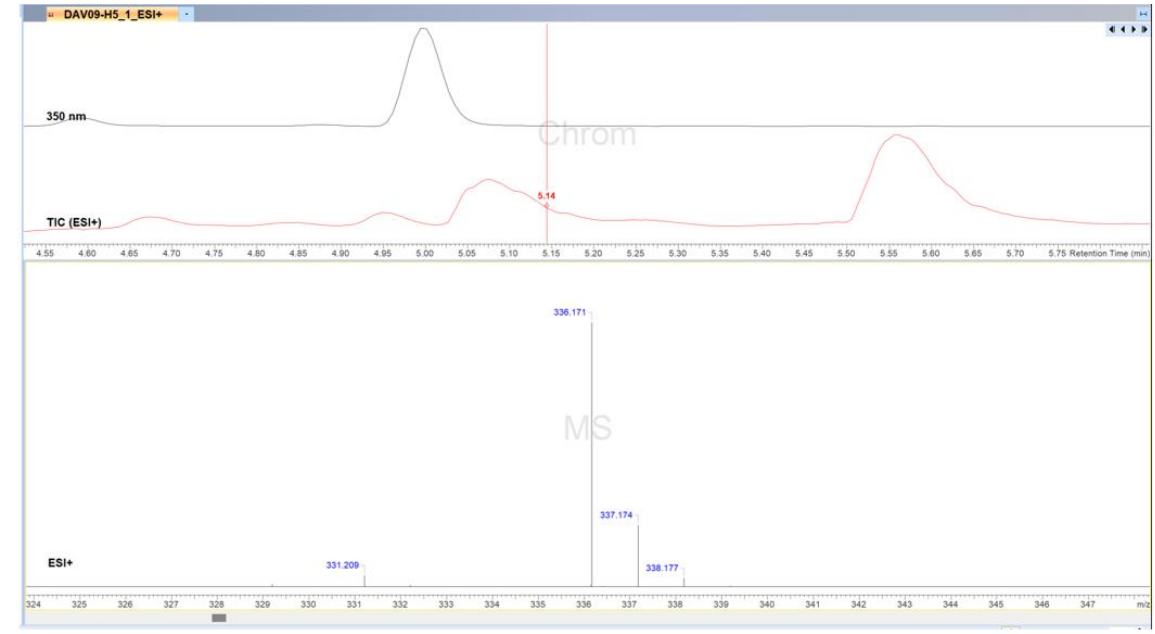

	Formula	Monoisotopic Mass	Error (Da)	FFQ	RDBE
	C22H24O3	336.173	-0.002		23.0
	C20H22N3O2	336.171	0.000		19.5;20.5;2
	C18H20N6O	336.170	0.001		16.0 - 22.0

Figure 2.5.24: Makaluvamine A LC-HRMS chromatogram

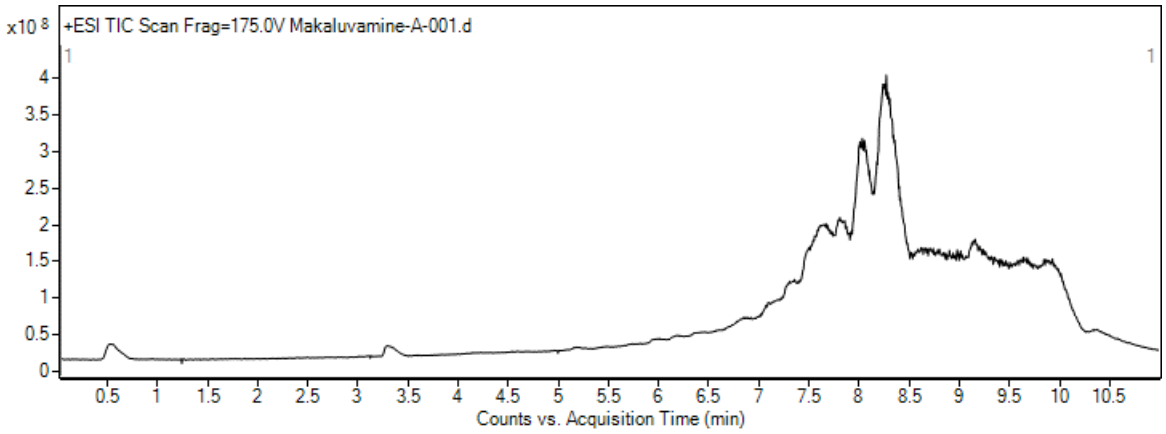

Figure 2.5.25: Makaluvamine A LC-HRMS mass spectra

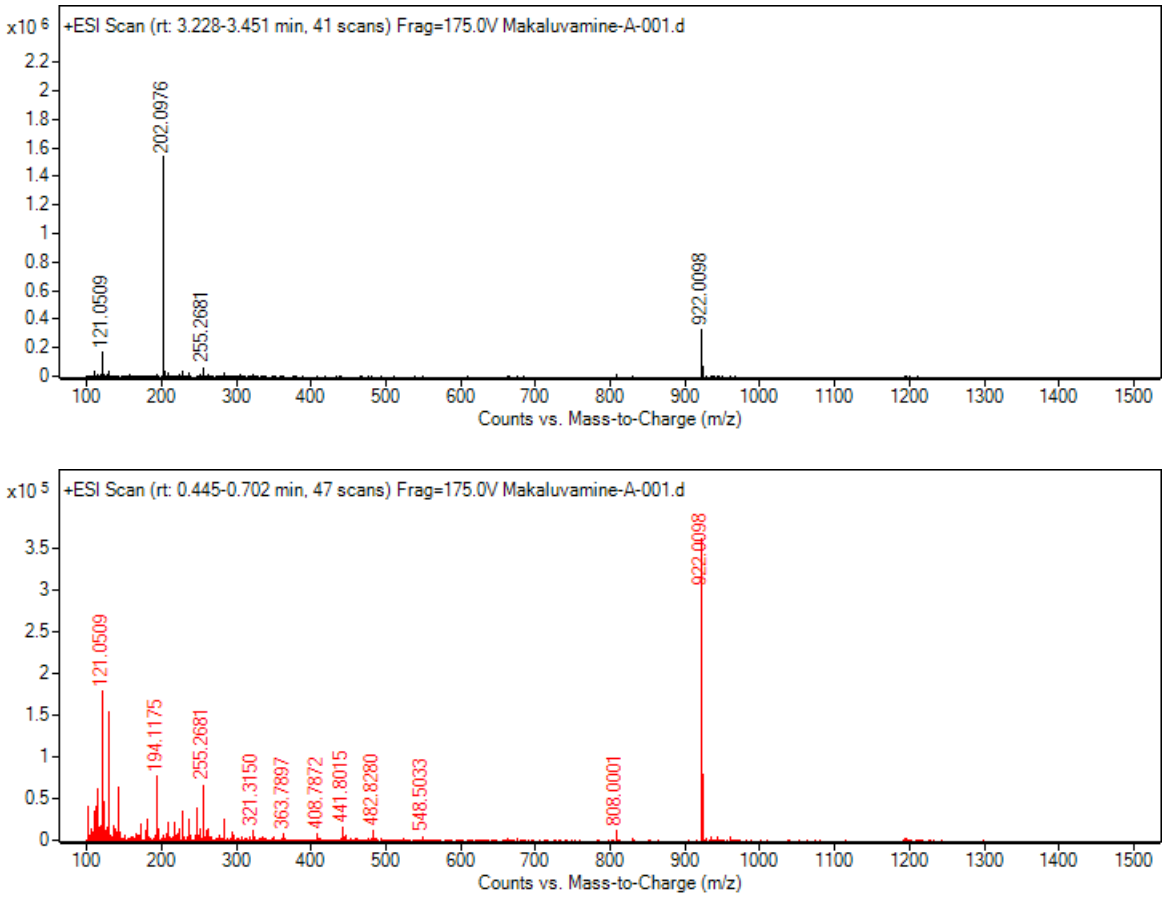

Figure 2.5.26: Makaluvamine A LC-HRMS MS/MS mass spectra

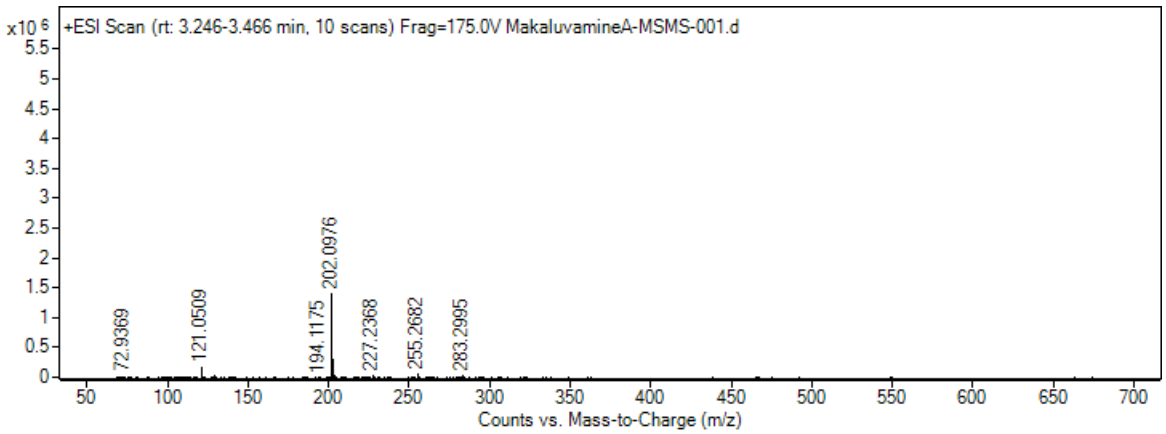

Figure 2.5.27: Makaluvamine C LC-HRMS chromatogram

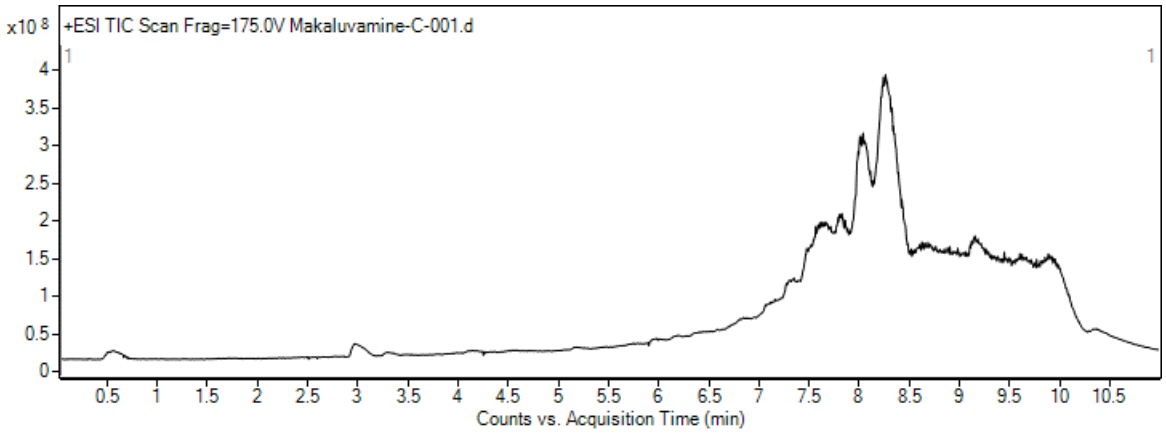

Figure 2.5.28: Makaluvamine C LC-HRMS mass spectra

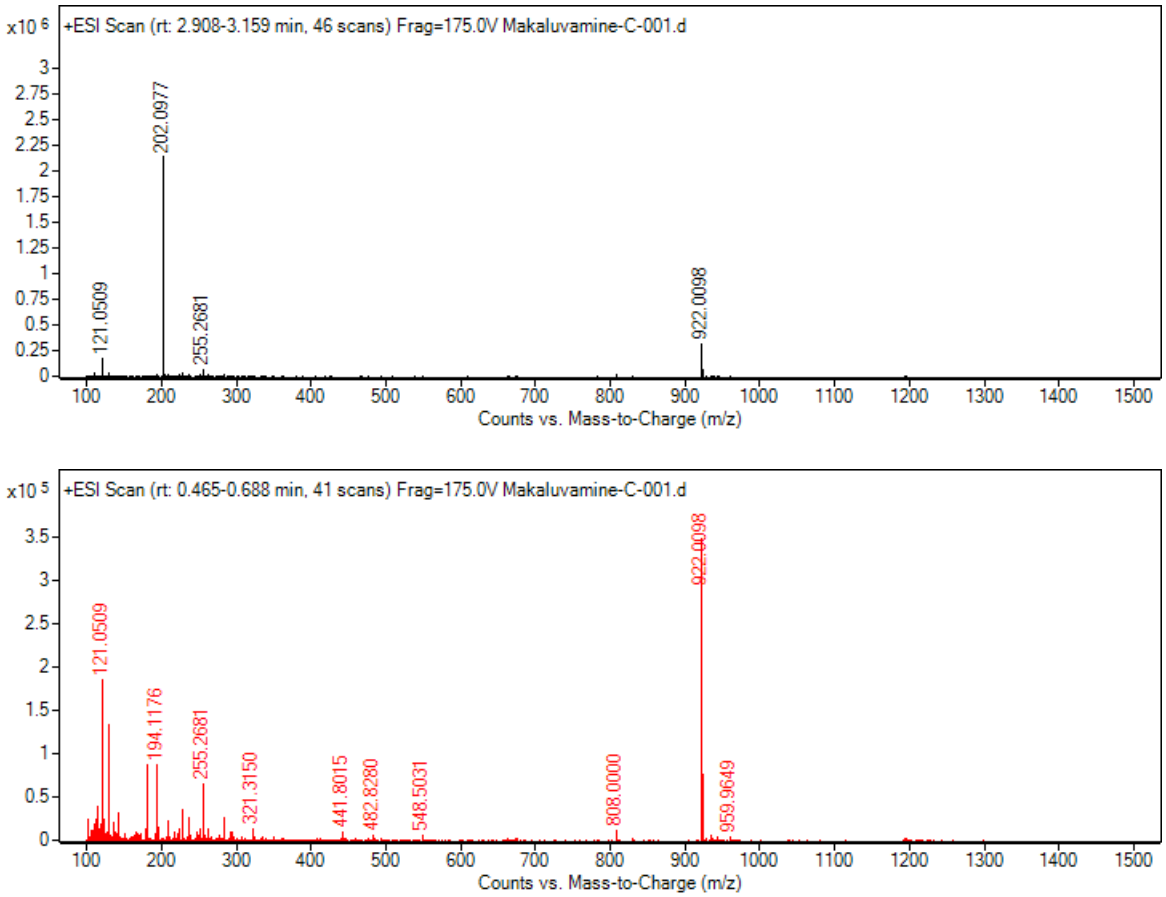

Figure 2.5.29: Makaluvamine C LC-HRMS MS/MS mass spectra

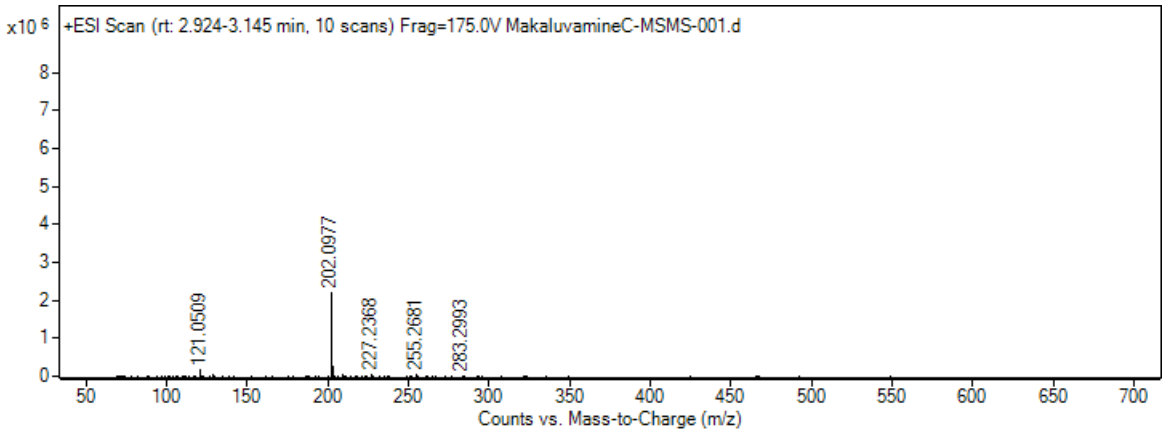

Figure 2.5.30: Makaluvamine P LC-HRMS Chromatogram

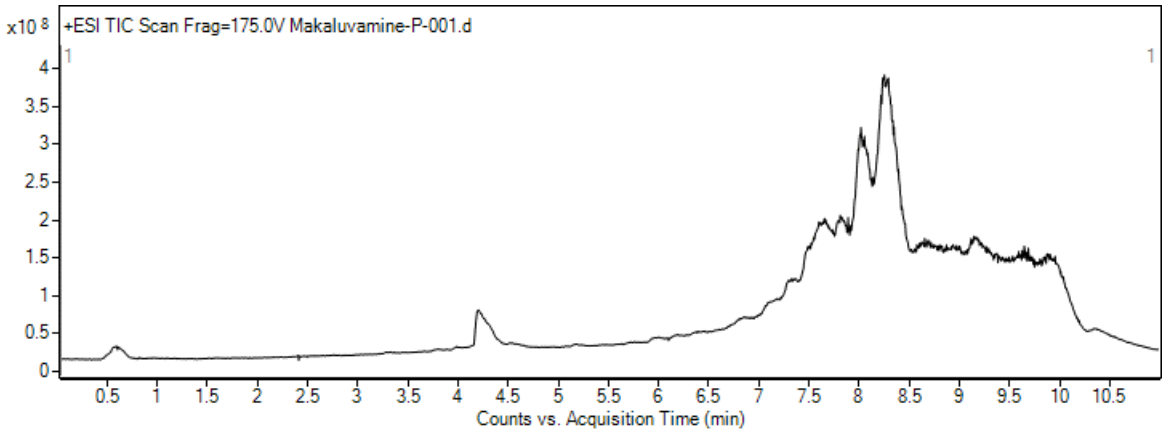

Figure 2.5.31: Makaluvamine P LC-HRMS mass spectra

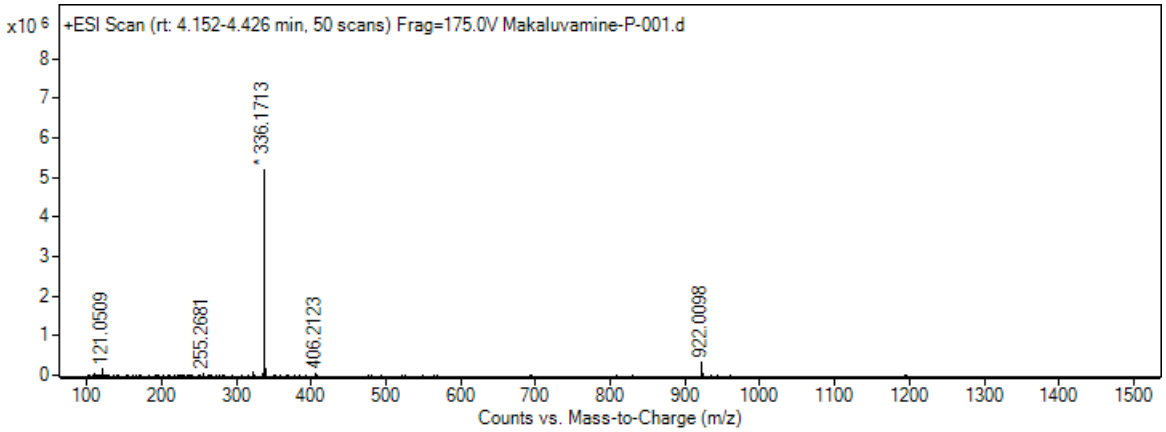

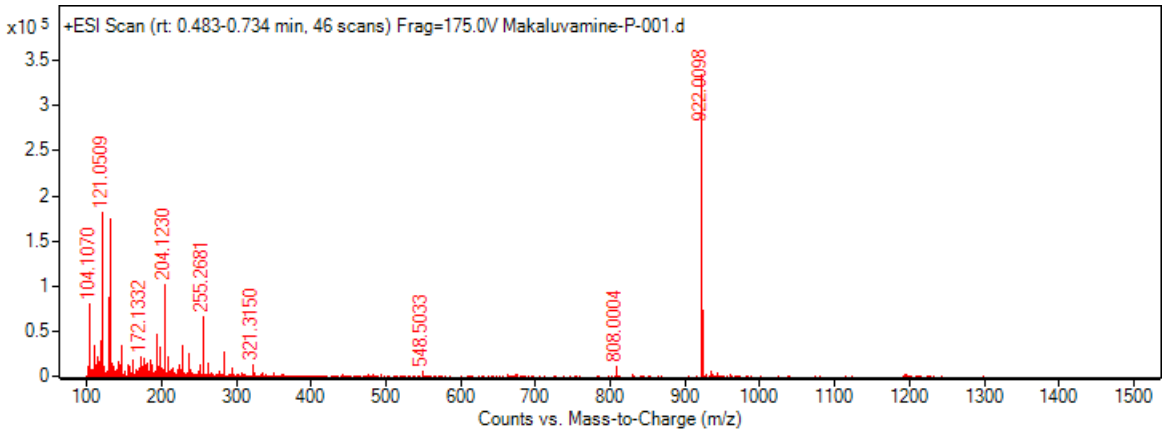

Figure 2.5.32: Makaluvamine P LC-HRMS MS/MS mass spectra

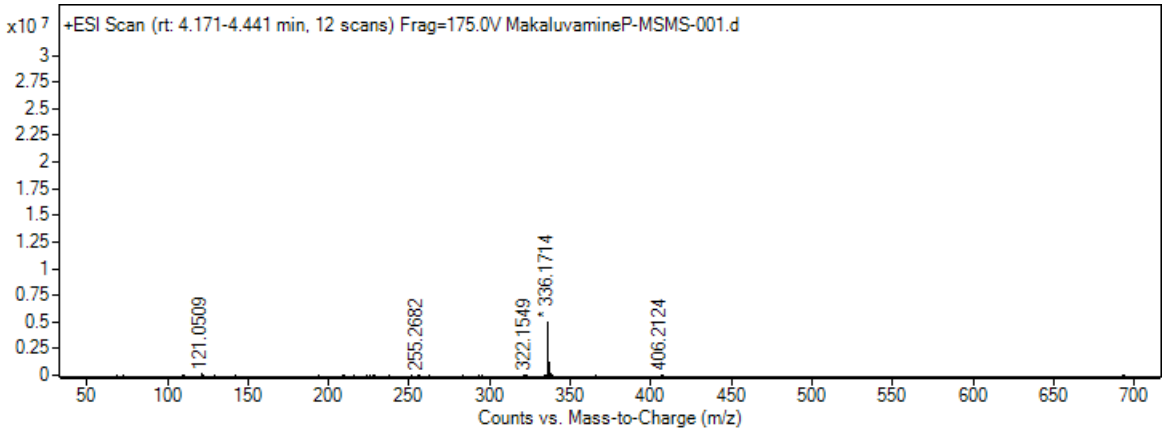

Figure 2.5.33: DAV-09-H3 Sephadex® 4 LC-HRMS chromatogram

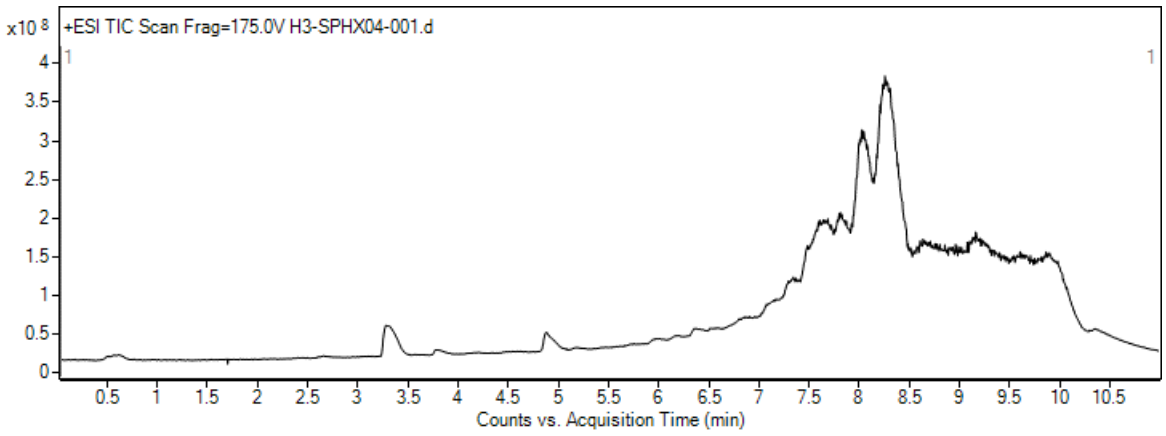

Figure 2.5.34: DAV-09-H3 Sephadex® 4 LC-HRMS mass spectra

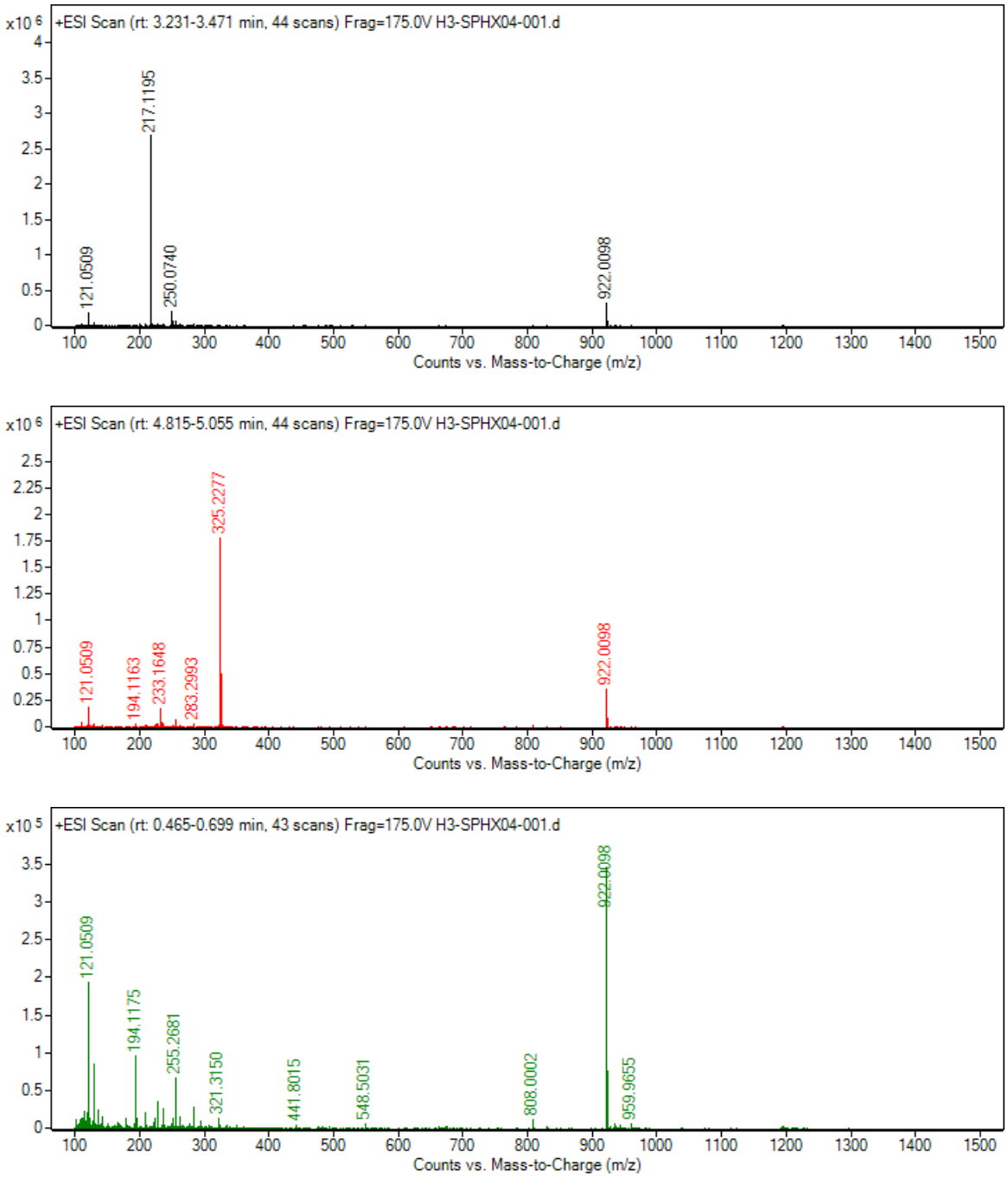

Figure 2.5.35: DAV-09-H3 Sephadex® 5 LC-HRMS chromatogram

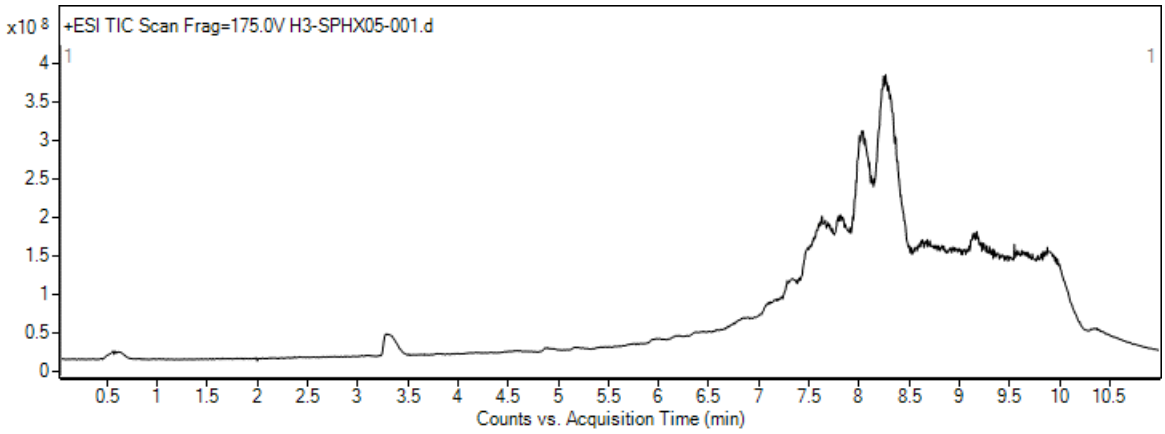

Figure 2.5.36: DAV-09-H3 Sephadex® 5 LC-HRMS mass spectra

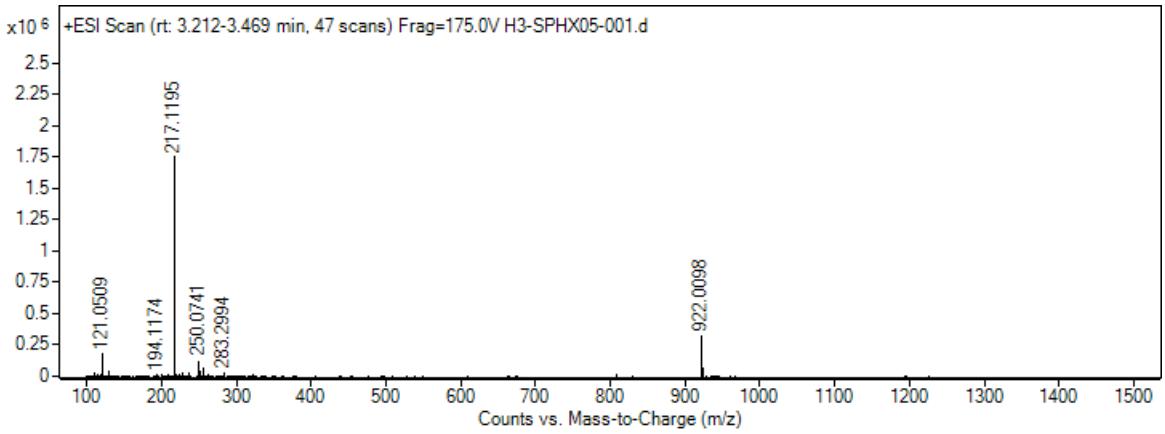

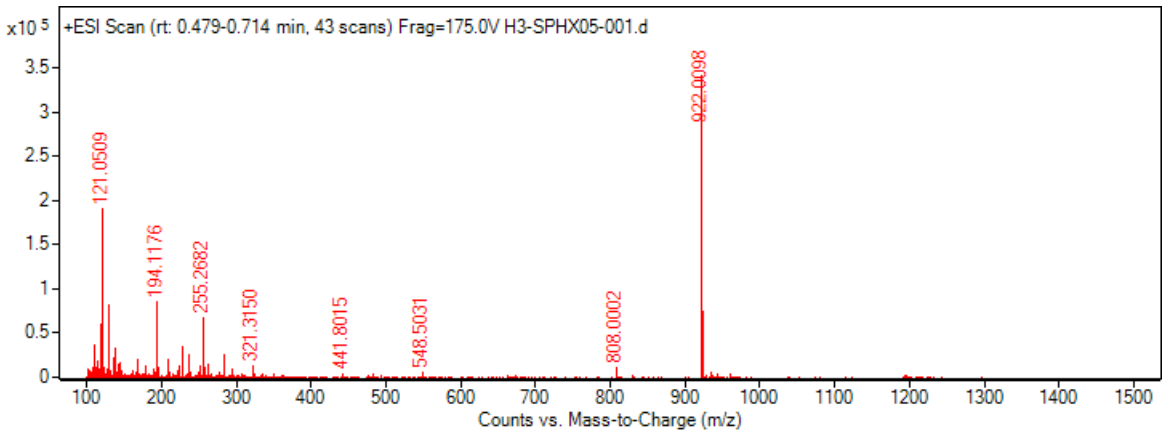

Figure 2.5.37: DAV-09-H3 re-Sephadex® Fraction LC-HRMS chromatogram

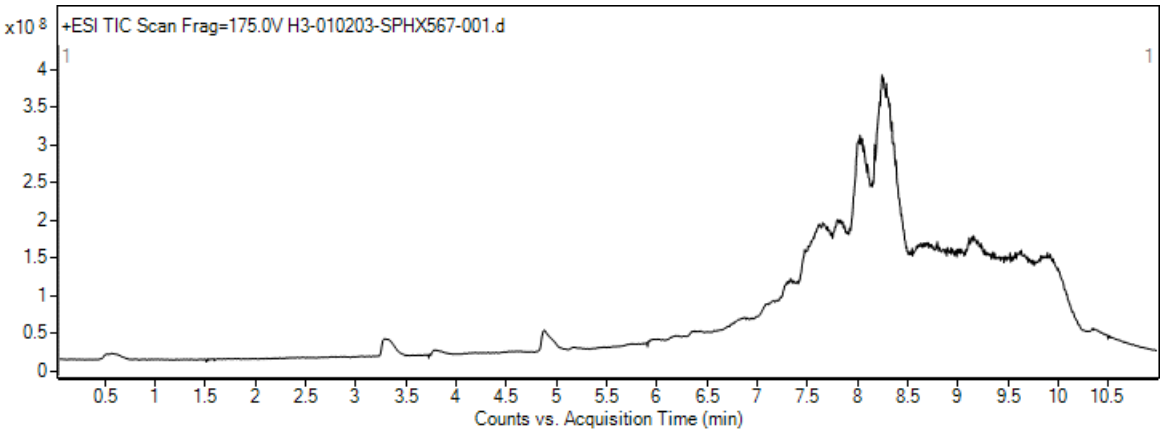

Figure 2.5.38: DAV-09-H3 re-Sephadex® Fraction LC-HRMS mass spectra

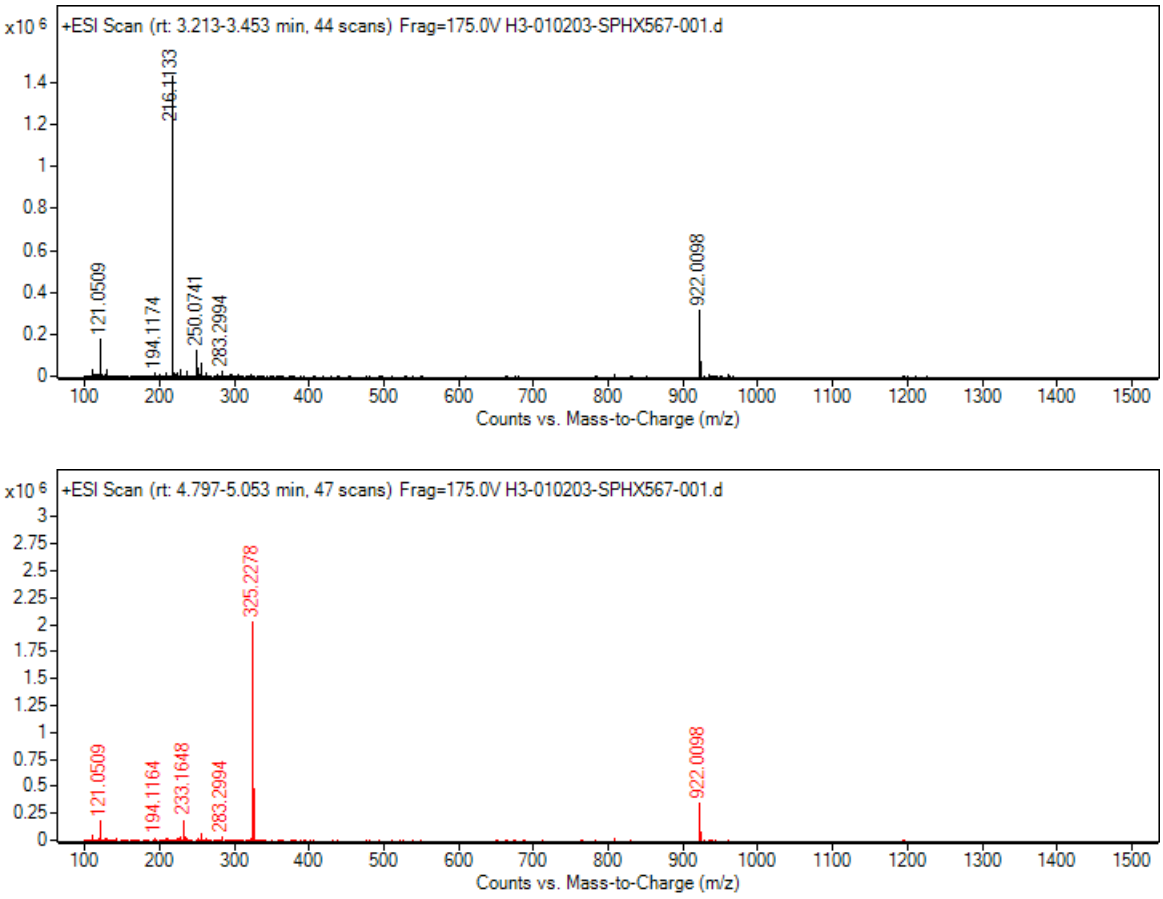

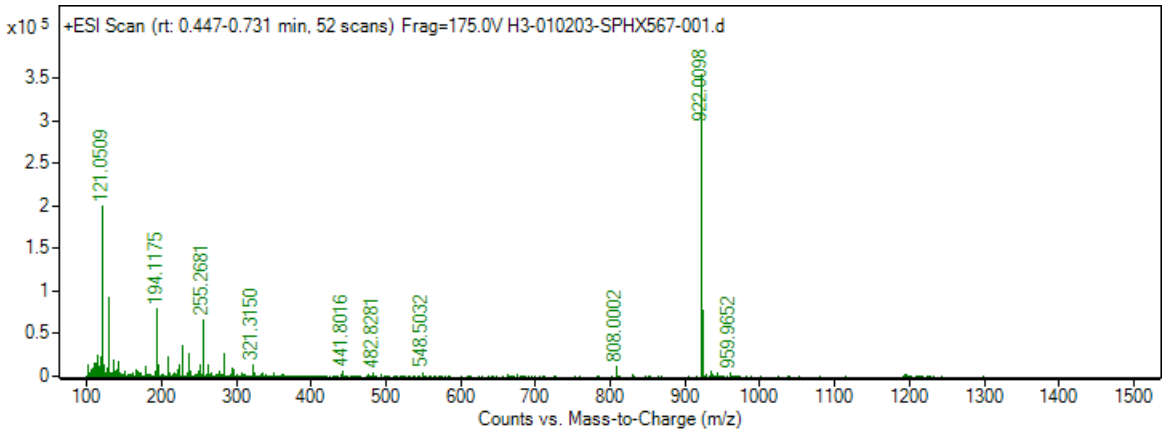

Figure 2.5.39: Method configuration for Agilent 6546 Quadrupole Time-of-Flight (Q-TOF) mass spectrometer

Acquisition Method Report — Agilent Technologies

TOF/Q-TOF Mass Spectrometer

Component Name	MS Q-TOF	**Component Model**	G6546A
Ion Source	Dual AJS ESI	**Stop Time (min)**	No Limit/As Pump
Can wait for temp.	Disable	**Fast Polarity**	False
MS Abs. threshold	200	**MS Rel. threshold(%)**	0.010
MS/MS Abs. threshold	5	**MS/MS Rel. threshold(%)**	0.010
BioConfirm Max Ent	No		

Time Segments

Time Segment #	Start Time (min)	Diverter Valve State	Storage Mode	Ion Mode
1	0	MS	Both	Dual AJS ESI

Time Segment 1

Acquisition Mode MS1

Min Range (m/z)	100
Max Range (m/z)	1500
Scan Rate (spectra/sec)	3.00

Instrument Parameters

Parameter	Value
Gas Temp (°C)	320
Gas Flow (l/min)	8
Nebulizer (psig)	35
SheathGasTemp	350
SheathGasFlow	11

Scan Segments

Scan Seg #	Ion Polarity	Collision Energy
1	Positive	0

Scan Segment 1

Scan Source Parameters

Parameter	Value
VCap	3500
Nozzle Voltage (V)	1000
Fragmentor	175
Skimmer1	65
OctopoleRFPeak	750

ReferenceMasses

Ref Mass Enabled	Enabled
Use Bottle A RefNebulizer	True
Ref Nebulizer (psig)	0

AutoRecalibration

Average Scans	1
Detection Window (ppm)	100
Min Height (counts)	1000

Reference Masses

<Positive>
121.05087300
922.00979800

Chromatograms

Chrom Type	Label	Expt. Type	Polarity Type	Offset	Y-Range
TIC	TIC	MS	Both	15	10000000

Report generation date: 1/4/2024 7:11:59 PM

Page 2 of 4

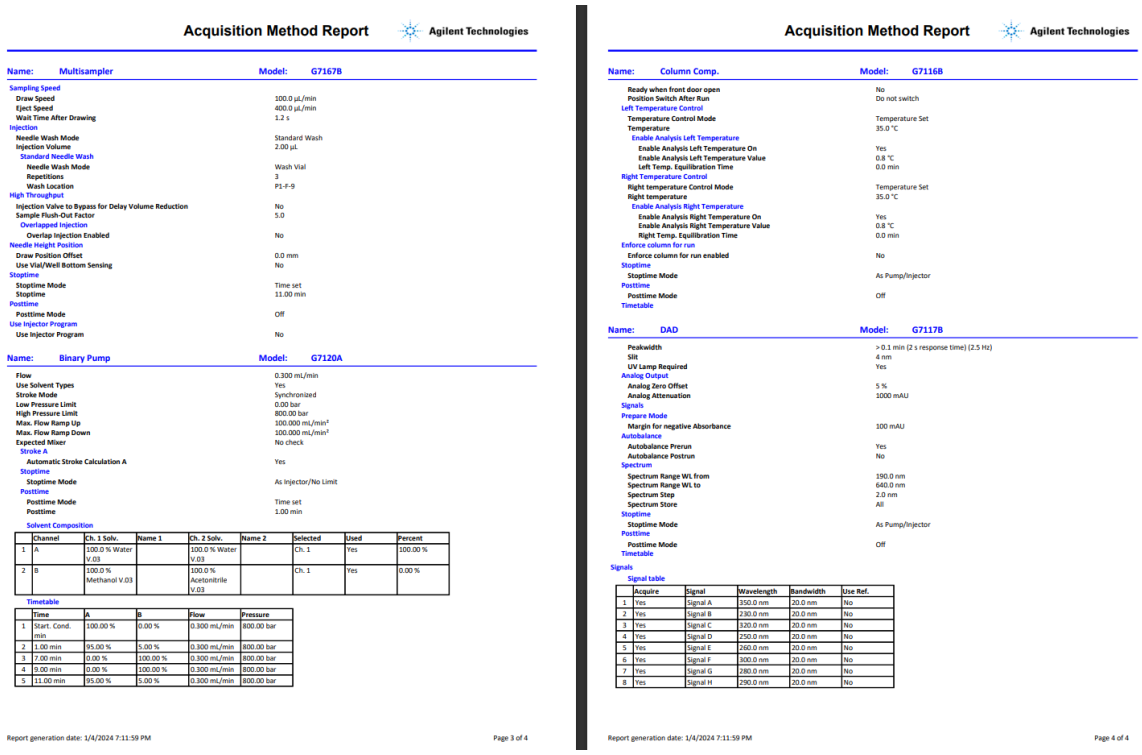

Acquisition Method Report — Agilent Technologies

Name: Multisampler — Model: G7167B

Sampling Speed	
Draw Speed	100.0 µL/min
Eject Speed	400.0 µL/min
Wait Time After Drawing	1.2 s
Injection	
Needle Wash Mode	Standard Wash
Injection Volume	2.00 µL
Standard Needle Wash	
Needle Wash Mode	Wash Vial
Repetitions	3
Wash Location	P1-F-9
High Throughput	
Injection Valve to Bypass for Delay Volume Reduction	No
Sample Flush-Out Factor	5.0
Overlapped Injection	
Overlap Injection Enabled	No
Needle Height Position	
Draw Position Offset	0.0 mm
Use Vial/Well Bottom Sensing	No
Stoptime	
Stoptime Mode	Time set
Stoptime	11.00 min
Posttime	
Posttime Mode	Off
Use Injector Program	
Use Injector Program	No

Name: Binary Pump — Model: G7120A

Flow	0.300 mL/min
Use Solvent Types	Yes
Stroke Mode	Synchronized
Low Pressure Limit	0.00 bar
High Pressure Limit	800.00 bar
Max. Flow Ramp Up	100.000 mL/min²
Max. Flow Ramp Down	100.000 mL/min²
Expected Mixer	No check
Stroke A	
Automatic Stroke Calculation A	Yes
Stoptime	
Stoptime Mode	As Injector/No Limit
Posttime	
Posttime Mode	Time set
Posttime	1.00 min

Solvent Composition

	Channel	Ch. 1 Solv.	Name 1	Ch. 2 Solv.	Name 2	Selected	Used	Percent
1	A	100.0 % Water V.03		100.0 % Water V.03		Ch. 1	Yes	100.00 %
2	B	100.0 % Methanol V.03		100.0 % Acetonitrile V.03		Ch. 1	Yes	0.00 %

Timetable

	Time	A	B	Flow	Pressure
1	Start. Cond. min	100.00 %	0.00 %	0.300 mL/min	800.00 bar
2	1.00 min	95.00 %	5.00 %	0.300 mL/min	800.00 bar
3	7.00 min	0.00 %	100.00 %	0.300 mL/min	800.00 bar
4	9.00 min	0.00 %	100.00 %	0.300 mL/min	800.00 bar
5	11.00 min	95.00 %	5.00 %	0.300 mL/min	800.00 bar

Report generation date: 1/4/2024 7:11:59 PM — Page 3 of 4

Acquisition Method Report — Agilent Technologies

Name: Column Comp. — Model: G7116B

Ready when front door open	No
Position Switch After Run	Do not switch
Left Temperature Control	
Temperature Control Mode	Temperature Set
Temperature	35.0 °C
Enable Analysis Left Temperature	
Enable Analysis Left Temperature On	Yes
Enable Analysis Left Temperature Value	0.8 °C
Left Temp. Equilibration Time	0.0 min
Right Temperature Control	
Right temperature Control Mode	Temperature Set
Right temperature	35.0 °C
Enable Analysis Right Temperature	
Enable Analysis Right Temperature On	Yes
Enable Analysis Right Temperature Value	0.8 °C
Right Temp. Equilibration Time	0.0 min
Enforce column for run	
Enforce column for run enabled	No
Stoptime	
Stoptime Mode	As Pump/Injector
Posttime	
Posttime Mode	Off
Timetable	

Name: DAD — Model: G7117B

Peakwidth	> 0.1 min (2 s response time) (2.5 Hz)
Slit	4 nm
UV Lamp Required	Yes
Analog Output	
Analog Zero Offset	5 %
Analog Attenuation	1000 mAU
Signals	
Prepare Mode	
Margin for negative Absorbance	100 mAU
Autobalance	
Autobalance Prerun	Yes
Autobalance Postrun	No
Spectrum	
Spectrum Range WL from	190.0 nm
Spectrum Range WL to	640.0 nm
Spectrum Step	2.0 nm
Spectrum Store	All
Stoptime	
Stoptime Mode	As Pump/Injector
Posttime	
Posttime Mode	Off
Timetable	

Signals

Signal table

	Acquire	Signal	Wavelength	Bandwidth	Use Ref.
1	Yes	Signal A	350.0 nm	20.0 nm	No
2	Yes	Signal B	230.0 nm	20.0 nm	No
3	Yes	Signal C	320.0 nm	20.0 nm	No
4	Yes	Signal D	250.0 nm	20.0 nm	No
5	Yes	Signal E	260.0 nm	20.0 nm	No
6	Yes	Signal F	300.0 nm	20.0 nm	No
7	Yes	Signal G	280.0 nm	20.0 nm	No
8	Yes	Signal H	290.0 nm	20.0 nm	No

Report generation date: 1/4/2024 7:11:59 PM — Page 4 of 4

Figure 2.5.40: Enzyme kinetics controls *Streptomyces* (black/red) and *Trichoderma* (green) comparison

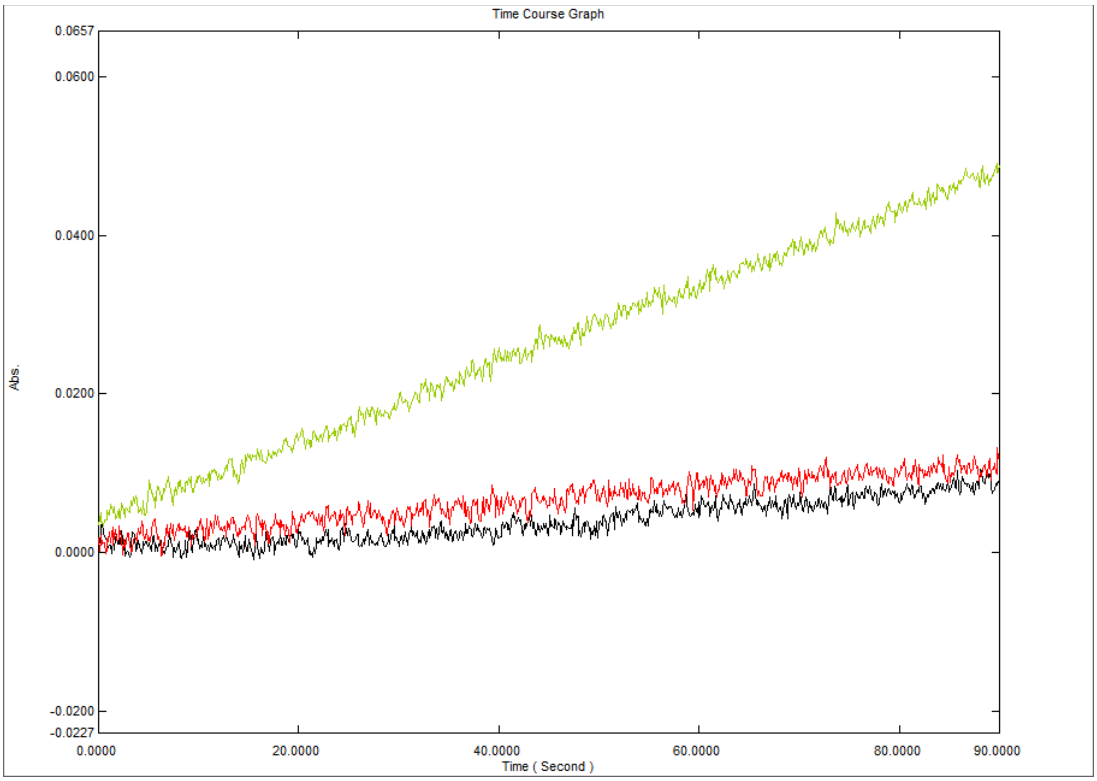

Figure 2.5.41: Strep. Enzyme kinetics of Makaluvamine A (blue)

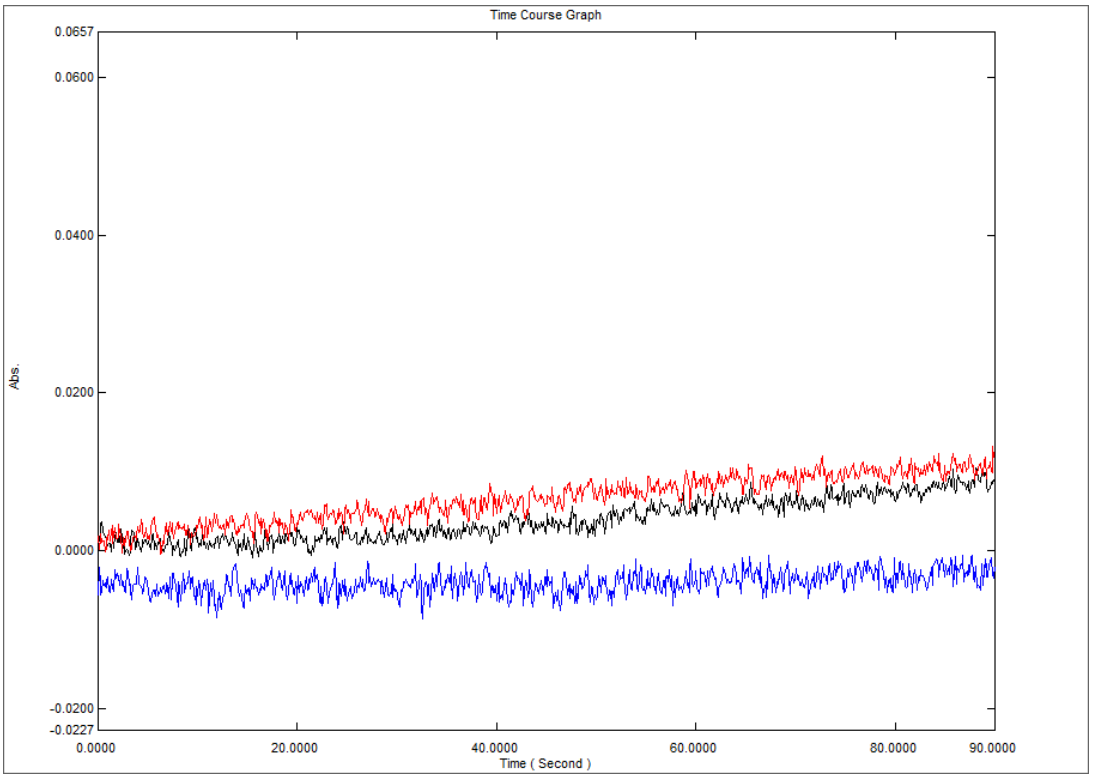

Figure 2.5.42: Strep. Enzyme kinetics Makaluvamine A (maroon) – diluted.

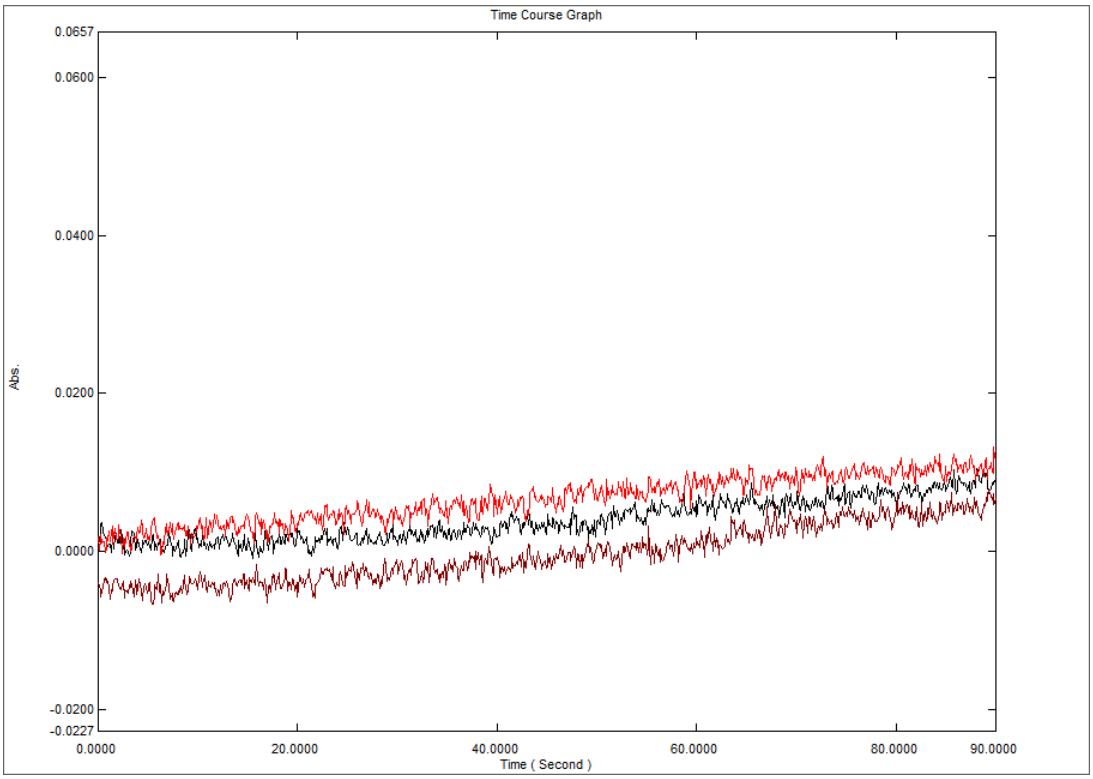

Figure 2.5.43: Strep. Enzyme kinetics Makaluvamine C (green)

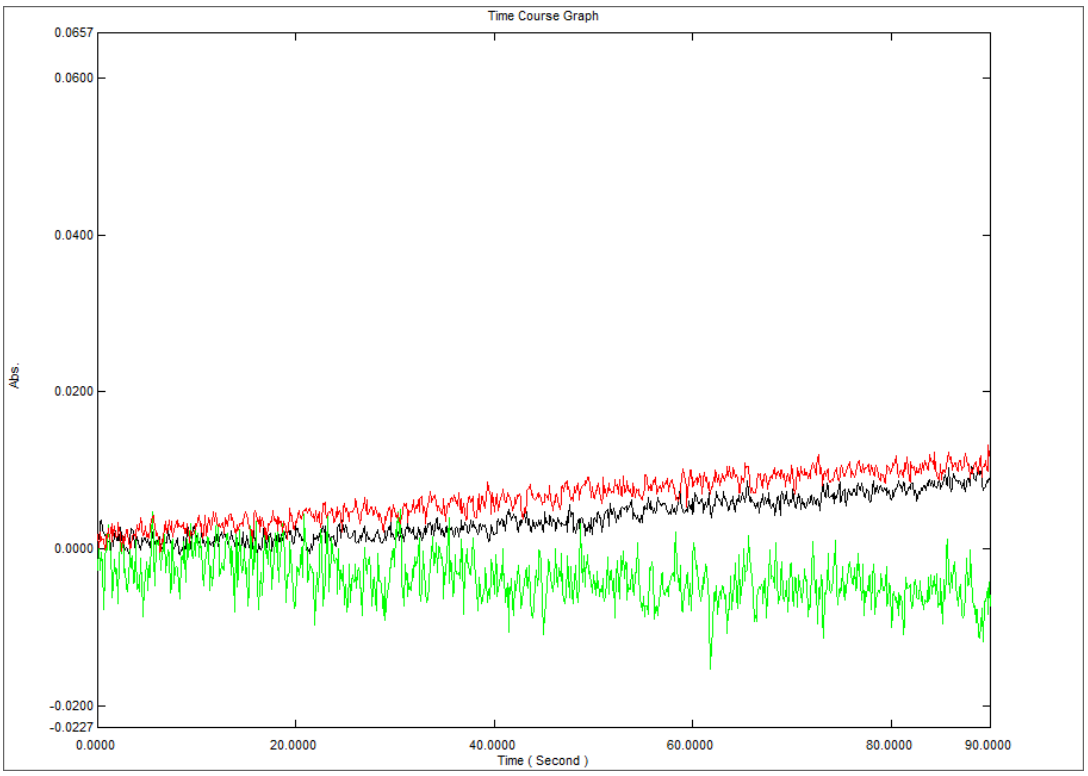

Figure 2.5.44: Strep. Enzyme kinetics Makaluvamine C (purple) – diluted.

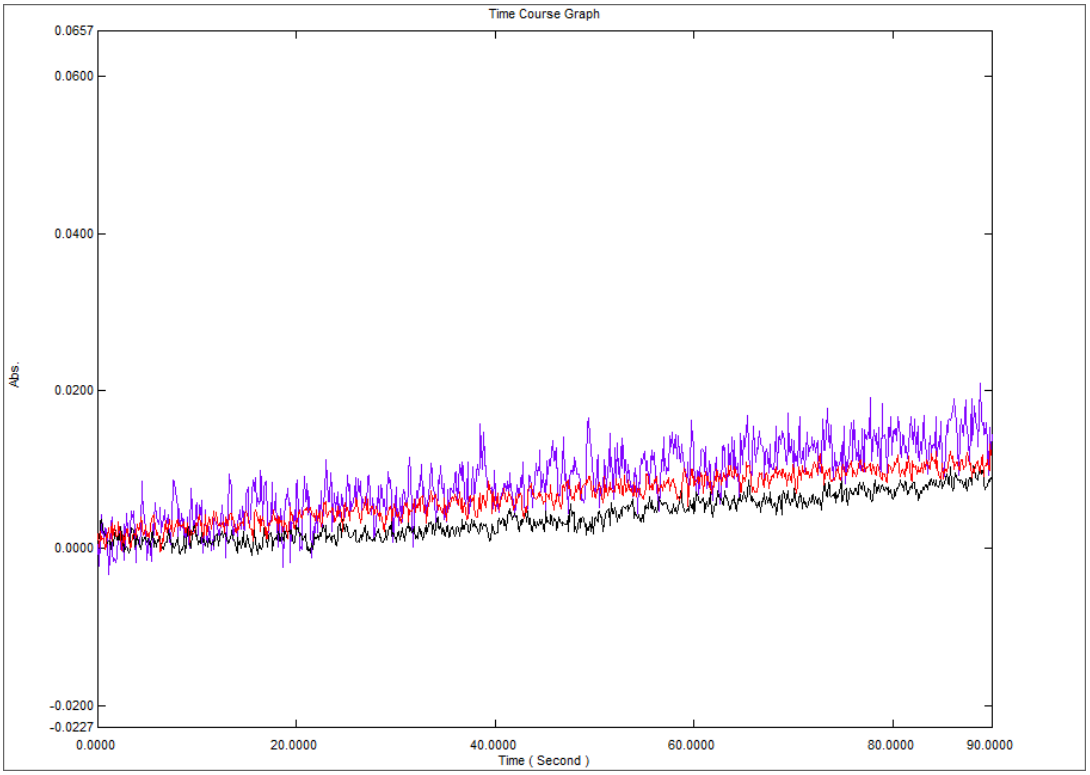

Figure 2.5.45: Strep. Enzyme kinetics Makaluvamine H (orange)

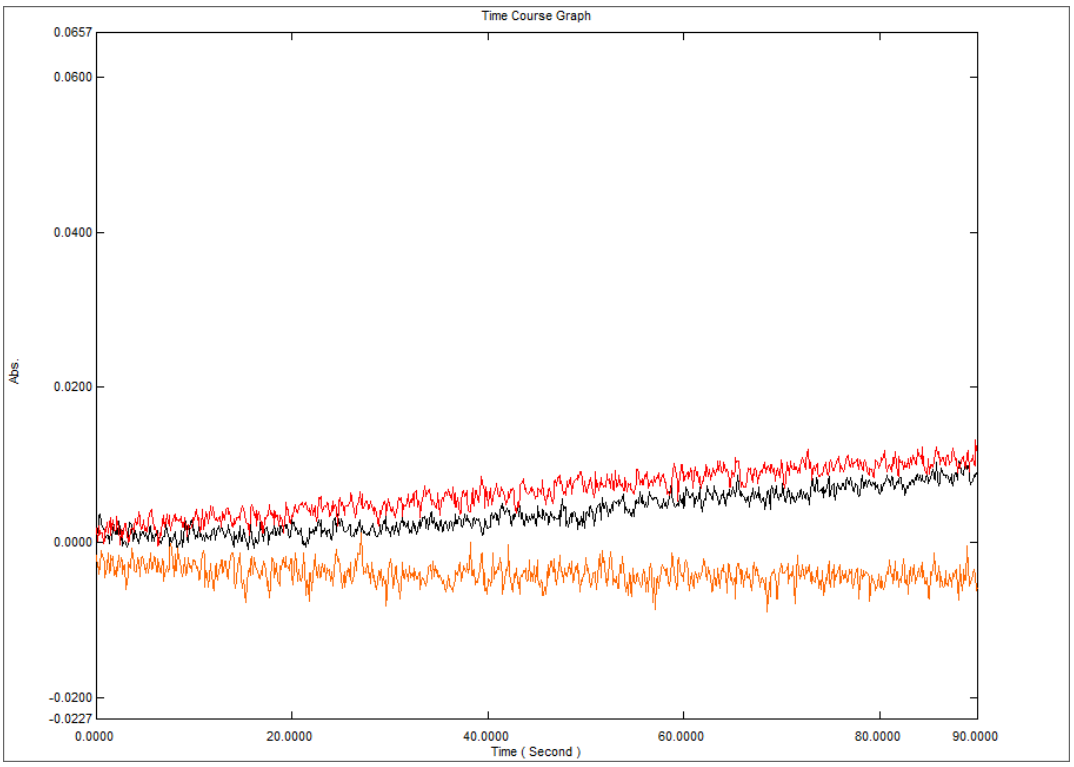

Figure 2.5.46: Strep. Enzyme kinetics Makaluvamine H (purple) – diluted.

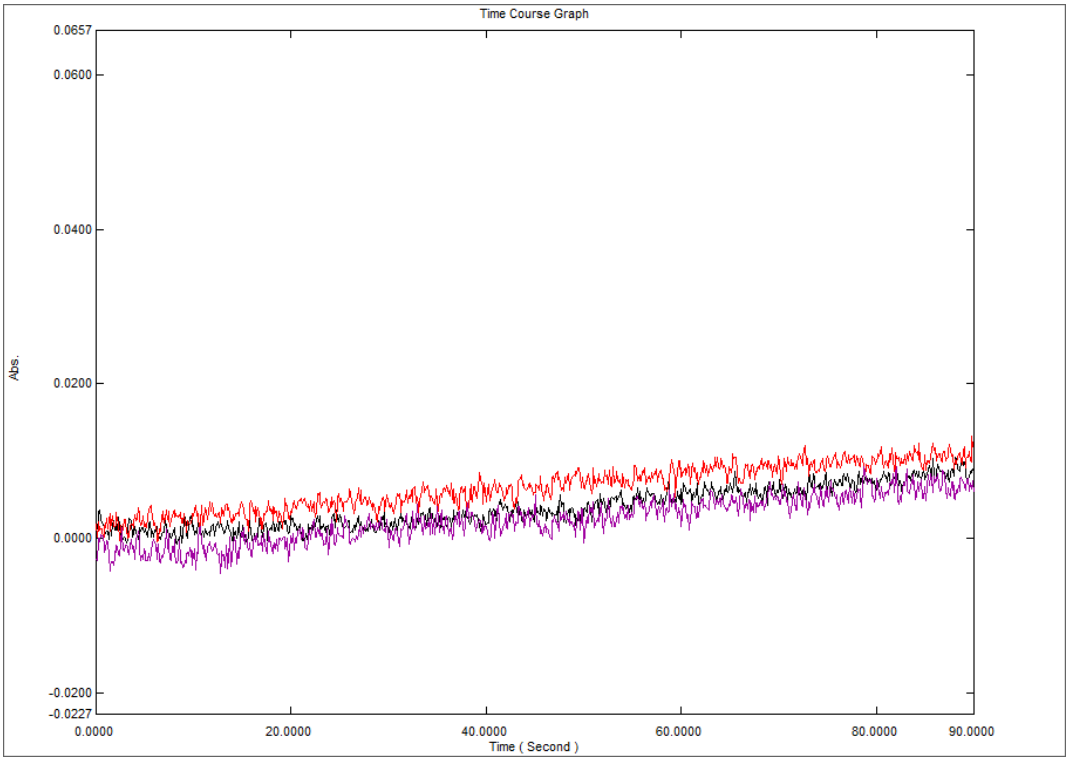

Figure 2.5.47: Strep. Enzyme kinetics Makaluvamine P (pink)

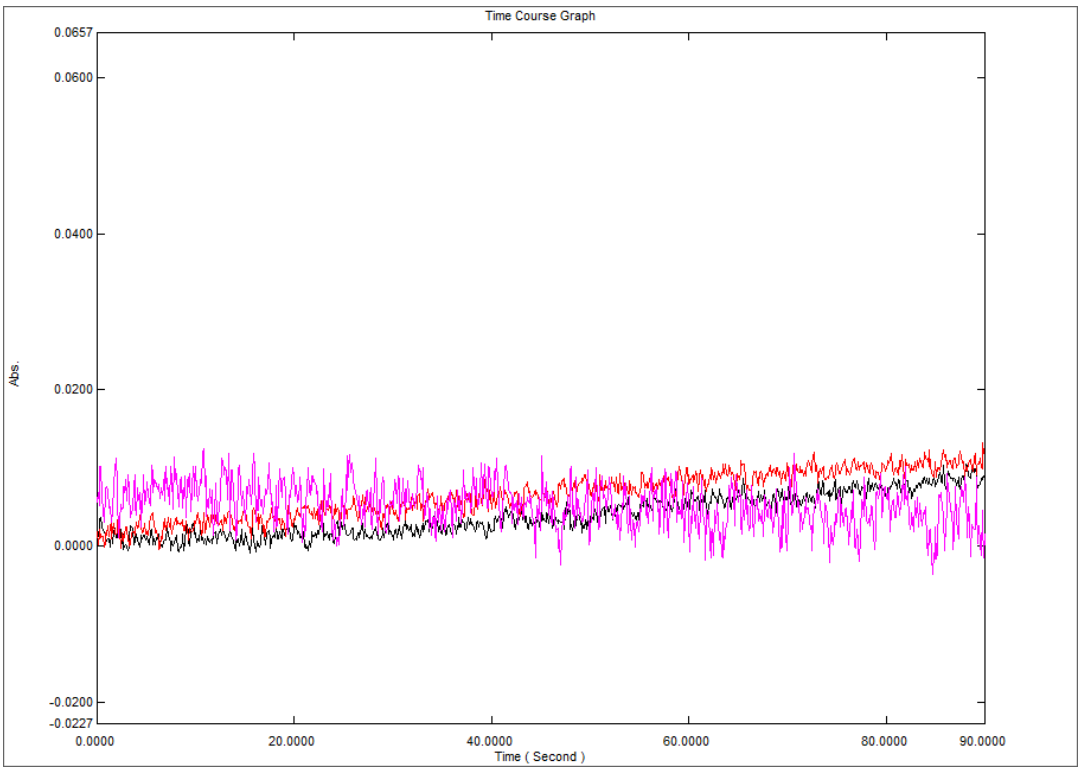

Figure 2.5.48: Strep. Enzyme kinetics Makaluvamine P (grey) – dilution 1

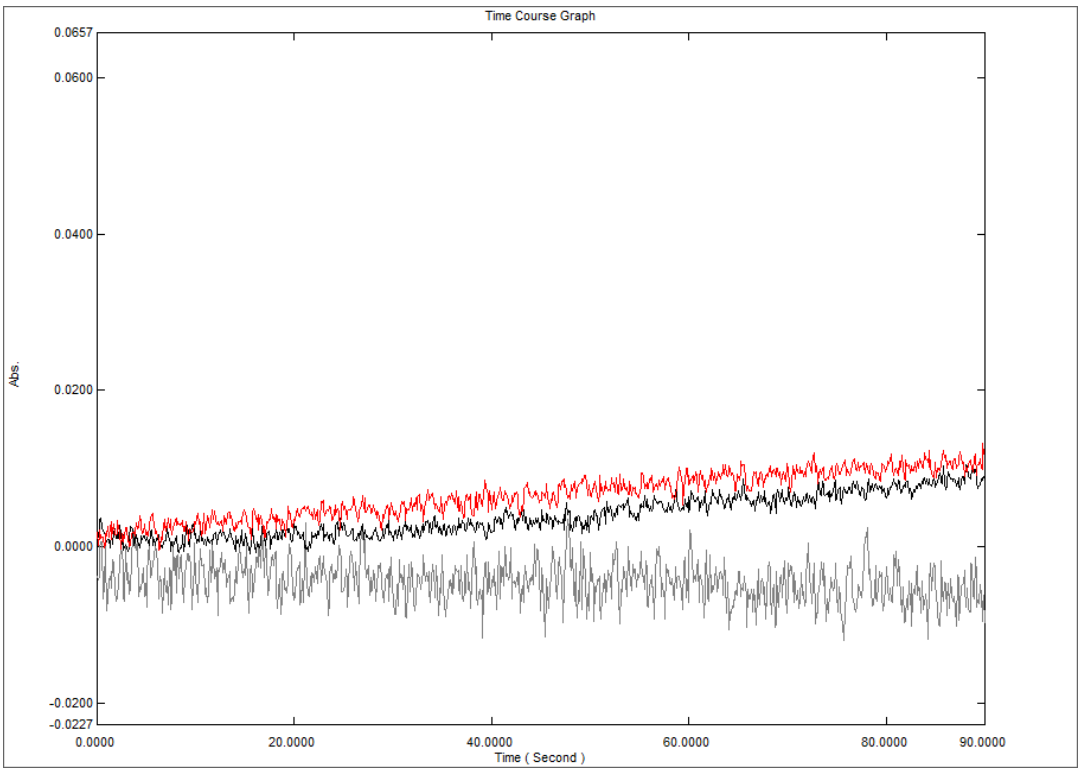

Figure 2.5.49: Strep. Enzyme kinetics Makaluvamine P (teal) – dilution 2

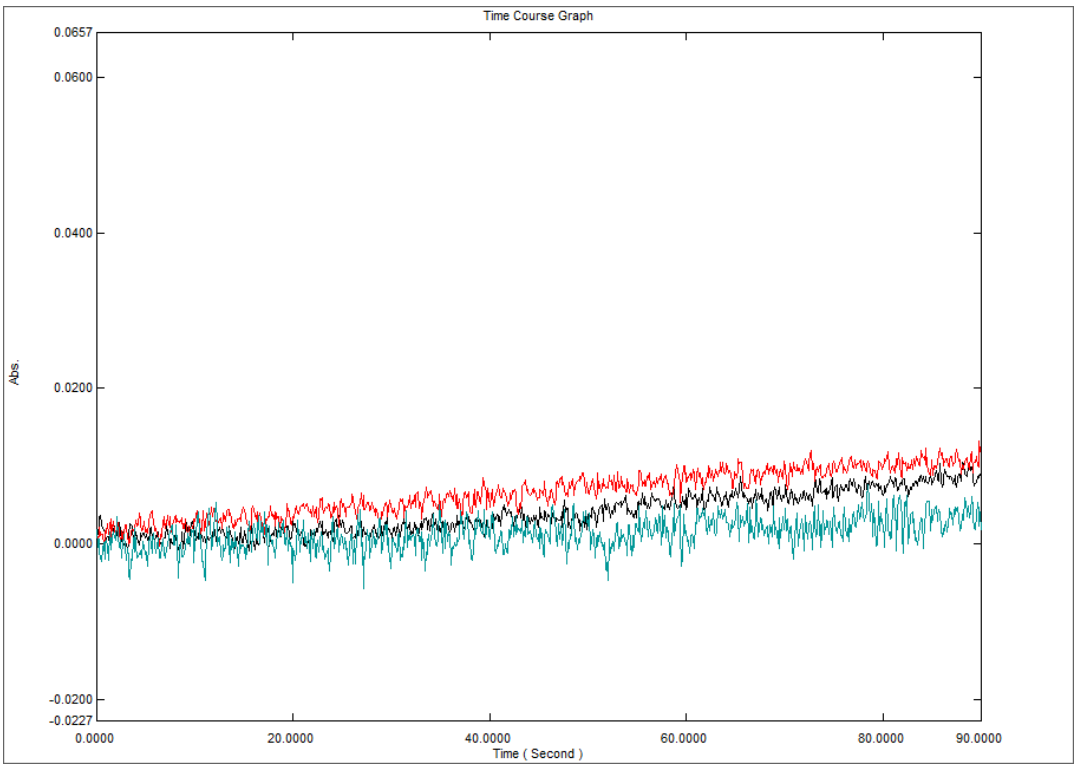

Figure 2.5.50: Trich. Enzyme kinetics Makaluvamine C (black)

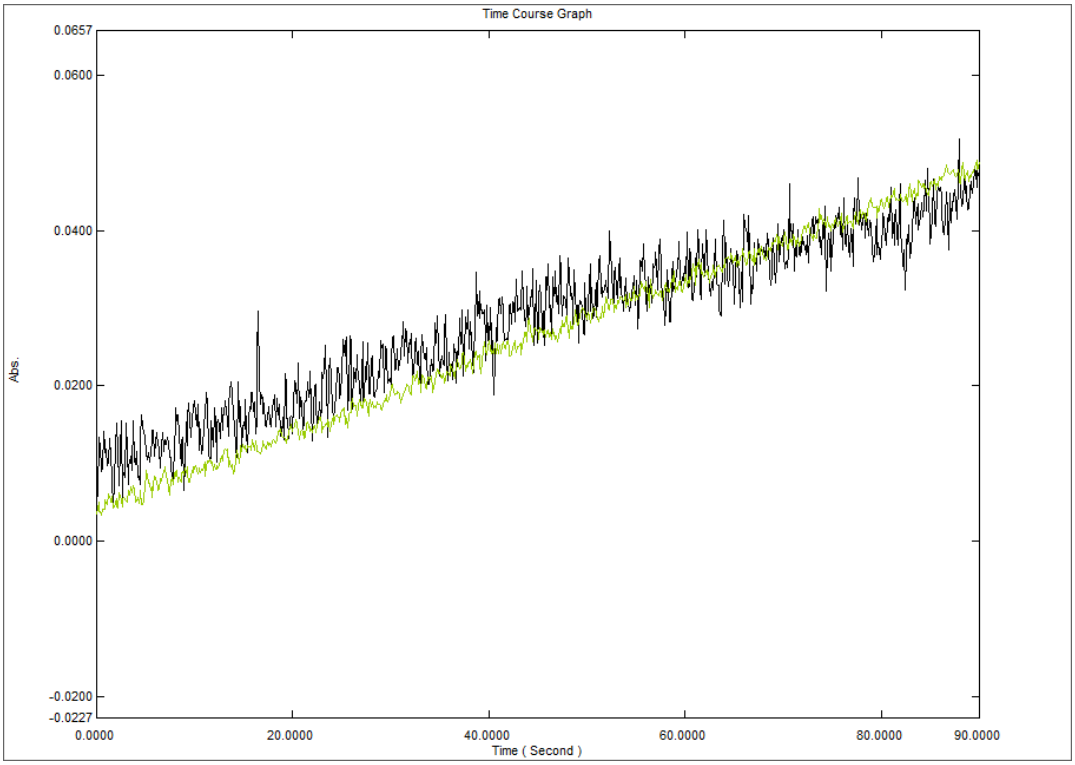

Figure 2.5.51: Trich. Enzyme kinetics Makaluvamine H (red)

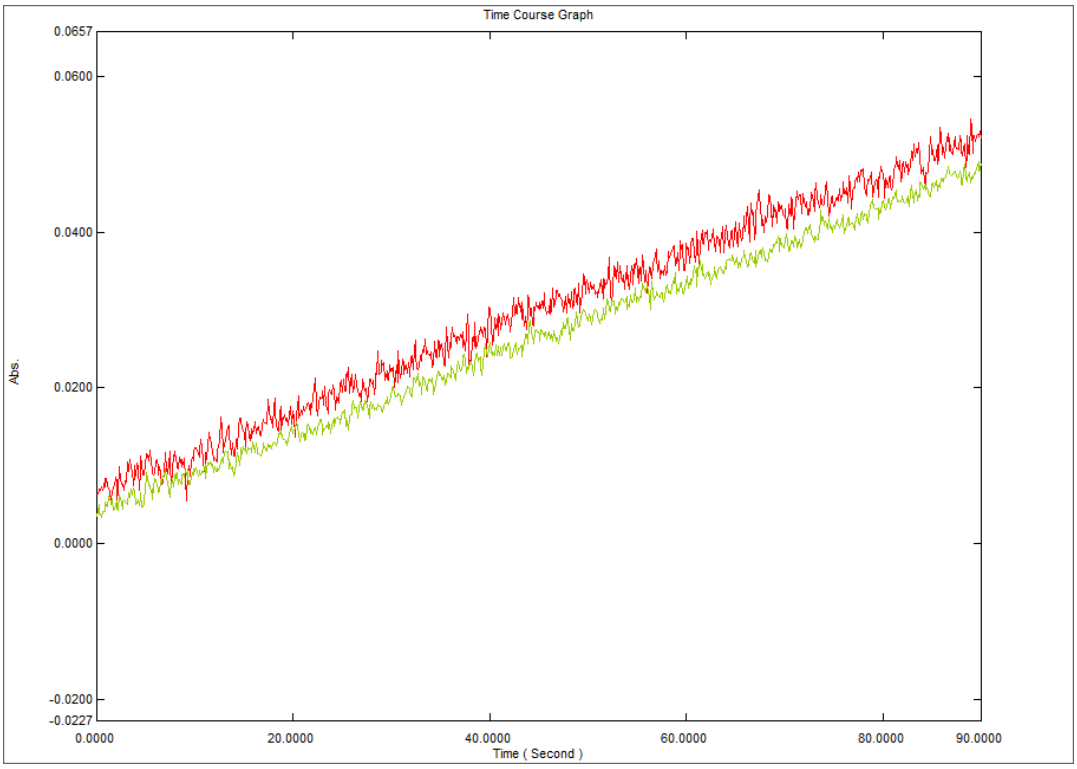

Figure 2.5.52: Trich. Enzyme kinetics Makaluvamine H (yellow) – diluted.

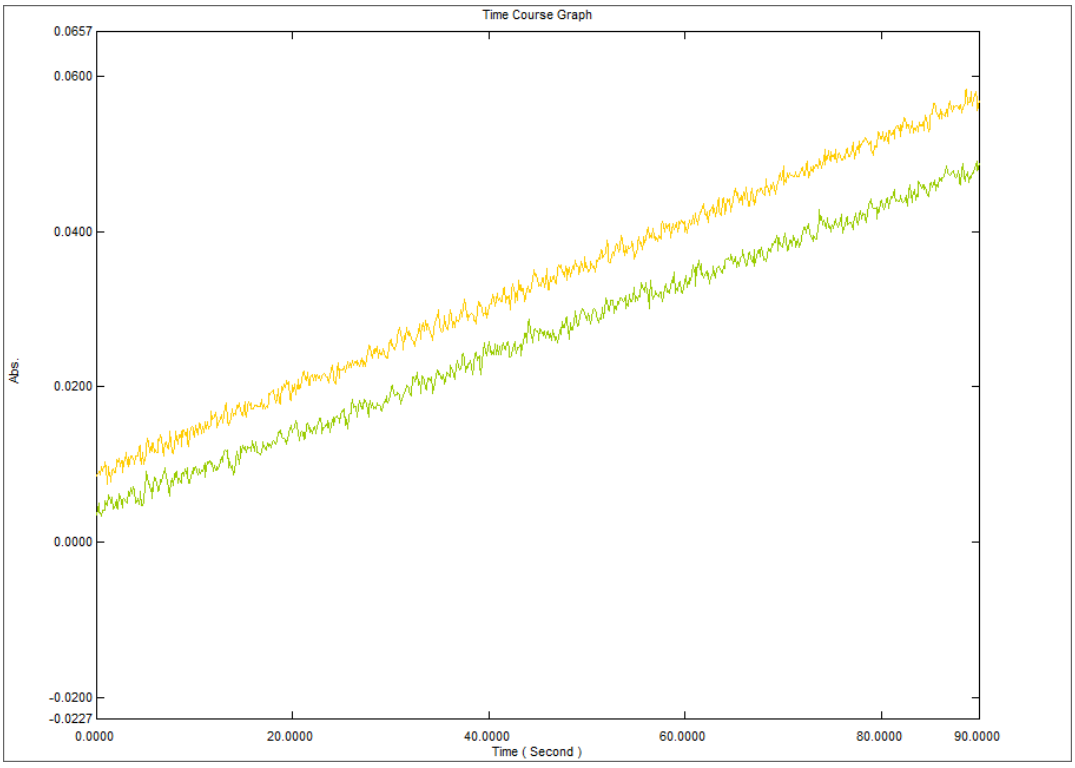

Figure 2.5.53: Chemical structure of 4-Nitrophenyl *N*, *N*'-diacetyl-β-D-chitobioside [73]

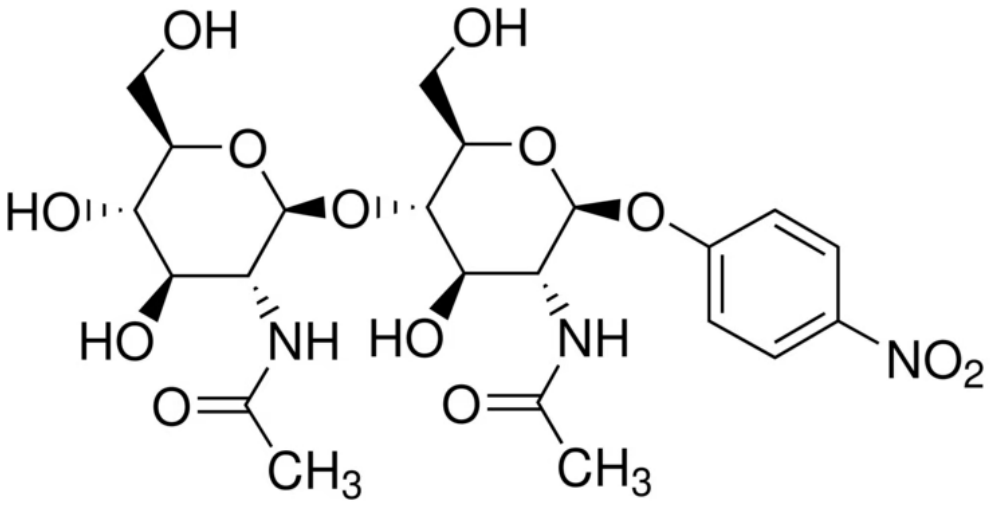

Figure 2.5.54: Chemical structures of select members of the Makaluvamine family [74]

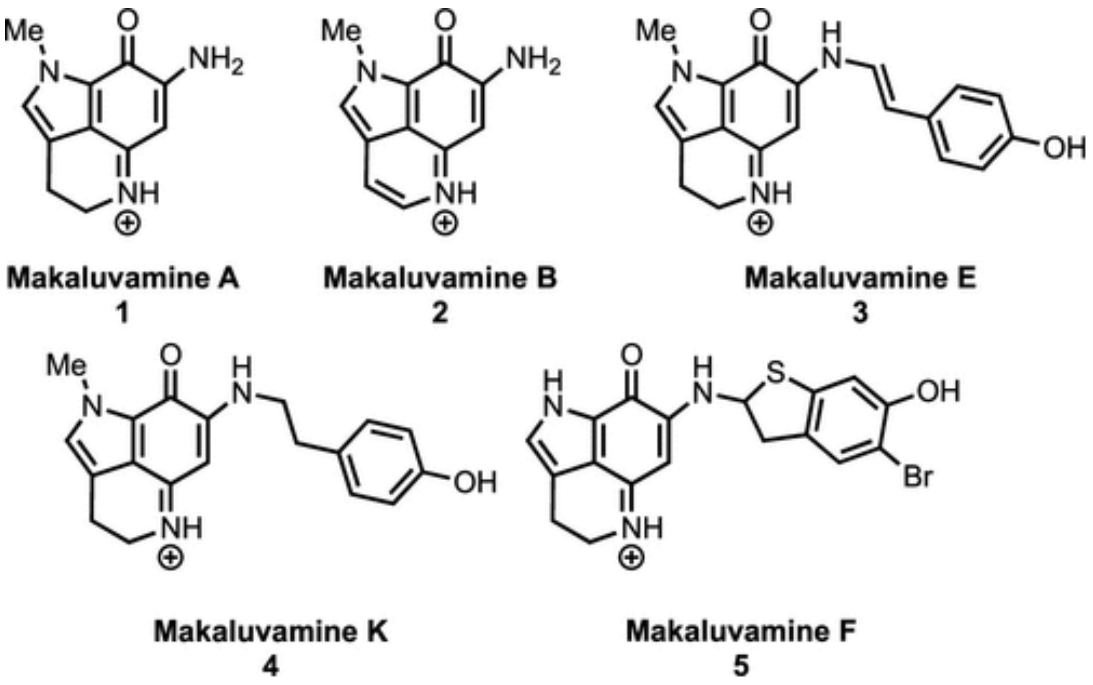

Figure 2.5.55: Chemical structures of 14 Makaluvamine analogues (A) free pyrrole NH and (B) tosyl group on pyrrole N [69]

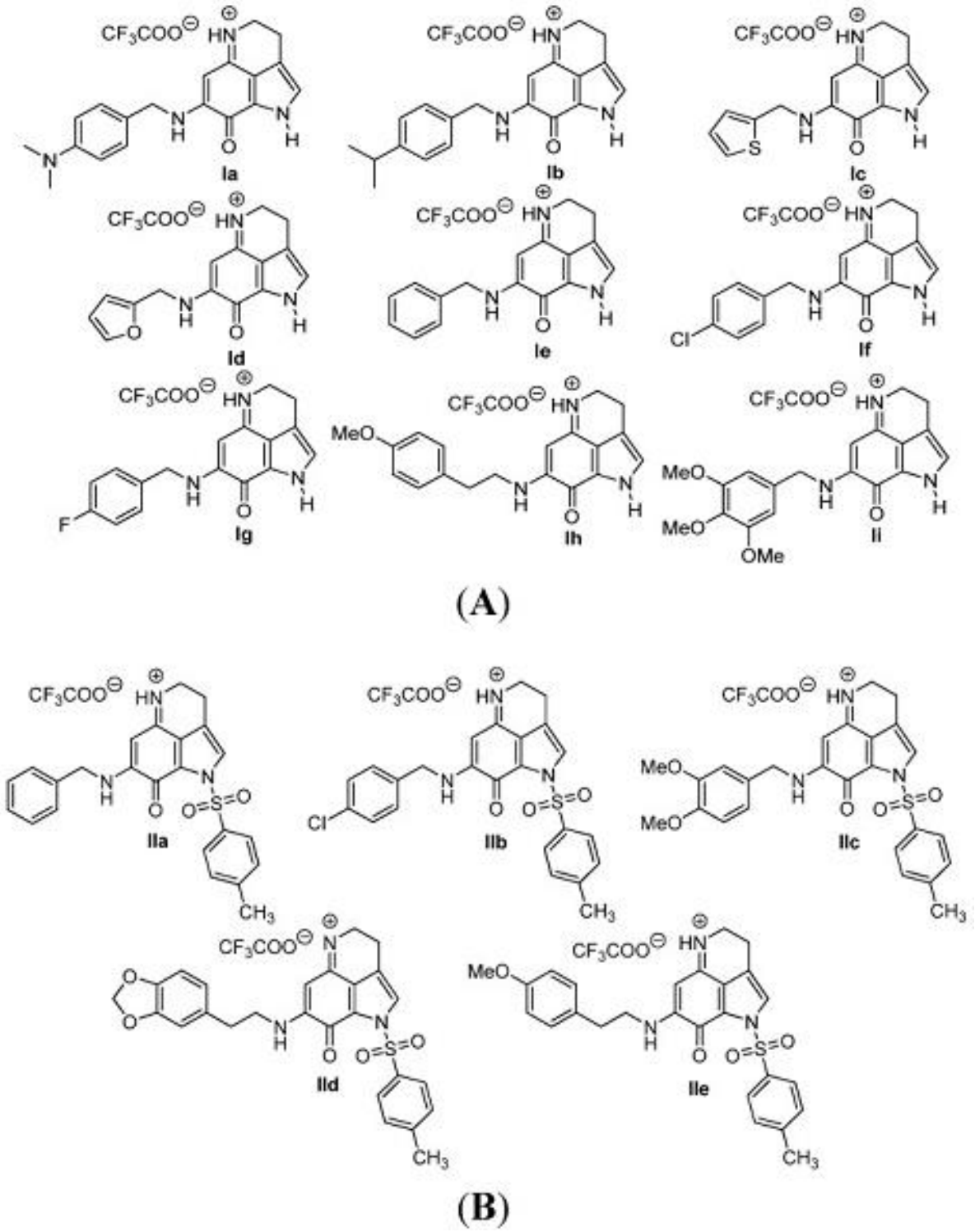

Figure 2.5.56: Comprehensive flow chart overview of the purification scheme.

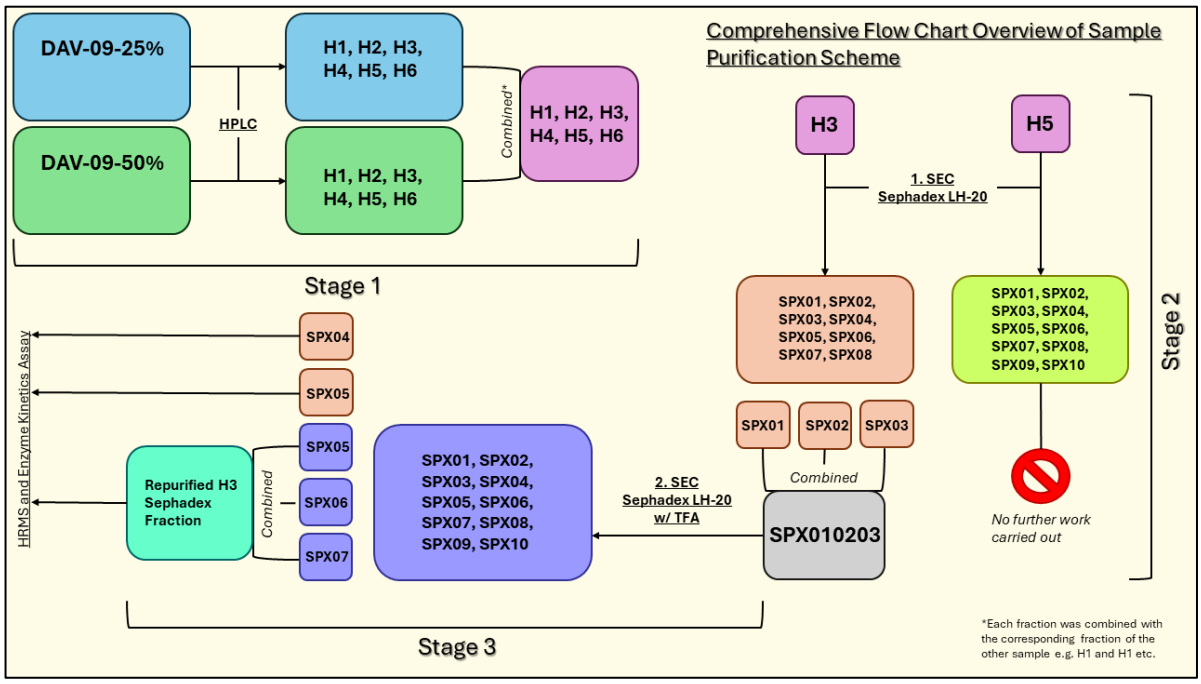

2.6 References

1. Dias DA, Urban S, Roessner U. A Historical Overview of Natural Products in Drug Discovery. Metabolites. 2012; 2(2): 303 – 336.

2. Demain AL, Vaishnav P. Natural Products for Cancer Chemotherapy. Microbial Biotechnology. 2011; 4(6): 687 – 699.

3. National Cancer Institute. Natural Products. Centre for Cancer Research. [Website]. 2023 (Cited). Available from: https://ccr.cancer.gov/news/horizons/article/natural-products#:~:text=Natural%20products%20have%20given%20us,isolated%20from%20a%20sea%20squirt.

4. Demain AL, Fang A. The Natural Functions of Secondary Metabolites. Advances in Biochemical Engineering and Biotechnology. 2000; 69: 1 – 39.

6. Solecki RS. Shanidar IV, a Neanderthal Flower Burial in Northern Iraq. Science. 1975; 190(4217): 880 – 881.

7. Ji HF, Li XJ, Zhang HY. Natural Products and Drug Discovery. Can Thousands of Years of Ancient Medical Knowledge Lead us to New and Powerful Drug Combinations in the Fight Against Cancer and Dementia? EMBO Reports. 2009; 10(3): 194 – 200.

8. Atanasov AG, Zotchev SB, Dirsch VM, Supuran CT. Natural Products in Drug Discovery: Advances and Opportunities. Nature Reviews Drug Discovery. 2021; 20(3): 200 – 216.

9. Norn S, Permin H, Kruse PR, Kruse E. From Willow Bark to Acetylsalicylic Acid. Dansk Medicinhistorisk Arbog. 2009; 37: 79 – 98.

10. Murphy PB, Bechmann S, Barrett MJ. Morphine. StatPearls Publishing. 2023.

12. Christensen SB. Natural Products That Changed Society. Biomedicines. 2021; 9(5).

13. NCI Staff. Nature's Bounty: Revitalizing the Discovery of New Cancer Drugs from Natural Products. National Cancer Institute. 2019. [Website]. 2023 (Cited).

    Available from:

    https://www.cancer.gov/news-events/cancer-currents-blog/2019/cancer-drugs-natural-products-nci-

program#:~:text=Paclitaxel%20(Taxol)%2C%20for%20example,from%20compounds%20found%20in%20fungi.

15. Govardhanagiri S, Bethi S, Nagaraju GP. Small Molecules and Pancreatic Cancer Trials and Troubles. Breaking Tolerance to Pancreatic Cancer Unresponsiveness to Chemotherapy. 2019; 117 – 131.

16. Tewari D, Atanasov AG, Semwal P, Wang D. Natural Products and Their Applications. Current Research in Biotechnology. 2021; 3: 82 – 83.

17. Cancer Research UK. Cancer Statistics for the UK. [Website]. 2023 (Cited). Available from: https://www.cancerresearchuk.org/health-professional/cancer-statistics-for-the-uk

19. Cancer Research UK. Trabectedin (Yondelis). 2022. [Website]. 2023 (Cited). Available from: https://www.cancerresearchuk.org/about-cancer/treatment/drugs/trabectedin

20. Cragg GM, Newman DJ. Biodiversity: A Continuing Source of Novel Drug leads. Pure and Applied Chemistry. 2005; 77(1): 7 – 24.

21. Zhong G, Wan F. An Outline on the Early Pharmaceutical Development Before Galen]. Zhonghua Yi Shi Za Zhi. 1999; 29(3): 178 – 182.

22. Newman DJ, Cragg GM, Snader KM. The Influence of Natural Products Upon Drug Discovery (Antiquity to Late 1999). Natural Product Reports. 2000; 17(3): 215 – 234.

24. Liang X, Luo D, Luesch H. Advances in Exploring the Therapeutic Potential of Marine Natural Products. Pharmacological Research. 2019; 14(7): 104 - 373.

25. McGivern JG. Ziconotide: a Review of its Pharmacology and Use in the Treatment of Pain. Neuropsychiatric Disease and Treatment. 2007; 3(1): 69 – 85.

26. PharmaMar. Plitidepsin. 2022. [Website]. 2023 (Cited).

Available from: https://pharmamar.com/en/products/aplidin/

27. Elgoud Said AA, Mahmoud BK, Attia EZ, Abdelmohsen UR, Fouad MA. Bioactive Natural Products from Marine Sponges Belonging to Family Hymedesmiidae. RSC Advances. 2021; 11(27): 16179 – 16191.

28. Utkina NK, Makarchenko AE, Denisenko VA. Zyzzyanones B-D, Dipyrroloquinones from the Marine Sponge Zyzzya Fuliginosa. Journal of Natural Products. 2005; 68(9): 1424 – 1427.

29. Sipkema D, Franssen MCR, Osinga R, Tramper J, Wijffels RH. Marine Sponges as Pharmacy. Marine Biotechnology (NY). 2005; 7(3): 142 – 162.

30. Abdelaleem ER, Samy MN, Desoukey SY, Liu M, Quinn RJ, Abdelmohsen UR. Marine Natural Products from Sponges (Porifera) of the Order Dictyoceratida: A Promising Source for Drug Discovery. RSC Advances. 2020; 10(57):34959 – 34976.

31. Cancer Research UK. Cytarabine (Ara-C, Cytosine Arabinoside). [Website]. 2023 (Cited).

Available from: https://www.cancerresearchuk.org/about-cancer/treatment/drugs/cytarabine

32. El Gamal AA. Biological Importance of Marine Algae. Saudi Pharmaceutical Journal. 2010; 18(1): 21 – 25.

33. Mahmoud AM, Bin-Jumah M, Abukhalil MH. Anti-Inflammatory Natural Products from Marine Algae. Inflammation and Natural Products. 2021; 131 – 159.

34. Davis A, Robson J. The Dangers of NSAIDs: Look Both Ways. British Journal of General Practice. 2016; 66(645): 172 – 173.

35. National Geographic Society. Ocean. National Geographic. [Website]. 2023 (Cited). Available from: https://education.nationalgeographic.org/resource/ocean/

36. Marta Fava. How Much of the Ocean Has Been Explored? Ocean Literacy Portal: Unesco. 2022. [Website]. 2023 (Cited).

Available from:

https://oceanliteracy.unesco.org/ocean-exploration/#:~:text=It%20might%20be%20shocking%20to,ocean%20exploration%20throughout%20the%20centuries.

37. Becky Oskin. Mariana Trench: The Deepest Depths. LiveScience. 2022. [Website]. 2023 (Cited).

Available from: https://www.livescience.com/23387-mariana-trench.html

38. Newman DJ, Cragg GM. Natural Products of Therapeutic Importance. Comprehensive Natural Products II. 2010; 623 – 650.

39. Yan Y, Liu Q, Jacobsen SE, Tang Y. The Impact and Prospect of Natural Product Discovery in Agriculture. EMBO Reports. 2018; 19(11).

40. Agrios GN. Plant Diseases Caused by Prokaryotes: Bacteria and Mollicutes. Plant Pathology. 2005; 615 – 703.

41. San-Martin A, Negrete R, Rovirosa J. Insecticide and Acaricide Activities of Polyhalogenated Monoterpenes from Chilean Plocamium Cartilagineum. Phytochemistry. 1991; 30(7): 2165 – 2169.

42. Canola Council of Canada. Canola Encyclopedia. Aster Leafhopper. [Website]. 2023 (Cited).

Available from: https://www.canolacouncil.org/canola-encyclopedia/insects/aster-leafhopper/

43. Fukuzawa A, Masamune T. Laurepinnacin and Isolaurepinnacin: New Acetylenic Cyclic Ethers from the Marine Red Alga Yamada. Tetrahedron Letters. 1981; 22(41): 4081 – 4084.

44. Kirst HA. The Spinosyn Family of Insecticides: Realizing the Potential of Natural Products Research. Journal of Antibiotics (Tokyo). 2010; 63(3): 101 – 111.

45. Owen WJ, Yao C, Myung K, Kemmitt G, Leader A, Meyer KG, et al. Biological Characterization of Fenpicoxamid, a New Fungicide with Utility in Cereals and Other Crops. Pest Management Science. 2017; 73(10): 2005 – 2016.

46. Bhattacharyya C, Roy R, Tribedi P, Ghosh A, Ghosh A. Biofertilizers as Substitute to Commercial Agrochemicals. Agrochemicals Detection, Treatment and Remediation. 2020; 263–90.

47. Tripathi S, Srivastava P, Devi RS, Bhadouria R. Influence of Synthetic Fertilizers and Pesticides on Soil Health and Soil Microbiology. Agrochemicals Detection, Treatment and Remediation. 2020; 25 – 54.

48. Manjunath R, Hemavathi, Reddy NT, Chaithra C, Mishra P. Pesticides and its Toxicity. Encyclopedia of Toxicology. 2024; 7: 419 – 428.

49. Nijampatnam B, Dutta S, Velu SE. Recent Advances in Isolation, Synthesis, and Evaluation of Bioactivities of Bispyrroloquinone Alkaloids of Marine Origin. Chinese Journal of Natural Medicine. 2015; 13(8): 561 – 577.

50. Zhang QW, Lin LG, Ye WC. Techniques for Extraction and Isolation of Natural Products: A Comprehensive Review. Chinese Medicine. 2018; 13(1): 20.

51. Ito T, Masubuchi M. Dereplication of Microbial Extracts and Related Analytical Technologies. Journal of Antibiotics (Tokyo). 2014; 67(5): 353 – 360.

52. Avery VM, Camp D, Carroll AR, Jenkins ID, Quinn RJ. The Identification of Bioactive Natural Products by High Throughput Screening (HTS). Comprehensive Natural Products II. 2010; 3: 177 – 203.

53. Reynolds WF. Natural Product Structure Elucidation by NMR Spectroscopy. Pharmacognosy. 2017; 567–96.

54. Attene-Ramos MS, Austin CP, Xia M. High Throughput Screening. Encyclopedia of Toxicology. 2014; 916 – 917.

55. Perera N, Hikkaduwa Koralege RS. High Throughput Screening. Encyclopedia of Toxicology. 2024; 297–301.

56. Jia Q. Generating and Screening a Natural Product Library for CYclooxygenase and Lipoxygenase Dual Inhibitors. Studies in Natural Products Chemistry. 2003; 29: 643 – 718.

57. ThermoFisher Scientific Inc. High-Throughput Screening (HTS) for Drug Discovery. [Website]. 2023 (Cited).

Available from: https://www.thermofisher.com/uk/en/home/industrial/pharma-biopharma/drug-discovery-development/screening-compounds-libraries-hit-identification/high-throughput-screening-drug-discovery.html

58. Farooq S, Mir SA, Shah MA, Manickavasagan A. Extraction Techniques. Plant Extracts: Applications in the Food Industry. 2022; 23–37.

59. Popova M, Bankova V. Contemporary Methods for the Extraction and Isolation of Natural Products. BMC Chemistry. 2023; 17(1): 68.

60. Aurora Instruments Ltd. Aurora Biomed Inc. A Breakdown of Liquid-Liquid Extraction and Solid Phase Extraction. [Website]. 2023 (Cited). Available from: https://www.aurorabiomed.com/a-breakdown-of-liquid-liquid-extraction-and-solid-liquid-extraction/

61. Elieh-Ali-Komi D, Hamblin MR. Chitin and Chitosan: Production and Application of Versatile Biomedical Nanomaterials. International Journal of Advanced Research (Indore). 2016; 4(3): 411 – 427.

62. Song EH, Shang J, Ratner DM. Polysaccharides. Polymer Science: A Comprehensive Reference. 2012; 9: 137 – 55.

63. Hamid R, Khan MA, Ahmad M, Ahmad MM, Abdin MZ, Musarrat J, et al. Chitinases: An Update. Journal of Pharmacy and BioAllied Sciences. 2013; 5(1): 21 – 29.

64. Rathore AS, Gupta RD. Chitinases from Bacteria to Human: Properties, Applications, and Future Perspectives. Enzyme Research. 2015; 7(9): 190 - 197.

65. Suzuki S, Nakanishi E, Ohira T, Kawachi R, Nagasawa H, Sakuda S. Chitinase Inhibitor Allosamidin is a Signal Molecule for Chitinase Production in its Producing Streptomyces I: Analysis of the Chitinase whose Production is Promoted by Allosamidin and Growth Accelerating Activity of Allosamidin. The Journal of Antibiotics (Tokyo). 2006; 59(7): 402 – 409.

66. Hirose T, Sunazuka T, Omura S. Recent Development of Two Chitinase Inhibitors, Argifin and Argadin, Produced by Soil Microorganisms. Proceedings of the Japan Academy, Series B Physical and Biological Sciences. 2010; 86(2): 85 – 102.

67. Kim LK, Morita R, Kobayashi Y, Eisenbarth SC, Lee CG, Elias J, et al. AMCase is a Crucial Regulator of Type 2 Immune Responses to Inhaled House Dust Mites. Proceedings of the National Academy of Sciences. 2015; 112(22).

68. Zhu Z, Zheng T, Homer RJ, Kim YK, Chen NY, Cohn L, et al. Acidic Mammalian Chitinase in Asthmatic Th2 Inflammation and IL-13 Pathway Activation. Science. 2004; 304(5677): 1678 – 82.

69. Nijampatnam B, Nadkarni D, Wu H, Velu S. Antibacterial and Antibiofilm Activities of Makaluvamine Analogs. Microorganisms. 2014; 2(3): 128 – 39.

70. Donlan RM. Biofilms: Microbial Life on Surfaces. Emerging Infectious Diseases. 2002; 8(9): 881 – 890.

71. Barrows LR, Radisky DC, Copp BR, Swaffar DS, Kramer RA, Warters RL, et al. Makaluvamines, Marine Natural Products, are Active Anti-Cancer Agents and DNA Topo II Inhibitors. Anti-Cancer Drug Design. 1993; 8(5): 333– 47.

72. Aburjania Z, Whitt JD, Jang S, Nadkarni DH, Chen H, Rose JB, et al. Synthetic Makaluvamine Analogs Decrease c-Kit Expression and are Cytotoxic to Neuroendocrine Tumor Cells. Molecules. 2020; 25(21).

73. 4-Nitrophenyl *N*,*N*'-diacetyl-β-D-chitobioside. Item N6133. *Sigma Aldrich*. [Website]. Accessed on 31.03.2024. Available at:

https://www.sigmaaldrich.com/GB/en/product/sigma/n6133

74. An J, Jackson III RK, Tuccinardi JP, Wood JL. Pyrroloiminoquinone Alkaloids: Total Synthesis of Makaluvamines A and K. Organic Letters. 2023; 25(11): 1868 – 1871.

2.7 Abbreviations

List of Abbreviations	
NMR	Nuclear Magnetic Resonance
HPLC	High-Pressure Liquid Chromatography
SPE	Solid-Phase Extraction
SEC	Size-Exclusion Chromatography
MeOH	Methanol
TFA	Trifluoroacetic Acid
IC50	Half maximal inhibitory concentration
UV-Vis	Ultraviolet-Visible Spectroscopy
DAV-09	Davies Reef marine tunicate sample / extract
DAV-09-X%	Solid-Phase extracted variant w/ X% of methanol
QTOF	Quadrupole Time-of-Flight
COSY	Correlation Spectroscopy
HSQC	Heteronuclear Single Quantum Coherence Spectroscopy
HMBC	Heteronuclear Multiple Bond Coherence Spectroscopy
HR-ESIMS	High Resolution Electrospray Ionisation Mass Spectrometry
MS/MS	Tandem Mass Spectrometry
CASE	Computer Aided Structural Elucidation